European Commission

JRC TECHNICAL REPORTS

Joint Probabilities of Storm Surge, Significant Wave Height and River Discharge Components of Coastal Flooding Events

Utilising statistical dependence methodologies & techniques

Thomas I. Petroliagkis
Evangelos Voukouvalas
Juliana Disperati
Jean Bidlot

2016

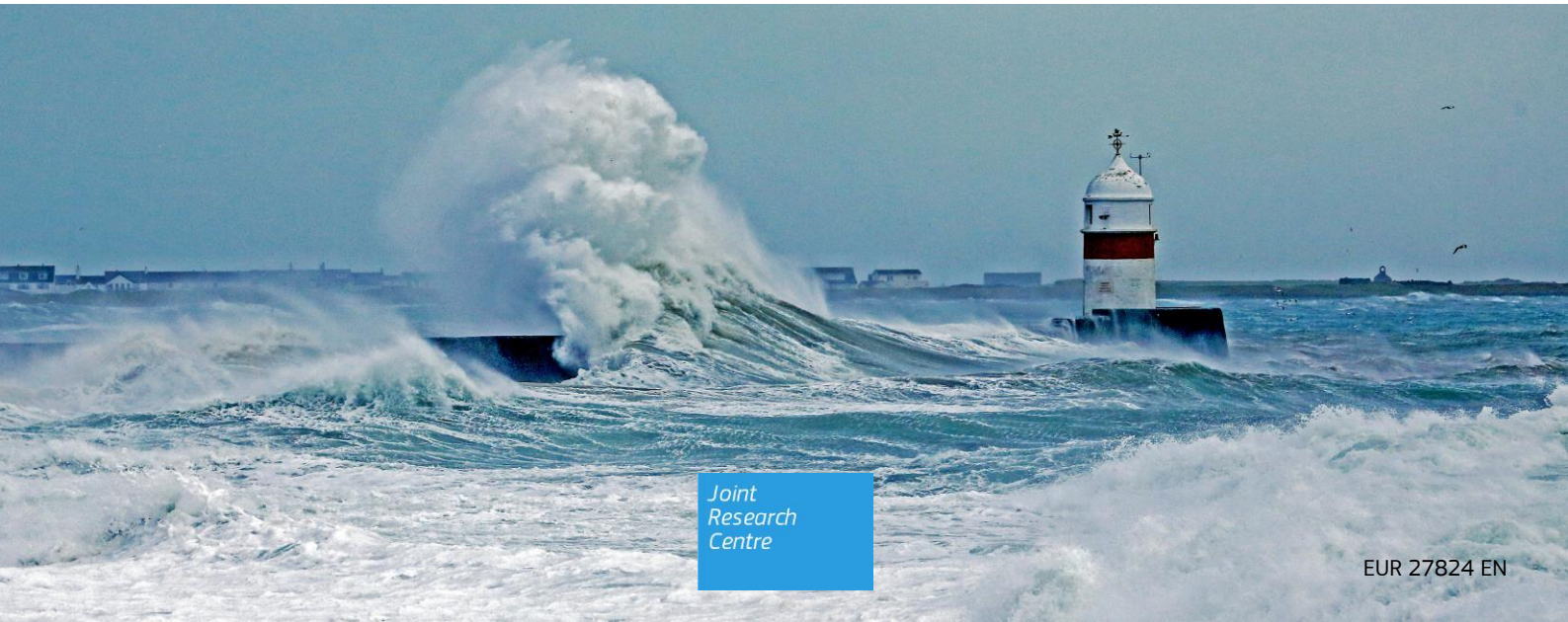

EUR 27824 EN

Joint Probabilities of Storm Surge, Significant Wave Height and River Discharge Components of Coastal Flooding Events

Utilising statistical dependence methodologies & techniques

Thomas I. Petroliagkis (JRC)
Evangelos Voukouvalas (JRC)
Juliana Disperati (JRC)
Jean Bidlot (ECMWF)

Contact information
Name: Thomas I. Petroliagkis
Address: Joint Research Center (JRC), Via E. Fermi 2749, I-21027 ISPRA (VA) - Italy
E-mail: thomas.petroliagkis@jrc.ec.europa.eu
Tel.: +39 0332 78 3907

JRC Science Hub
https://ec.europa.eu/jrc

JRC100839

EUR 27824 EN

ISBN 978-92-79-57665-2 (PDF)
ISBN 978-92-79-57666-9 (print)

ISSN 1831-9424 (online)
ISSN 1018-5593 (print)

doi:10.2788/677778 (online)
doi:10.2788/951583 (print)

How to cite:
Petroliagkis, T.I., Voukouvalas, E., Disperati, J. and J. Bildot, 2016. Joint Probabilities of Storm Surge, Significant Wave Height and River Discharge Components of Coastal Flooding Events. EUR 27824 EN. doi:10.2788/677778.

Compound events,
that is, two or more events occurring simultaneously, can lead to high impacts, even if the two single events are not extreme per se, i.e., only their combination (IPCC, 2012). Furthermore, compound events can be viewed as a special category of weather / climate extremes, which result from the combination of two or more events, and which are again 'extreme' either from a statistical perspective (tails of distribution functions of climate variables) or associated with a specific (critical) threshold.

The Exploratory Research Project Coastal-Alert-Risk (2015-16) of the Joint Research Center has been an initial effort of developing the first global integrated coastal flood risk management system with emphasis on such compound events, by linking satellite monitoring, coupled wave, tide and surge forecasting, inundation modelling and impact analysis …

Table of contents

Exploratory Research Project: CoastAlRisk 5
Acknowledgements 6
Abstract 7
1. Introduction 8
2. Joint probability and statistical dependence 12
2.1 Short review on the usage of joint probability methods 12
2.2 Methods for estimating joint probabilities 15
2.3 Introduction to statistical dependence concept and implications 18
2.4 Techniques to estimate statistical dependence 19
3. Data and methodology 25
3.1 Construction of hindcasts 28
3.2 Validation of hindcasts 31
3.3 Capability of hindcasts resolving correctly correlations & statistical dependencies 38
3.3.1 Correlations in observations and hindcast mode 38
3.3.2 Dependencies in observations and hindcast mode 41
4. Results 47
4.1 Correlation assessment of combined event components over RIEN points 47
4.1.1 Storm surge & wave height for MAX12 (maxima over 12 hours) 47
4.1.2 Storm Surge & wave height for MAX24 (maxima over 24 hours) 49
4.1.3 Storm surge & river discharge for MAX24 (maxima over 24 hours) 51
4.1.4 Wave height & river discharge for MAX24 (maxima over 24 hours) 53
4.2 Statistical dependence assessment of combined event components over RIEN points 55
4.2.1 Storm surge & wave height for MAX12 (maxima over 12 hours) 55
4.2.2 Storm surge & wave height for MAX24 (maxima over 24 hours) 58
4.2.3 Storm surge & river discharge for MAX24 (maxima over 24 hours) 61
4.2.4 Wave height & river discharge for MAX24 (maxima over 24 hours) 63
5. Discussion & conclusion 69
References 72
List of abbreviations and definitions 75
List of figures 76
List of tables 78

Exploratory Research Project: CoastAlRisk

Prototype of the first global integrated coastal flood risk management system with emphasis on compound events, by linking satellite monitoring, coupled wave, tide and surge forecasting, inundation modelling and impact analysis.

The current work provides evidence of statistical dependence and joint probability estimations between coastal flooding components such as storm surge, wave height and river discharge, and refers to the deliverable 21 of the "CoastAlRisk" Exploratory Research Project (JRC).

Project CoastAlRisk (CAR) aims to develop the first global integrated coastal flood risk management system that links satellite monitoring, coupled wave, tide and surge forecasting, inundation modelling and impact analysis. The CAR project aims also to perform novel research into: (i) model coastal extreme water levels, (ii) deriving joint return periods and inundation for concurring inland and coastal floods, and (iii) calculate flood impacts.

The CAR project is to create a ground-breaking prototype based on knowledge of IPSC, IES and IPTS. One of its deliverable (no. 21) focuses on the development of an optimal methodology for assessing the joint occurrence probability of coastal and riverine flooding events. It should be noted that flood risk is rarely a function of just one variable but usually more of two or three flooding components (source variables). Joint probability values provide the likelihood of source variables taking high values simultaneously resulting to a situation where flooding may occur.

The CAR is considered of significant importance since the interaction of flooding components (surge / wave / river discharge) is generally referred to as compound event (IPCC, 2012). The risk of such a compound event seems to become more and more important for the future as existing and developing coastal communities are to be threatened by rising sea levels and changing tidal regimes. CAR is a joint effort for the development of new methodologies for assessing the joint occurrence probability of coastal and river flooding in major deltas describing the historical data-analysis and numerical integration of the marginal probability distributions of river floods and extreme sea-levels for major deltas, taking into account return periods from the GloFAS (Global Flood Awareness System), GFDS (Global Flood Detection System) and SSCS (Storm Surge Calculation System) of GDACS (Global Disaster Alerts & Coordination System).

For deriving joint return periods and inundation for concurring inland and coastal floods, there exist various approaches focusing mainly on the assessment of coincident events, ranging from simple desk study assessments to full joint probabilistic analytical solutions. To determine the existing coincident flood risk in coastal and inter-tidal areas, it is necessary to understand and evaluate the interaction between the different physical factors, which include precipitation, river flow, storm surge, astronomical tide, wind and wave setup.

A key component of any coincident event assessment is, therefore, to understand the historical relationships between these different factors, which may lead to a coincident or compound flood event. Based on such coincident assessments, joint probability values are capable of providing the likelihood of source variables taking high values simultaneously. Acceptance of joint probability methods has been sparse so far mainly due to the lack of information on dependence among source variables and the intrinsic difficulty in usage and interpretation of the methods.

The current simple "desk study" approach – described in this Report – requires a certain number of extremes referring to the first source variable, the same number of extremes (for the second variable) and a single-parameter representation of dependence "chi" (χ) between the two.

Acknowledgements

Contributors to be acknowledged

- Peter Salamon, JRC / IES (technical assistance referring to river discharges)

- Michalis Vousdoukas, JRC / IES (technical assistance referring to storm surges)

- Lorenzo Mentaschi, JRC / IES (technical assistance referring to waves)

- Vasileios Syrris, JRC / IPSC (technical assistance referring to matlab functions & I/O routines)

- Prof. P. van Gelder, Delft University (technical assistance on dependence & joint probability estimations)

- Ricardo Tavares da Costa, LNEC / ARC (technical assistant on storm & wave hindcasts)

- Andre Fortunato, LNEC / ARC (technical assistance on storm & wave hindcasts)

- George Breyiannis, JRC / IPSC (technical assistance referring to modelling & routine optimisation)

- Daniele Brusa, JRC / IPSC (technical assistance referring to observations & data retrieval)

- Lorenzo Mancon, JRC / IPSC (technical assistance referring to observations & data retrieval)

- Pamela Probst, JRC / IPSC (technical assistance referring to meteorological & GIS graphical applications)

- Hara Melis, JRC / IRSC (technical assistance referring to meteorological & GIS graphical applications)

- Alessandro Annunziato, JRC / IPSC (technical assistance referring to storm surges & wave modelling)

Abstract

In this Report, the possibility of utilizing joint probability methods in coastal flood hazard component calculations is investigated, since flood risk is rarely a function of just one source variable but usually more of two or three variables such as river discharge, storm surge, wave etc. Joint probability values provide the likelihood of source variables taking high values simultaneously and resulting to a situation where flooding may occur. This report focuses on data preparation, parameter selection and methodology application. The source variable-pairs presented here, which include enough information for calculations, are: (i) surge & wave, (ii) surge & discharge and (iii) wave & discharge. The analysis is focused over 32 river ending (RIEN) points that have been selected to cover a variety of coastal environments along European riverine and estuary areas. In the absence of coincident long-term measurements, the methodology of simulating data observations by modelling was adapted resulting to a set of hindcasts for the three source variables (surge, wave height and discharge).

Storm surge hindcasts were performed by utilising the hydrodynamic model Delft3D-Flow that was forced by wind and pressure terms from ECMWF ERA-Interim reanalysis. In a similar way, wave hindcasts were generated by utilizing the latest version of ECMWF ECWAM wave (stand-alone) model, forced by neutral wind terms from ERA-Interim. For the construction of river discharge hindcasts the LISFLOOD model – developed by the floods group of the Natural Hazards Project of the Joint Research Centre (JRC) – was employed. Validation of hindcasts was made over the RIEN point of river Rhine (NL) where coincident observations were available. Considering the physical driver complexity behind interactions among surge, wave height and discharge variables, hindcasts were found to perform quite well, not only simulating observation values over the common interval of interest, but also in resolving the right type and strength of both correlations and statistical dependencies.

Results are presented by means of analytical tables and detailed maps referring to both correlation and dependence (χ) values being estimated over RIEN points. In particular, dependencies coming from such analytical tables can be used in an easy way to calculate the joint return period for any combined event by inserting χ in a simple formula containing the individual return periods of source variables. It is then straightforward to estimate the joint probability value as the inverse of the joint return period.

Overall, the highest values of (strong / very strong) correlations and dependencies were found between surges and waves mainly over North Sea and English Channel with (such combined) events to take place on the same day (zero-lag mode). Moderate to well category dependencies were found for most sea areas, also on a zero-lag mode. In the case of surge and river discharge, moderate to well category values were found in most cases but not in a zero-lag mode as in surge & wave case. It became clear that in order to achieve such (relatively high) values, a considerable lag time interval of a few days was required with surge clearly leading discharge values. For the case of wave and river discharge, well to strong category values were found but once more mostly in non-zero lag mode indicating the necessity of a considerable lag time interval for dependence to reach such (well / strong) values with wave distinctly leading discharge values.

1. Introduction

In the coastal and inter-tidal zones, high tides and extreme tidal surge events can occur simultaneously with extreme precipitation events and high river flows, leading to increased flood severity, duration or frequency. This interaction is generally referred to as coincident or compound events (IPCC, 2012).

Understanding the risk posed by these events is likely to become more important in the future as existing coastal communities become threatened by rising sea levels and changing tidal regimes. Towns close to tidal rivers and estuaries are at risk from the combination of both fluvial and tidal flooding. Expected rises in sea levels and increased precipitation resulting from climate change, coupled with pressure for increased urbanization of low-lying areas, is expected to create major flood risk problems for many coastal and estuarine towns.

Furthermore, a certain lack of knowledge seems to exist in the interaction between sea levels and river flows in riverine & estuarine environments as the risk of flooding posed by such an interaction is hard to quantify due to the dynamic nature of the hydrological variables and the complex interaction of catchment and tidal processes. Coastal-Alert-Risk (CoastAlRisk / CAR) project should be considered as a prototype of a Global Integrated Coastal Impact-based Flood Alert and Risk Assessment (Aids) Tool. The CAR project is focused on developing the first global integrated coastal flood risk management system that links satellite monitoring, coupled wave, tide and surge forecasting, inundation modelling and impact analysis. The CAR project aims to perform novel research in:

(i) *modelling coastal extreme water levels,*
(ii) *deriving joint return periods and inundation for concurring inland and coastal floods, and*
(iii) *calculating flood impacts.*

The CAR project plans to create a ground-breaking prototype based on knowledge of IPSC (Institute for the Protection and Security of the Citizen), IES (Institute for the Environment and Sustainability) and IPTS (Institute for Prospective Technological Studies), with key orientation the development of disaster detection and early warning systems as well as scientific and analytical services to support the Emergency Response Coordination Centre (ERCC) of the EC (European commission).

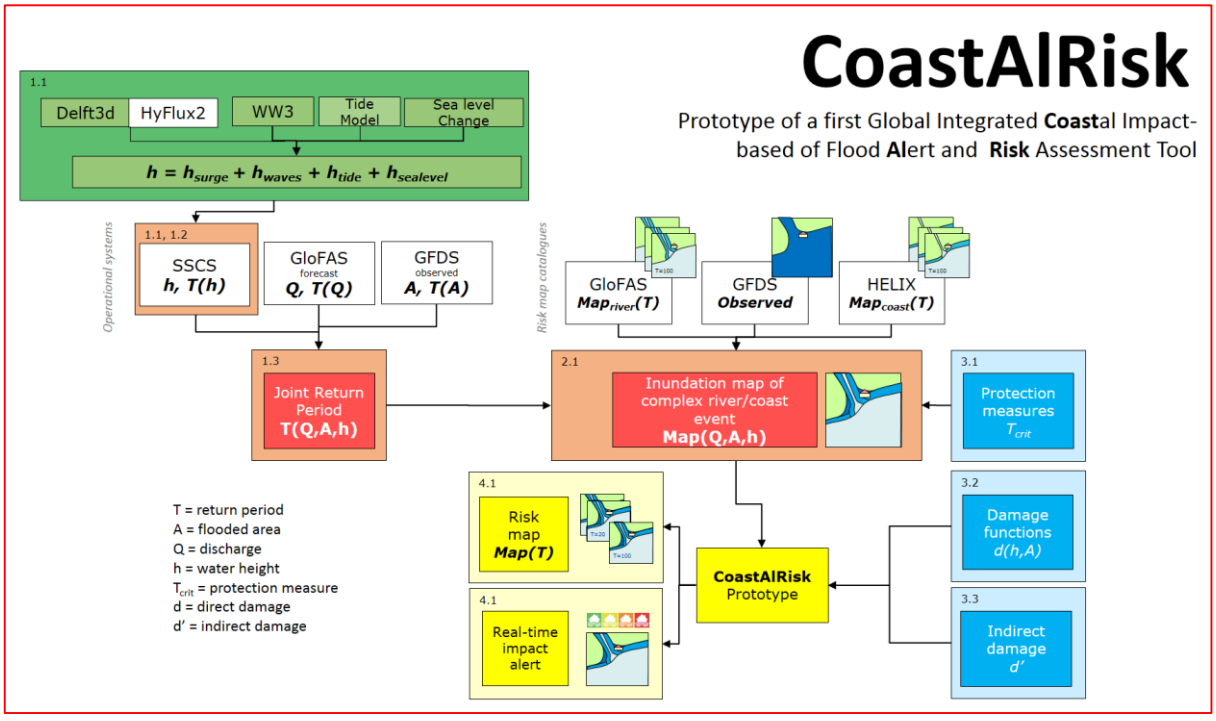

Figure 1.1. Main components of the Coast-Alert-Risk (CoastAlRisk / CAR) exploratory research project.

In simple words, CAR is a joint effort for the development of a new method for assessing the joint occurrence probability of coastal and river flooding in major deltas describing the historical data-analysis and numerical integration of the marginal probability distributions of river floods and extreme sea-levels for major deltas and taking into account return periods from GloFAS (Global Flood Awareness System), GFDS (Global Flood Detection System) and SSCS (Storm Surge Calculation System). The main components of CAR project are shown in Figure 1.1.

For deriving joint return periods and inundation for concurring inland and coastal floods (as shown graphically in Figure 1.2) various approaches are available focusing on the assessment of coincident events, ranging from simple desk study assessments to full joint probabilistic analytical solutions. To determine the existing coincident flooding risk in coastal and inter-tidal areas, it is necessary to understand and evaluate the interaction between the different physical factors, which include precipitation, river flow, storm surge, astronomical tide, wind and wave setup (AR & R Project 18, 2009).

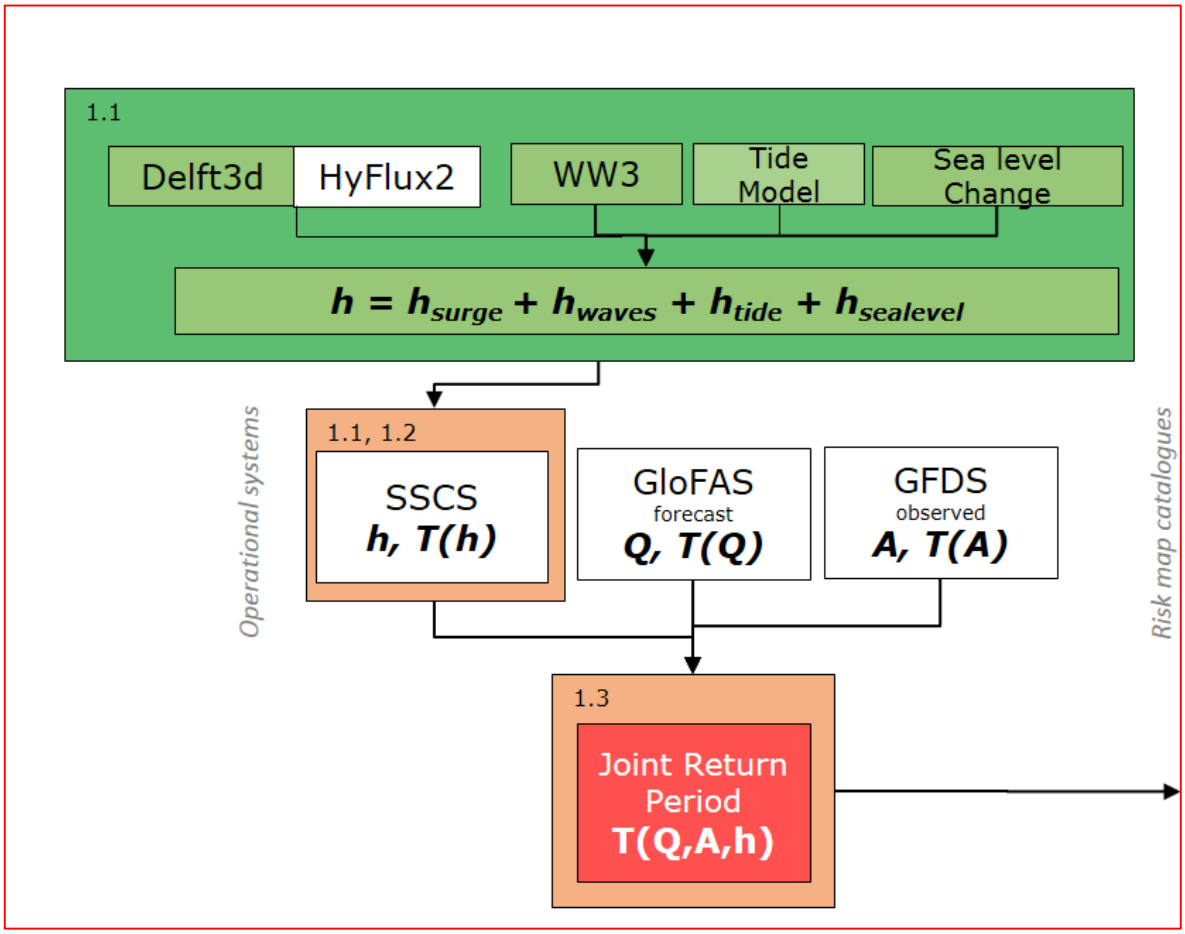

Figure 1.2. Main elements of the Joint Return Period module of CAR Project.

A key component of any coincident event assessment is, therefore, to understand the historical relationships between these different factors, which may lead to a coincident or compound flood event. However, assumptions are often made regarding how the different factors and variables coincide or combine, typically leading to either an under or an overestimation of the probability of flooding. In reality, while some events may indeed occur independently from one another, others involve an interaction, or may have compounding consequences when they occur simultaneously, and need to be treated as partially dependent.

Joint probability values provide the likelihood of source variables taking high values simultaneously resulting to a situation where flooding may occur. Acceptance of joint probability methods has been sparse so far mainly due to the lack of information on dependence among source variables and the intrinsic difficulty in usage and interpretation of the methods.

This report focuses on data preparation, parameter selection, methodology application and presentation of results. The variable-pairs presented in this report, which include enough information for calculations, are:

- *storm surge & wave height, relevant to most coastal flood defence studies,*
- *storm surge & river discharge, relevant to most riverine / estuary flood defence studies, and*
- *wave height & river discharge, relevant to most coastal flood defence studies*

Examples of coincident flood event studies, which incorporate a measure of the relationship (i.e. the dependence) between the input variables, are generally limited due to the complexity of the broader coincident events problem. However, more approachable and user-friendly methods, now exist to quantify the statistical dependence between the input variables (as noted in Hawkes 2004, White 2007). In the current Report, the estimation of joint probabilities among primary flooding components as storm surge, significant wave height and river discharge is being pursued by utilising statistical dependence methodologies and techniques.

An example of a combined event and its implications is given in Figure 1.3. A concurrent set of storm surge and wave height observations are plotted in a scatterplot diagram. Storm surge values were collected at the tide gauge station of Hoek van Holland (HVH) whereas significant wave height observations were recorded at the Lichteiland Goerre I (LIC) wave buoy platform a few kilometres away from HVH's location. Both time series comprise 1,114 records of daily maximum values for the time period of 22 September 2010 to 9 October 2013.

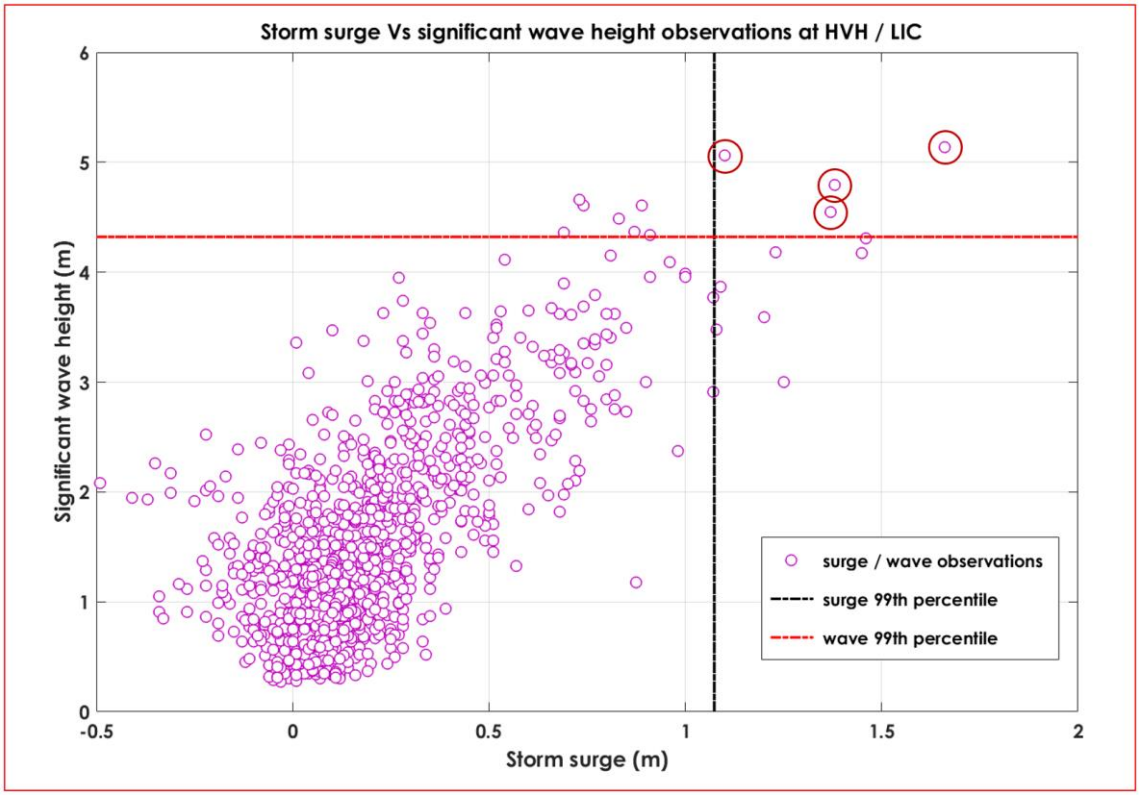

Figure 1.3. Storm surge Vs significant wave height observations at HVH / LIC.

By considering an extreme value threshold (99% percentile) for both surge and wave height observations, an area of (combined) extremes is defined by both variables exhibiting extreme values at the same time (day). These four cases (points) are clearly visible on the upper right corner of Figure 1.3. There are additional storm surge points that have values overshooting the 99% percentile (lower right corner) but they do not correspond to a concurrent extreme value of wave height. The same holds for some extreme wave height values (upper left corner) that they do not match to a coincident extreme storm surge value.

Taking into account the variability of such conditions, it seems quite important to find a way to identify extreme data within each of primary variables and statistically correlate their linkages and risk (probability) of occurring simultaneously. Understanding such risks, created by the combination of such extreme events is considered to be crucial for the design of adequate and cost effective river and coastal defences and for the true estimate of flood risk.

A methodology capable of correlating the linkage between extremes of primary variables and estimating the (joint) probability of occurring simultaneously, is called statistical dependence. Dependence determines the extent to which an observation of one variable is reliant on a value of another (variable). This is essential for a joint probability calculation. Dependence indicates the likelihood of two variables, (such as river discharge, storm surge, tide or wave height), producing high or extreme values at the same time (worst case scenario). In the equation shown below (Equation 1.1 being an exact copy of Equation 2.4.10), the dependence is denoted by the Greek letter chi (χ) and it is essential for the estimation of the joint (combined) return period ($T_{X,Y}$) as it is analytically explained in Subsection 2.4.

$$T_{X,Y} = \sqrt{\frac{T_x \, . \, T_y}{\chi^2}}$$	(1.1)

It should be noted that T_x stands for the return period of the first primary variable (in the current case: storm surge) for an event of a particular size, whereas T_y stands for the return period of the significant wave height for an event of another particular size. It is obvious that the probability of a storm surge event (of a particular or greater size) to occur in any year is equal to $1/T_x$. Same wise, the probability of a similar type of wave height event to take place in any year is equal to $1/T_Y$. If the source variables (surge & wave) are considered independent (chi = 0), then the combined probability would be given by: $1/T_x * 1/T_Y$ that usually corresponds to a low probability value. In case that events were fully dependent (chi = 1) then Equation 1.1 (or Equation 2.4.10) yields: $\mathbf{T_{X,Y} = T_x = T_Y}$.

It should be pointed out, that in most cases, prime (source) variables are not independent (chi = 0) or fully dependent (chi = 1) and the assessment of the exact value of dependence (chi) is considered crucial for the estimation of the joint return period and consequently the joint probability of the combined event to take place in any year, given as the inverse of joint return period $\boldsymbol{(T_{X,Y})^{-1}}$.

Based on the above, the organisation and set up of this Report follows an obvious path leading to the estimation of statistical dependence between primary components capable of resulting to a high-impact flood event.

In Section 2, the main details and characteristics of both the joint probability and statistical dependence concepts and implications are documented, while in Section 3, the data and methodology utilised is presented together with the validation of model hindcasts used for the simulation of missing long-term concurrent observation data.

Results are presented in Section 4 while discussion and conclusion is contained in Section 5.

2. Joint probability and statistical dependence

Joint probability determines the chance of two (or more) events occurring concurrently that may combine and produce a critical (high-impact) situation. The method for the estimation of the probability of extreme values from a single variable has been well understood. Such probabilities are usually expressed in the form of a return period. In a similar way, the probability of two (combined) variables producing high or extreme values together, assuming to be fully independent, is also considered to be straightforward (Hawkes 2003).

The basis of joint probability theory is to identify extreme data within each of primary variables and statistically correlate their linkages and risk (probability) of occurring simultaneously. Understanding such risks, created by the combination of such extreme events, is crucial for the design of adequate and cost effective river and coastal defences as well as for the true estimate of flood risk (AR & R Project 18, 2009). For the case that two (or more) variables, capable of producing high-impact events, are not totally independent, but may be partially dependent, probabilistic approaches are limited in both their reliability and scope (White 2007).

Statistical dependence on the other hand, determines the extent to which an observation of one variable is reliant on a value of another variable. This is essential for a joint probability calculation. Dependence indicates the likelihood of two variables (such as river discharge and storm surge for example), producing high or extreme values at the same time (worst case scenario).

2.1 Short review on the usage of joint probability methods

Acceptance of joint probability methods has been sparse so far mainly due to the lack of information on dependence among source variables and the intrinsic difficulty in usage and interpretation of such methods. Prior to the 1980s, the usage of joint probability methodology was almost non-existent in estimating coextensive flood risk. Studies of how a single flooding variable as astronomical tide for instance may affect two or more sites had been undertaken but no further research was taken place since investigations on how a possible combination of two (or more) flooding components could affect coastal areas had been somehow limited. Published research at that time referring to the possible interaction of storm surge (sea level) and river discharge was focusing on the inter-comparison of historical records and the frequency of combined water levels as the ones coming from the work of Weston (1979) and ten years later from Vongvisessomjai and Rojanakamthorn (1989).

In particular, Weston (1979) tried to quantify the magnitude and sum of river flow (River Dee) and sea level (of North Wales) components by combining them. That proved to be in harmony to the observed water levels but they were no joint probability estimates besides some comments on how much influence river flow could have on the resultant water levels in the tidal reach area of the river. On the same wavelength, Vongvisessomjai and Rojanakamthorn (1989) found that historical records of stage in estuary areas and tidal rivers in the United States presented the fact that an increase in the riverine discharge could have a dampening effect on incoming tides and such an event could reduce the tidal propagation speed that was contributing in the raising of water levels. Furthermore, Prandle and Wolf (1978) examined the interaction of surge and tide in the North Sea while Walden et al. (1982) in a similar approach investigated over the interaction of surge and tide on the south coast of England by assessing the level of tide and surge interaction from historical observations.

More detailed examples of joint probability research on tidal water levels has been carried out at Proudman Oceanographic Laboratory (POL), UK. Such research has been documented by the work of Coles and Tawn and Dixon and Tawn on the same year (1994). That work was focused in assessing the interaction of extreme surges and wave heights. One important aspect here, has been the enclosure of a measure of dependence between the input variables. On that same year (1994), Acreman also has published a study of assessing the joint probability of fluvial and tidal floods in the River Roding (UK). A year later (1995), Dwyer recognised and

also investigated over various approaches to the solution of joint probability problems with an emphasis on cases of river confluences.

A few years later (1999), Reed debated joint probability problems involving variables from both tidal and fluvial input for the determination of sea level(s). The importance of selecting a set of correct input variables in a joint probability analysis was recognised. Furthermore, the adoption of a time-blocking approach that is capable of selecting one value per high tide or per day was highlighted.

The appropriate definition of events (i.e. how to define independent extreme events) was also considered, and a recommendation was made that in extreme value analysis the approach of Peaks-Over-Threshold (POT) should be used rather than the typical annual maxima (AMAX) method. Furthermore, Reed (1999) incorporated results of his work as a summary of a joint probability approach based on a methodology of utilising structure functions. The case of inter-variable independence was also examined but no methods or techniques were produced for non-independent variables.

In more recent years, there have been various research programmes focusing on how joint probability theory could be exploited in environmental applications, such as flood dangers and risks. Statistical methodologies on flood risk analysis – developed mainly by UK research & academic institutions – had focused mostly on the application of joint probability theory to specific (selected) variable pairs. Such pairs were: sea level & wave and wind & sea swell source parameters (coming from research made by HR Wallingford, UK), tides & surges (coming from Proudman Oceanographic Laboratory, UK), rainfall & surge and surge & river flow (coming from CEH Wallingford, UK). The interesting point here is that even if joint probability methods had been applied by all institutions as mentioned above (i.e., HR Wallingford, Proudman Oceanographic Lab and CEH Wallingford) the dissemination or accompanied information on their use and exploitation had been limited. Subsequently, it came as no surprise that take-up of joint probability methods within the Civil Engineering and Hydrology communities had been limited.

As part of the R&D joint probability programme (funded by Defra Institute), Hawkes and Tawn (2000), pointed out that although methods for assessing single extremes of tidal water levels or waves at a single location were in common use, the estimation of joint probability of both water level and wave variables was somehow more complex and difficult to comprehend. This (R&D) project concluded with the successful production of a joint probability software package (named as Join-Sea) developed jointly by HR Wallingford and the University of Lancaster (details can be found in Hawkes and Tawn, 2000).

The Join-Sea statistical package (written mainly in the old-fashion Fortran 77 code) had been a program primarily designed to calculate the joint probability between waves and still water levels at the same location by extrapolating the original source variables to extreme values. Such statistical processes made use the fitting of various statistical models to the distribution of variables. Then an extreme statistical distribution was fitted to the top few percent of each variable, and a statistical correlation model was applied to the datasets. There was a need of a large sample of synthetic records, so Monte Carlo techniques were used by utilising the same fitted distributions as the input data. Extreme values (identified by joint exceedance criteria) were extracted from the Monte Carlo dataset using a count-back approach.

The main conclusion based on Join-Sea simulations had been the fact that although a degree of dependence should be expected between surge and wave values as both data sets are linked to common prevailing weather system and meteorological conditions, the degree of statistical dependence differs from one site to another (most probably due to different topographical and local weather / atmospheric circulation characteristics). Nevertheless, the Join-Sea code has remained in the old-fashion Fortran 77 code and it is not easy by any means to run it in most of nowadays operating systems as clearly stated by his own developer Peter Hawkes (personal communication, November 2015).

The issue of locally varying values of dependence does not seem to be a simple issue by any means especially since Hawkes (2003) documented that in some estuary areas the significance of wave or surge parameters

might be even higher (other than upstream river flows and downstream tidal levels) and obviously need to be considered in joint probability analyses. In some estuaries, surge and wave variables may have such an important effect on water levels that then may require the need of at least a trivariate joint probability approach as clearly suggested by White (2007). Such an introduction of a third variable (i.e., in case of trivariate analysis) could make probability calculations extremely complex. Based on this unavoidable complexion, Defra, UK, in collaboration with HR Wallingford, CEH Wallingford and Proudman institutions, have produced a guide for the optimal usage of joint probabilities in the flooding sector as documented in Hawkes, (2004), Svensson and Jones (2003) & Hawkes and Svensson (2003).

Even if no new developments were made, the aim of joining efforts (by the four leading institutions involved here) had been to pool previously unpublished research and methodologies in an attempt to compile an "official" type of methodology. Each of the institutions had reported its joint probability results following its own preferred methodology. However, the whole effort resulted to a relatively limited exercise.

It should be noted here that Hawkes (2004) documented two main methodologies concerning joint probability analysis. The first, named as SA (Simplified Approach) was compiled as a desk study methodology aimed at non-specialist users. The SA methodology was capable of producing a basic extreme joint exceedance output in annual return periods, to be used in the case that original time series of the input variable pairs were not available. The SA approach proved to be reliant on estimating the correlation between the variable pairs from pre-calculated colour-coded small scale maps of the UK, although there were inherent problems relating to the precision of the maps that eventually resulted to the decision that some of the mapping ideas that were eventually dropped. Based on such (intrinsic) limitations it has been questionable whether a non-specialist user could appreciate the full implications of assumptions and methods used.

There was also a second method, named as AA (Applied Approach) that was actually a revisit of the work performed by Hawkes and Tawn (2000). Unfortunately, the AA proved to be more complicated and difficult to be handled by non-specialist users as explained in Hawkes et al. (2005).

On the other hand, in the south hemisphere, Teakle et al. (2005) and a few years later Gould et al. (2008) described a joint probability assessment that had to be taken in order to define water level boundaries in an estuary system in southeast Queensland. Furthermore, Gould et al. (2008) had pointed out some possible implications of climate change on the results and recommendations were provided on assessing possible climate change impacts referring to the future estimation of water levels plus 0.5 m to define planning levels. This was somehow unsubstantiated since the climate change impacts were not specifically incorporated in the modelling.

More practical results were provided by Need et al. (2008) referring to an assessment taking into account the fact that both the 100-year return period water level along a river reach and the 100-year return period downstream depth were combined (superimposed) and compared to a joint probability approach, while a similar approach was followed by White (2007) on a catchment in southeast England.

In the first case (Need et al., 2008), results show that the upstream region is dominated by the inflow boundary while the downstream depth seems to be the dominating factor downstream. It is only in a limited area of around 10 kilometres from the downstream boundary, where joint behaviour is most evident. In this relatively small area the simple (independent) approach noticeably underestimates the risk of coincident flood levels.

Similar conclusions were also established by White (2007) who documented that fluvial river flow and tide dominate water levels were acting mostly independently in different parts of the tidal river system of a catchment in Sussex (UK), but there existed a small section (of the river system) in which the combination of tide and river flow was likely to be combined for dominating over the maximum flood risk level.

2.2 Methods for estimating joint probabilities

Various approaches are available for assessing the probability of coincident events, ranging from simple desk study assessments to full joint probabilistic analytical solutions. To determine the existing coincident flooding risk in coastal and inter-tidal areas, it is necessary to understand and evaluate the interaction between the different physical factors, which include precipitation, river flow, storm surge, astronomical tide, wind and wave setup. A number of different methodologies for estimating joint probabilities are presented below in Table 2.1 that is based partly on the AR & R Project 18 (2009) analysis:

Table 2.1. Different methodologies for estimating joint probabilities.

Direct Analysis	A number of existing compound flooding studies use a non-probabilistic direct (one source variable) approach at the point or close to the point of interest using historical observed data, in an effort to avoid potentially complex joint probability studies. This is not always conceivable due to the lack of gauge stations (near the site of interest) or due to poor measurement records. Such simplistic methodologies include an assumption of independence between the probabilities of the boundary variables – as the downstream tide and upstream river flow for instance – when using combinations of selected design events to determine a 'joint' probability of flood risk in the system. Based on such an assumption Teakle et al. (2005), suggested that current practice in a joint probability analysis of water levels in estuary flood modelling (referring in southeast Queensland), should include an analysis of two boundary cases to obtain the 100-year average return period flood level that might typically combine: (i) the 100-year average return period river discharge with a downstream (tidal) level at mean high sea level and (ii) the 20 year average return period freshwater inflow with a 100 year downstream (tidal) level.
Continuous simulation	The term "continuous simulation" refers to a direct numerical hydraulic model simulation that involves co-existing measurements of river flow and sea level observations at the extremities of the model (forcing terms), producing a corresponding modelled output time series at an intermediate point of interest within the length of the hydraulic model (output terms) as analysed by Jones (1998). Jones also presented an approach for continuous simulation modelling, suggesting that this could be undertaken as a long-term or event-based exercise. What someone should expect from such an exercise should be a set of time series at each modelled cross-section for the same time period as the input variables. These time series could provide a real-time output enabling extraction of extreme values (i.e., maximum values during a day or a year) or specific hydrological events at any point of interest within the model cycle as suggested by Reed (1999). It is important to notice that Hawkes (2003) also suggests the use of a continuous simulation of water levels, commending that such an approach could benefit from the fact of not needing to know the type and strength of the dependence between the source variables, although this specific methodology seems to be time consuming and limited by the length and availability of input records.

Historical emulation	The main requirement of the continuous simulation approach presented above, is the requirement of two simultaneous historical data series (i.e., storm surge and river discharge) for simulating an output variable (in a continuous mode). In contrary the historical emulation approach makes use of a structure function matrix upon input data series in order to select, corresponding values at the point of interest. Such structure function(s) is to be derived through extensive trials and model runs as recommended by Reed (1999). Once the structure function found it is applied to potential flood (extreme) events being extracted from the historical records. In this way a series of extreme output values are constructed for further exploitation. Applying such 'historical reconstruction' approach on a tributary area of River Thames (UK), Acreman (1994) utilised a set of statistical distributions to be fitted onto input variables with the combined use of a one-dimensional hydraulic model. As a result, he managed to reconstruct water levels from historical records of river flow and sea level through structure functions. Acreman also found that the estimated water level for a specified return period was determined on a great extent by the extrapolated input data. The obvious implication here is coming from the short duration of the historical input variables that might miss completely the most extreme coincidences of sea levels and river discharges, resulting in a relatively large extrapolation of the output data. The author came to a conclusion that historical emulation appears to be both flexible and adaptable. He also recommended the careful use of a sensitivity test that seemed to be necessary for satisfactory results. Another effort of documenting this methodology – presenting a historical emulation exercise – was made by Jones (1998). Jones (1988) in addition, provided examples of its use on tributaries of the river Thames. The author finally concluded that the historical emulation approach is quite straightforward to be used when compared to complex joint probability analyses, but it is limited to the length of the available records for such a study.
Structure functions and matrices	This method relates an output variable, for instance the water level at some point of interest, to two input variables (storm surge and river discharge taken as an example here). It is described in details by various authors as Ibidapo-Obe and Beran (1988), Dwyer (1995), Jones (1998) and Reed (1999). It seems that two direct methods of calculating water levels in tidal rivers and estuaries exist. The first uses numerical hydraulic model for simulating water levels while the second makes use of a simple formula that in most cases is the outcome product of a regression analysis as pointed out by Hawkes (2003). One obvious drawback of this approach is that the length of the historical datasets as relevant equations may differ under conditions of extreme discharge/surge level events for instance that might not be included in (historic) data series. As mentioned above, Jones (1998) performed a historical emulation exercise on tributaries of the river Thames. He also carried out an extensive structure function analysis of the tidal reaches in the same areas. This gave him the opportunity to evaluate both the (hydraulic) modelling but also the formula-based structure function methodologies used in the experiment. He documented that the most accurate method for determination of overall water levels would be the modelling process since it had been found capable of evaluating intermediate water-levels

	for any possible combination of the input variables, including pronounced extreme loading conditions as well. On the same subject, the optimal and most reliable structure function approach seems to be by utilising matrices as suggested by Reed (1999). It follows that for a bivariate analysis, two matrices are to be constructed and used (defined as 'double matrix method'. The first matrix is to contain the output variables generated by hydraulic model runs. The setup of matrix should be as such that input values would be at opposing axes while the generated 'structure' values at the point of intersection corresponding to the "crossing" of input pair. The second matrix is to contain a joint density function matrix of probabilities. Such probabilities are referring to the same input variable pairs as the structure value matrix. For the calculation of matrix elements, the density functions of the two input variables are to be considered. Applying such methodology, the peak levels of water at a tidal river site can be estimated taking into account both the peak sea levels and peak river discharges for a desired range of probabilities linked directly to the (inverse of) return periods. One important issue here as noted by Hawkes (2003) would be the difficulty in practice to generate so many hydraulic model output data (for each possible pairing) as there could be a very high number (thousands actually) of combinations. Nowadays, the applications utilising numerical modelling of sea levels and hydraulic flows have been established as an optimal tool of studying in detail flood frequency estimation. Such modelling is capable of enabling complex calculations that are necessary in fluid dynamics with relative ease and high accuracy. It comes with no surprise that current models can simulate a wide range of specified (extreme) events or perform continuous (real-time) simulations, and can be used for the estimation of structure functions based on two or more input data records.
Utilising statistical dependence (χ)	For the estimation of compound flooding events all methodologies mentioned so far can be utilised although the most accurate approach appears to be an optimal combination of the methods presented so far while incorporating an estimation of dependence (χ). The concept of the dependence (as defined by Reed, 1999) refers to the tendency for critical values of source variables to occur at the same time resulting to an increase in frequency of an extreme (defined by a selected critical threshold value). This increase in frequency means that dependence could increase the magnitude of the output variable (combined event) for a given annual return period that defines the rarity of the event under consideration. Even if someone considers a small value of dependence between extremes of storm surge and river discharge for instance, this most probably could have a significant impact on the resultant water levels as pointed out by Svensson and Jones (2004b), White (2007). The methodology of using statistical dependence for estimating joint probabilities is analytically explained in the following Subsection 2.3 (Introduction to statistical dependence and implications).

In the current Report the methodology of utilising statistical dependence for the estimation of joint probabilities (by assessing joint return periods) of the combined events considered in this study (surge & wave / surge & discharge / wave & discharge) is adapted. One important issue to be mentioned here is that the number of available coincided observations of the source variables (surge / wave height / discharge) is limited and this proved to be the main reason behind the usage of model hindcasts.

2.3 Introduction to statistical dependence concept and implications

To assess the probability of flooding as a result of such combined high (extreme) values, the dependence between source variables needs to be calculated as analytically documented in AR & R Project 18 (2009). This is an essential part of joint probability analysis, yet quantification of dependence can be difficult and extreme values hard to define.

If two events are independent, the probability that they occur at the same time is the product of their probabilities (Blank, 1982). As independent events, the chance of one event occurring is not changed by the occurrence of the other event. However, if the occurrence of one event is dependent on the occurrence of a second event then the events are termed conditional. For example, both high wave height and storm surge values may be attributed to a common weather event prevailing over the area of interest. The conditional probability of both events occurring at the same time is then different than the product of their individual probabilities. Furthermore, it is more complicated to estimate such conditional probabilities.

What someone should anticipate is the fact that dependence is likely to occur when different processes are linked for example to common weather prevailing (forcing) conditions. It may also arise when the same process is studied at different spatial locations or over different time periods (Coles et al., 2000). In an estuarine or river ending area, an example would be a low atmospheric (weather) pressure system accompanied of high winds and intense precipitation. These phenomena are likely to create high river discharges and storm surge conditions that may interact with each other, increasing the risk of flooding.

The estimation of dependence between source variables as river flow, tide, wave and surge could determine the (joint) probability of a critical water level taking place, caused by such a combination of events.

At present for coastal flood risk assessments, extreme combined events are either assumed to be independent, or an arbitrary level of dependence is applied such as the one(s) mentioned for example in the Report of AR & R Project 18 (2009). The estimation of dependence is essential since joint probability determines the chance of two (or more) conditions occurring simultaneously that may be combined resulting to a high-impact event. The method for calculating the probability of extreme values prevailing at a given location from a single variable has been well understood. Such probabilities are usually expressed in the form of a return period. Same way, if two variables are assumed to be fully independent from each other, their joint probability producing high-impact values together, is also quite straight forward as presented in details in Hawkes (2003).

The basic idea behind joint probability theory is the identification of extreme data within each of the input variables and statistically correlate their linkages and risk of simultaneous occurrence. Quantifying such dangers referring to the combination of high-impact events is crucial for the estimation of flood risk and the optimal design of adequate and cost effective river and coastal defences. In tidal and estuarine environments, assessing the probability of flooding from the joint occurrence of both high river discharge and high sea level values is not an easy process, as high river discharges and storm surge tides might be related to the same prevailing meteorological conditions, thus independence cannot and should not always be assumed. For instance, if we assume independence between input variables, this might underestimate considerably the likelihood of flooding resulting in higher risk for the coastal community. Similarly, assuming total dependence could be too conservative. This can be considered as a 'worst case' approach whereby an optimal combination

of variables might be a 100-year average return period for river discharge combined with a 100-year average return period of high sea level conditions.

Based on the above, it seems quite appropriate that the level of dependence between individual variables should be taken into account to ascertain a true joint probability calculation. However, the typical variables required for a joint occurrence flooding study are quite often spatially dependent, temporally dependent or both. Therefore, the type and level of dependence between the variables will likely affect the analysis approach adopted (AR & R Project 18, 2009).

2.4 Techniques to estimate statistical dependence

A methodology for estimating statistical dependence was developed in the early 1990s mainly to establish the probability of simultaneous occurrences of extreme hydrological values as described in details in Tawn (1992), Coles and Tawn (1991 & 1994), Dixon and Tawn (1994). The main concept of the so-called dependence measure χ (chi) is related to two or more simultaneously observed variables of interest – for instance storm surge and river discharge – known as observational pairs. If one variable exceeds a certain (extreme / hi-impact) threshold, then the dependence (χ) representing the risk of the other variable will also exceed an extreme (hi-impact) threshold.

Following Coles et al. (2000), if all of the extreme observations of two variables exceed a given threshold at the same time, this indicates total dependence ($\chi = 1$). If the extreme observations of one variable exceed a given threshold but the second variable does not, this indicates total independence ($\chi = 0$). Similarly, if the extreme observations of one variable exceed a given threshold but the other variable produces lower observations than would normally be expected, this indicates negative dependence ($\chi = -1$). In practice, hydro-meteorological analyses based on real data often lead to an assessment of complete independence that could result to an under-estimation of the joint probability of concurrent extreme events, whereas, an assumption of complete dependence could result to an over-estimation of joint probabilities.

The dependence as a term appears in the Flood Estimation Handbook noted by Reed (1999) and refers to the tendency for potentially critical values of source variables to occur at the same time interval with a frequency higher than by chance alone. Reed also described some simple methods for assessing inter-parameter dependence referring to both scatterplots of source variables and their correlation coefficients. Unfortunately, such methods seem more likely to lead to a considerable underestimation of extremes. Reed's conclusion has been that more complex multivariate statistical methods of extreme values were necessary and pointed to suggestions made by Coles and Tawn (1994) as an extension to the Flood Estimation Handbook methodologies. One obvious drawback here is that such multivariate methods are highly specialised (complex) and not easy (straightforward) to be applied. Another important point in Reed's analysis has been the fact that the type and strength of statistical dependence should be calculated taking into account simultaneous only records that in most cases have a shorter duration than their corresponding return periods in case of flood estimation. Consequently, such results in most cases would be highly sensitive to the (small) number of extreme events taking place in relatively short data series (input values).

Following Coles (2001) it becomes obvious that the identification of simultaneously occurring extreme events (defined as dependent events) in a multivariate extreme value environment should be considered distinctly important since the impact of such a compound event may be much noticeable than if extremes of either source variable take place alone. Based on this, it comes natural for Coles (2001) to suggest that both the assessment of dependence between source variables at extreme levels and their extreme behaviour are necessary for an accurate simulation during the application of extreme multivariate models. Furthermore, the marginal distributions of two primary variables (storm surge and wave height for instance) may not necessarily be identical. An optimal approach concerning such non-identical marginal distributions is given by Coles et al. (2000) pointing out that for a successfully estimation of dependence, the two primary variables

require identical marginal distributions, so, it seems necessary to be transformed to identical ones. Such an approach could be achieved by implementing their empirical distributions. One could rank each set of observations separately and divide each rank with the total number of observations in each dataset. In such simple way both datasets are to be transformed to a common distribution with uniform [0,1] margins. This relatively simple method has a clear advantage by using such transformed distributions for the two source variables as cited by Coles and Tawn (1994) when compared to single variable approaches in which variables are considered as a combination of input factors (Reed, 1999).

As mentioned already in Subsection 2.2 the most accurate method for the estimation of coincident flooding is by using an optimal combination of various methods and incorporating an estimate of dependence "chi" (denoted as χ). Examples of estimating joint probabilities by utilising the dependence measure χ exist (for instance, Svensson and Jones, 2000 & 2004a) although they mainly focused on the assessment and calculation of an accurate value of χ rather than how to use dependence (χ) in the final stage of a joint probability assessment. It is interesting to point out that Svensson and Jones (2002) document in their work the position(s) of simultaneously extreme river discharge and storm surges values. The estimation of the actual water levels by considering the variable of astronomical tide as well (in a trivariate exercise) was not analysed. Furthermore, no analysis was made concerning time lag periods between storm surges and extreme river discharges. Such analysis would be an attempt to model the catchment processes and associated spatial and temporal time lag periods between the river discharge and sea level values.

A method for the interpretation of the dependence (chi) proposed by Svensson and Jones (2000) using daily and annual return periods is contained in Equation 2.4.1. It involves an expression for the probability of non-exceedance of a critical threshold (u) by two source (flood components) variables U and V with identical probabilities of non-exceedance and dependence chi (χ). Equations 2.4.1 to 2.4.10 follow closely the methodology of Svensson and Jones (2000) as applied in AR & R Project 18 (2009):

$$P(U \leq u, V \leq u) = P(U \leq u)^{2-\chi}$$	(2.4.1)

Considering identical probabilities of non-exceedance and dependence chi (χ),

$$P(U \leq u) = P(V \leq u)$$	(2.4.2)

it becomes handy if in Equation 2.4.2 the probability of non-exceedance of the threshold (u) could be expressed in terms of a return period T for identical probabilities, thus:

$$P(U \leq u) = P(V \leq u) = 1 - \frac{1}{T}$$	(2.4.3)

So, if period T is known, the marginal probability of exceedance could then be expressed as:

$$P(U > u) = P(V > u) = \frac{1}{T}$$	(2.4.4)

Considering the probability of exceeding the selected extreme threshold (u) by both sources variables with identical probabilities, a rearrangement could be applied in terms of the identical return period **T** and dependence (χ) as follows:

$$P(U > u, V > u) = 1 - 2P(U \leq u) + P(U \leq u, V \leq u)$$	(2.4.5)

$$= 1 - 2\left(1 - \frac{1}{T}\right) + \left(1 - \frac{1}{T}\right)^{2-\chi}$$	(2.4.6)

$$= \left(1 - \frac{1}{T}\right)^{2-\chi} + \frac{2}{T} - 1$$	(2.4.7)

From Equation 2.4.7 it is possible to derive an expression for the joint return period $\mathbf{T_{X,Y}}$ of two variables (X, Y). Both source variables are considered of having uniform marginal distributions and an estimated dependence measure χ while exceeding an identical threshold u with identical return periods. Then the joint return period $\mathbf{T_{X,Y}}$ is given by Equation 2.4.8:

$$T_{X,Y} = \frac{1}{\left(1 - \frac{1}{T}\right)^{2-\chi} + \frac{2}{T} - 1}$$	(2.4.8)

Svensson and Jones (2000) performed a number of inter-comparisons referring to a wide range of dependence values between 0 and 1 against predefined return periods. It was found that the consideration of a dependence measuring into joint probability calculations had a significant impact on the resultant joint return period when compared to results based on the assumption of total independence. Results were profound for both day- and year-periods. It became obvious that neglecting dependence in a joint probability assessment exercise would likely result in an underestimation of maximum water levels for a given frequency. Surprisingly, even if the assessment of dependence for estimating joint probabilities had proved being so robust, no further analysis was undertaken to explore the suitability of this application on source variables with non-identical return periods. So, it appears that such an approach would be limited to variables with similar marginal distributions and identical return periods.

Furthermore, focusing over different parts of a coastal or riverine area of interest seems logical to assume that the water level in a riverine area will be most probably influenced to varying degrees by combined source variables (sea level and river discharge for instance). Consequently, the estimated (single value) joint return period of a combined event should not be considered as an indication of the true return period of the water level as pointed out by Svensson and Jones (2000).

In such a case, a structure function approach for the estimation of intermediate water levels is recommended. Such structure function should contain a detailed description of how the source variables could combine to influence the critical output variable. On the same subject, both Hawkes (2004) and Meadowcroft et al. (2004) managed to use a rather simplistic joint variable exceedance method that was involving a set of dependence correlation factors including dependence (χ). It is important here to stress that in order to obtain the joint return period $\mathbf{T_{X,Y}}$ (of cases exceeding the critical / extreme threshold u) of source variables (X & Y) with an identical (common) return period of **T** and dependence value of (χ), $\mathbf{T_{X,Y}}$ could be (logically) expressed by Equation 2.4.9:

$$T_{X,Y} = \frac{T}{\chi}$$	(2.4.9)

The estimation of joint return period utilising Equation 2.4.9 is based on the assumption that marginal distributions of source variables should be identical and no further transformation is required. Such an assumption constitutes a clear limitation of the approach (as explained above). To overcome this, Hawkes (2004) developed an approach based on a spreadsheet as part of the SA (Simplified Approach) methodology for the R&D (Defra Institution, UK) Project of joint probability. Based on such spreadsheet values it was possible to generate graphical curves of joint exceedance taking into account predetermined values of chi (χ). These curves were relating to four levels of correlation (low, moderate, high and super) between the source variable pairs. Applying this methodology, it became clear that in many cases, the return periods of two source variables were not always identical.

Finally, the limitation posed by Svensson and Jones (2000) was overcome by derivations of both Hawkes (2004) and Meadowcroft et al. (2004) as mentioned above in their effort to obtain the joint probability $\mathbf{T_{X,Y}}$ of threshold levels $\mathbf{(x^*, y^*)}$ corresponding to threshold u, with non-identical return periods (T_X , T_Y) for source variables (X, Y) and dependence measure chi (χ), making use of the average of T_X and T_Y, as expressed in:

$$T_{X,Y} = \sqrt{\frac{T_x \, . \, T_y}{\chi^2}} \qquad (2.4.10)$$

In Equation 2.4.10 it is assumed that return periods of source variables are not required to be identical for the estimation of the joint return period. The assumption of the existence of many forms of combined probabilities that correspond to the same joint return period (when using non-identical return periods) was made by Hawkes (2004). In his examples, if someone would consider a 1:100-year joint return period, this could be the outcome of event combinations such as a 1:10 and 1:10, 1:20 and 1:5, 1:50 and 1:2, 1:100 and 1:1 concerning the return periods of source variables). Hawkes (2004) also had mentioned that this joint return period approach of non-identical return periods approach (as defined by Equation 2.4.10) might lead to an underestimation of the magnitude for a given joint return period, and recommended that a factor of around 2 may be required for the adaptation of dependence (χ) but this is still open for investigation. In the current Report the somehow "conservative" factor of one (1) has been utilised as in most studies related to statistical dependence estimation so far.

How to estimate statistical dependence (hands on coding main components of dependence equations)

In this Report, the dependence (χ) is estimated by techniques documented by Svensson and Jones (2000) but being adapted by suggestions form Hawkes (2004) resulting to Equation 2.4.11.

$$\chi(u) = 2 - \frac{ln\, P(U \leq u, V \leq u)}{ln\, P(U \leq u)} \qquad (2.4.11)$$

The terms of Equation 2.4.11 are straightforward to be calculated considering a common percentile threshold ($u = x^* = y^*$) and taking into consideration that the main term of fraction's numerator can be estimated as:

$$P(U \leq u, V \leq u) = \frac{Number\ of\ (X,Y)\ such\ that\ X \leq x^*\ and\ Y \leq y^*}{Total\ number\ of\ (X,Y)} \qquad (2.4.12)$$

whereas, its denominator term is estimated as:

$$ln\, P(U \leq u) = \frac{1}{2}\, ln[\, \frac{Number\ of\ X \leq\ x^*}{Total\ number\ of\ X} * \frac{Number\ of\ Y \leq\ y^*}{Total\ number\ of\ Y}\,] \qquad (2.4.13)$$

In the current Report, MATLAB (matlab) routines were coded following closely Equations 2.4.11 to 2.4.13. Details of additional modules and routines (also utilised for estimating dependence terms and parameters) based on the integrated statistical package R are given in Table 2.2. Complimentary (matlab & R) routines were also coded and compiled referring to techniques and methodologies found in Coles (2001). Emphasis was given to "taildep" routine of the module "extRemes" of the package R that is capable of estimating dependence values when a critical percentile (extreme) threshold is considered. Another "powerful" routine capable of providing dependence graphs & plots as well (besides single values of χ) was the 'chiplot' routine of the module "evd" of R. Routine "chiplot" is also capable of providing and plotting confidence intervals of selected levels. The routine "retlevel.gev" of the R module MCMC4-Extremes (referring to Monte Carlo simulations) was also used in sensitivity estimations of dependence (χ).

Table 2.2. Statistical modules & routines used for the estimation of dependence.

mat_chi	*MATLAB routines estimating dependence values based on the application of equations 2.4.11 to 2.4.13 utilising the POT (Peaks-Over-Threshold) methodology as described in Hawkes and Svensson (2003).*
mat_chi_lag	*As in mat_chi routines but also capable to estimate lag dependencies besides identifying the leading source variable(s).*
taildep routine of module extRemes (R)	*Function to calculate the estimated tail dependence parameters chi (χ) and "chibar". Values of dependence chi (χ) provide a measure summarizing the strength of dependence within the class of asymptotically dependent variables, whereas chibar values provide a corresponding measure within the class of asymptotically independent variables.*
chiplot routine of evd module (R)	*Routines of evd (Extreme Value Distributions) extends simulation, distribution, quantile and density functions to univariate and multivariate parametric extreme value distributions, and provides fitting functions which calculate maximum likelihood estimates for univariate and bivariate maxima models & for univariate and bivariate threshold models.*
retlevel.gev routine of MCMC4-Extremes module (R)	*MCMC4Extremes module provides some function to perform posterior estimation for some distribution, with emphasis to extreme value distributions. It contains some extreme datasets, and functions that perform the runs of posterior points of the GPD and GEV distribution. The package calculate some important extreme measures like return level for each t periods of time, and some plots as the predictive distribution & return level plots.*

Besides applying the general POT (Peaks-Over-Threshold) methodology (described in detail by Hawkes and Svensson, 2003) and the adaption of an optimal threshold for the data values not allowing more than ~2.3 to ~2.5 events per year to exceed (as suggested by Svensson and Jones, 2005), emphasis was also given in the stability of dependence (graph) curves as pointed out by Prof. Van Gelder of Delft University (personal communication, 2016).

This stability issue is considered important when a relatively small amount of observation values (combined extreme events in this case) is considered resulting to a graph containing intense fluctuating features. Furthermore, small differences were found in estimates made by chiplot of evd (R), taildep of extRemes (R) and mat_chi & mat_chi_lag (matlab) most probably due to the specific criteria being imposed on both mat_chi & mat_chi_lag routines concerning the selection of POT extremes.

In order to satisfy the criterion for the statistical independence between successive extreme events, a separation interval of 3 days is considered in this study, as in Svensson and Jones (2004a). Figure 2.1 presents an example of the declustering algorithm, where the extreme events of points 471 (5 January 2012) and 472 (6 January 2012) are considered as part of the same storm event, so, the extreme corresponding to 472 point is neglected from the POT extreme value analysis.

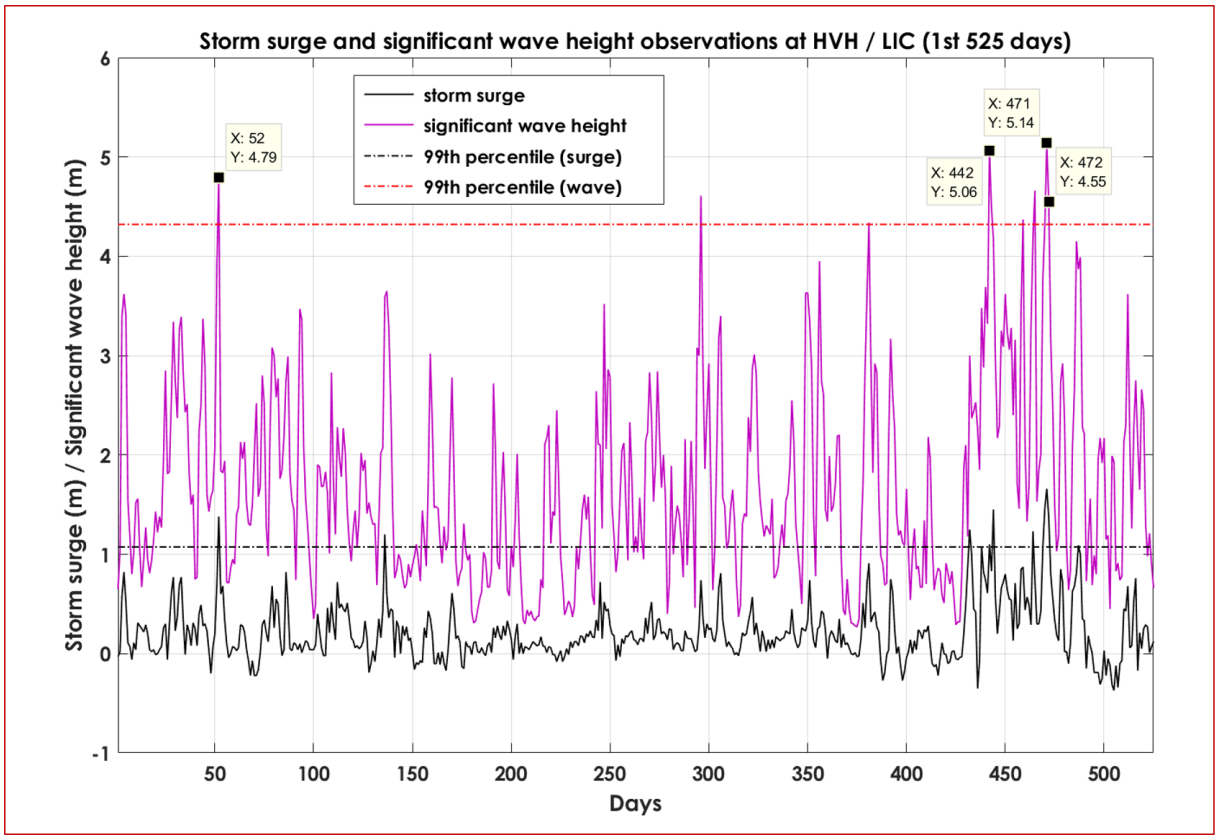

Figure 2.1. Storm surge and significant wave height time series of observations at HVH / LIC.

This latter imposed (declustering) criterion imposed by both mat_chi & mat_chi_lag routines, is an additional criterion to the one referring to the maximum yearly number of compound events (not to become higher than ~2.3 to ~2.5). Such declustering approach takes into account that extremes must not occur on consecutive days, but to be separated by at least 3 days, being in harmony with methodologies and techniques documented by Svensson and Jones (2004a). Lastly, an example is given below displaying how dependence modulates joint return periods and consequently joint probability values (Table 2.3).

Table 2.3. Example of utilising dependence to estimate joint return periods.

	100 RP (surge)	*100 RP (wave)*	*chi*	*JRP*
Hindcast total surge / wave	*1.78*	*6.05*	*0.57*	*174.53*

By considering a set of total hindcast series of surge and significant wave height (valid for the RIEN of river Rhine) and utilising the matlab function "gevfit" an estimation of the return levels having a 100-year return period for both surge and wave height variables can be retrieved (1.78 and 6.05 meters respectively). By inserting their chi (χ) value (0.57) in the formula 2.4.10, the joint return period (JRP) of this extreme combined event is estimated to 174.95 years. This JRP value (174.95 years) is significantly different than the value of 10,000 years that represents the estimated JRP in case that surge and waves were considered to be independent (since in a case like this, the dependence (χ) should had been considered equal to zero).

By considering total independence between surge and wave, the (joint) probability of the combined event (of surge = 1.78 and wave height = 6.05) to be equal or to be exceeded at any of the 100 years will be equal to 0.0001, whereas in the (real) case of an existing dependence (0.57), the appropriate joint probability value should be equal to 0.0057 (i.e., 57 times higher).

3. Data and methodology

In a multivariate statistical analysis, the estimation of dependence seems to be the most important aspect for assessing joint probabilities among variables. In the current study such an analysis is referring to the combinations of two applied on the three primary variables examined here (i.e., storm surge, significant wave height and river flow discharge).

A thorough estimation of the design conditions at the coastal zone would require to include the wave period analysis and/or the contribution of the wind and wave set-up at the total water level, but this analysis is beyond the scope of this study. In terms of the required duration of time series for a proper joint probability analysis, earlier studies (Hawkes, 2005, Hawkes and Svensson, 2005) tend to indicate that at least five years of simultaneous data for all the relevant input variables are required

In statistical analysis it is often more efficient to work in terms of the original variables, even if there are different types, as this retains the greatest knowledge of the problem, and later to convert to end products such as the overall induced water level. This can be harder to do, and provides more scope for errors in interpretation, but offers the possibility of greater insight into the problem and more faith in the extrapolations.

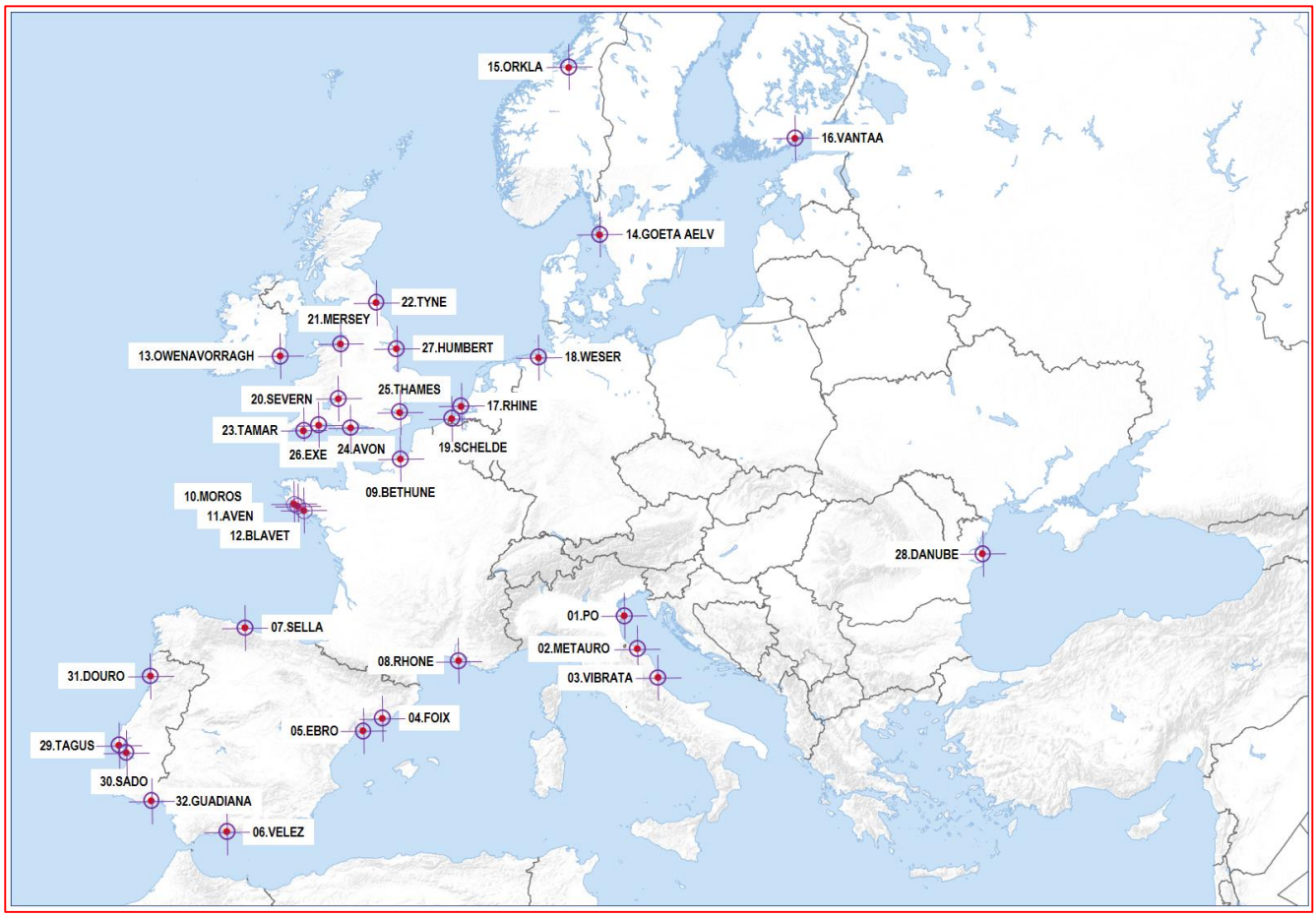

Figure 3.1. Positions of the 32 RIEN points used in the study.

The current analysis is focusing over 32 river ending points that have been selected to cover a variety of coastal environments found in European sea areas. These points were selected mainly to their proximity to tide gauge recorders although not many observations were found suitable to be exploited mainly due to the lack of corresponding wave and river discharge observations. The sea areas used in the study refer to Mediterranean Sea (central and north Adriatic Sea, Balearic Sea, Alboran Sea and Gulf of Lion), Bay of Biscay, English Channel, Irish Sea, North Sea, Black Sea and North-eastern Atlantic Ocean.

A map containing the position of the RIEN (RIver ENding) points used in the study is shown in Figure 3.1. Additional details can be found in Table 3.1 that contains both the name of rivers & RIEN points and their exact location (lat, lon). Arrows used in Table 3.1 denote the merging of the rivers involved.

Table 3.1. List of the River Ending (RIEN) points.

	River	River Ending point (RIEN)	Lat	Lon
1	Po (IT)	Po Della Pila	44.96	12.49
2	Metauro (IT)	Madonna Del Ponte	43.83	13.05
3	Vibrata (IT)	Martinsicuro	42.84	13.93
4	Foix (ES)	El Foix	41.20	1.67
5	Ebro (ES)	Illa de Buda	40.71	0.89
6	Salia / Velez (ES)	Rio De Velez	36.72	-4.11
7	Sella (ES)	Punta Del Arenal	43.47	-5.07
8	Saona → Rhone (FR)	Aries	43.34	4.84
9	Bethune (FR)	Dieppe	49.91	1.09
10	Moros (FR)	Concarneau	47.86	-3.92
11	Aven (FR)	Riviere De Belon	47.81	-3.72
12	Blavet (FR)	Larmor-Plage	47.71	-3.38
13	Owenavorragh (IE)	Muir Eireann	52.65	-6.22
14	Goeta Aelv (SE)	Kattegat	57.77	11.76
15	Orkla (NO)	Trondheimsfjord	63.32	9.82
16	Vantaa (FI)	Vanhankaupunginselka	60.24	24.99
17	Maas <--> Rhine (NL)	Rockanje	51.87	4.01
18	Weser (DE)	Wurster Arm	53.65	8.14
19	Schelde (BE)	Western Scheldt	51.43	3.55
20	Severn (UK)	Severn Bridge	51.61	-2.65
21	Mersey (UK)	Wallasey	53.44	-3.04
22	Tyne (UK)	South Tynesid	55.01	-1.43
23	Tamar (UK)	Fort Picklecombe	50.34	-4.17
24	Avon (UK)	Christchurch District	50.72	-1.74
25	Thames (UK)	Sheerness	51.45	0.74
26	Exe (UK)	Exmouth	50.62	-3.42
27	Trent → Humber (UK) Ouse → Humber (UK)	Spurm Point	53.57	0.11
28	Danube (RO)	Musura Bay	45.22	29.73
29	Tagus (PT)	Carcavelos	38.69	-9.26
30	Sado (PT)	Setubal	38.53	-8.89
31	Douro (PT)	Matosinhos	41.18	-8.71
32	Guadiana (ES)	San Bruno	37.18	-7.39

In a rich data analysis environment, the variable to be simulated more accurately as possible is the maximum overall water level at particular locations of an estuary or riverine area. If there happens to be a water surface elevation gauge in the vicinity it may be possible to work directly from its measurements. Otherwise, it is necessary to estimate the increase in water level at particular points induced by a series of other variables such as sea levels, river flows and waves, possibly measured or synthesised at other locations.

Another option is by utilising models since the data need not be particularly close to the site of application, but should be such that site conditions can be inferred using modelling techniques and the degree of correlation with other variables is well represented.

In the current analysis, water level data coinciding with wave and river discharge observations directly at the exact sites of interest (river ending points) were not available with the exception of RIEN point of river Rhine (NL). For this RIEN concurrent observations (with no gaps) of sea level, astronomical tide, storm surge, wave and river discharge were available for a period of about 4.5 years. It is important to understand that a full set of observation data are needed over a relatively long time period (at least five years) for all primary variables of this study (storm surge, river discharge and wave height) that need to be analysed, as presented in full details in Hawkes (2005).

Nevertheless, due to the lack of longer time concurrent observations, lesser duration data were used for the validation of hindcasts over Rhine RIEN point. Furthermore, in the absence of widespread coincident long-term measurements of storm surge, wave height and river discharge, a decision was made to utilise the methodology of simulating data observations by modelling resulting to a set of long series data (hindcasts). Three types of simulation data were considered in this study (and being analysed in detail):

- *Storm surge hindcasts*
- *Wave height hindcasts*
- *River discharge hindcasts*

The exact type and period of simulations (hindcasts) is shown in Table 3.2. The wave records (shaded in light blue) consist of significant wave height (HS) in metres with centimetre resolution, maximum wave height (Max) in meters with centimetre resolution, mean wave direction (Direction) in degrees North with one-degree resolution and mean wave period (Period) in seconds, with tenths resolution. Storm surge values (light yellow) are in meters while river discharge values (light green) are given in m**3/s.

Table 3.2. Duration of simulations (Hindcasts).

Variables	*Start*	*End*	*No. of days*
Storm Surge	*1 Jan 1980*	*31 Dec 2014*	*12,784*
Waves – HS	*1 Jan 1979*	*31 Dec 2014*	*13,149*
Waves – Max	*1 Jan 1979*	*31 Dec 2014*	*13,149*
Waves – Direction	*1 Jan 1979*	*31 Dec 2014*	*13,149*
Waves – Period	*1 Jan 1979*	*31 Dec 2014*	*13,149*
River Discharge	*1 Jan 1990*	*9 Oct 2013*	*8,683*

At this point it should be noted that both surge and wave hindcasts were obtained by utilising input parameters (forcing terms) from ERA-Interim reanalysis data set of ECMWF (Dee et al., 2011). ERA-Interim is a global atmospheric reanalysis from 1979 to present. It is produced with a 2006 version of the IFS (Cy31r2) and continues to be updated in real time.

ERA-Interim main products include global atmospheric and surface parameters from 1 January 1979 to present, at T255 spectral resolution (~75 km) on 60 vertical levels. The time discretization corresponds to 6-hourly atmospheric fields on model levels, pressure levels, potential temperature and potential vorticity. For surface parameters 3-hourly fields and daily vertical integrals are available. Monthly averages of daily means and synoptic monthly averages at 00 UTC, 06 UTC, 12 UTC, 18 UTC have also been produced and archived. Furthermore, for the reference climatology used in the Global Flood Awareness System (GloFAS) –a potential component of CAR prototype project – the ERA-Interim precipitation dataset has been bias-corrected utilising the Global Precipitation Climatology Project (GPCP, http://precip.gsfc.nasa.gov/).

3.1 Construction of hindcasts

In the current analysis, storm surge, wave height and river discharge hindcasts were obtained for the RIEN points of interest. The exact positions of RIEN (lat / lon) and their closest model grid points, (slat / slon) for surge, (wlat / wlon) for wave height and (rlat / rlon) for river discharges are shown in Table 3.3.

Table 3.3. Positions of RIEN points Vs model grid points used for hindcasts.

	River	lat	lon	slat	slon	wlat	wlon	rlat	rlon
1	Po (IT)	44.96	12.49	45.10	12.50	44.96	12.75	44.96	12.49
2	Metauro (IT)	43.83	13.05	43.90	13.10	44.01	13.05	43.83	13.05
3	Vibrata (IT)	42.84	13.93	42.90	14.10	42.84	14.34	42.84	13.93
4	Foix (ES)	41.20	1.67	40.90	1.50	40.99	1.67	41.20	1.67
5	Ebro (ES)	40.71	0.89	40.70	1.10	40.71	1.01	40.71	0.89
6	Salia / Velez (ES)	36.72	-4.11	36.70	-3.90	36.72	-4.00	36.72	-4.11
7	Sella (ES)	43.47	-5.07	43.30	-5.10	43.60	-4.99	43.47	-5.07
8	Saona → Rhone (FR)	43.34	4.84	43.10	4.70	43.24	4.84	43.34	4.84
9	Bethune (FR)	49.91	1.09	50.10	1.10	50.01	1.09	49.91	1.09
10	Moros (FR)	47.86	-3.92	47.50	-4.30	47.74	-3.92	47.86	-3.92
11	Aven (FR)	47.81	-3.72	47.50	-3.50	47.74	-3.72	47.81	-3.72
12	Blavet (FR)	47.71	-3.38	47.50	-3.50	47.65	-3.38	47.71	-3.83
13	Owenavorragh (IE)	52.65	-6.22	52.70	-5.90	52.65	-6.21	52.65	-6.22
14	Goeta Aelv (SE)	57.77	11.76	57.50	11.30	57.70	11.70	57.77	11.76
15	Orkla (NO)	63.32	9.82	64.30	9.50	63.75	9.75	63.32	9.82
16	Vantaa (FI)	60.24	24.99	59.90	25.10	60.00	25.00	60.24	24.99
17	Maas <--> Rhine (NL)	51.87	4.01	52.10	3.90	52.01	4.00	51.87	4.01
18	Weser (DE)	53.65	8.14	53.90	7.90	53.76	8.14	53.65	8.14
19	Schelde (BE)	51.43	3.55	51.70	3.30	51.51	3.55	51.43	3.55
20	Severn (UK)	51.61	-2.65	50.30	-2.70	51.25	-3.25	51.61	-2.65
21	Mersey (UK)	53.44	-3.04	53.70	-3.30	53.51	-3.37	53.44	-3.04
22	Tyne (UK)	55.01	-1.43	55.10	-1.10	55.01	-1.28	55.01	-1.43
23	Tamar (UK)	50.34	-4.17	50.10	-4.30	50.24	-4.17	50.34	-4.17
24	Avon (UK)	50.72	-1.74	50.30	-1.90	50.49	-1.74	50.72	-1.74
25	Thames (UK)	51.45	0.74	51.50	1.30	51.50	1.00	51.45	0.74
26	Exe (UK)	50.62	-3.42	50.30	-3.30	50.49	-3.42	50.62	-3.42
27	Trent → Humber (UK) Ouse → Humber (UK)	53.57	0.11	53.90	0.30	53.60	0.43	53.57	0.11
28	Danube (RO)	45.22	29.73	44.70	29.70	45.20	29.82	45.20	29.29
29	Tagus (PT)	38.69	-9.26	38.70	-9.10	38.90	-9.34	38.69	-9.34
30	Sado (PT)	38.53	-8.89	38.10	-9.30	38.25	-9.00	38.53	-8.89
31	Douro (PT)	41.18	-8.71	41.10	-8.70	41.18	-8.81	41.18	-8.71
32	Guadiana (ES)	37.18	-7.39	36.90	-7.70	36.99	-7.39	37.18	-7.39

a. Hindcasts of storm surge

The Delft3D-Flow hydrodynamic module of the open source model Delft3D (Deltares, 2014) has been utilised to estimate storm surge time-series due to the combined effect of the wind and the atmospheric pressure gradient. The model has been used successfully in similar applications in the past (Sembiring et al., 2015). The model module set-up that was adopted solves the 2-D non-linear shallow water equations on a staggered Arakawa C-grid, according to an implicit finite difference approximation on a vertical sigma-coordinate system. Details of the model setup are contained in Table 3.4.

Table 3.4. Details of Delft3D model setup.

Model setup	*Characteristics*
Storm surge model	Delft3D version 5.01.00.4018
Processes simulated	Wind/pressure-driven ocean circulation
Grid	Regular, 0.2° (40° W-47° E; 26° N-73° N)
Atmospheric forcing	ERA-INTERIM (simulation)

Long term storm surge level time series for the RIEN points have been obtained from a 35-year hindcast set (Vousdoukas et al., 2016) This set was obtained by the Deflt3D-Flow hydrodynamic module (of Delft3D model) being forced by the 6-hourly wind and pressure fields from the ERA-Interim reanalysis (Dee et al. 2011). The storm surge levels span from 1/1/1980 to 31/12/2014, with a time interval of three hours and spatial resolution of 25 km along the European coastline and the NE Atlantic Ocean.

Furthermore, the hindcast storm surge levels have been validated with measurements from 110 tide gauges from the JRC Sea Level Database (http://webcritech.jrc.ec.europa.eu/SeaLevelsDb). The relative RMS error for more than 105 stations was less than 20% and for more than 60 stations less than 15%. Although in some cases the extreme storm surge levels were underestimated, the overall model performance is considered satisfactory.

For a successful historical reconstruction of storm surge datasets, ERA-Interim reanalysis represents a valuable source of meteorological forcing terms, but due to its limitation in terms of spatial and temporal resolution, higher resolution forcing terms have to be considered for finer (resolution) fields. This can be achieved utilising the dynamical downscaling approach, as in the current case, by utilizing the Delft3D-Flow model in a resolution considerably higher than ERA-Interim's one.

For each RIEN point, 3-hourly hindcast storm surge data time series for the period of 1 January 1980 to 31 December 2014 were obtained (over 12,784 days) by considering the closest model grid (sea) point, with no missing records. The exact position of the 32 grid points relative to 32 (RIEN) locations is given in Table 3.3. Columns shaded in light orange correspond to lat / lon of RIEN points whereas columns shaded in light yellow (wlat / wlon) contain the grid points of Delft3D model closest to RIEN locations. The resulted 102,272 records refer to 3-hourly storm surge hindcast values.

b. Hindcasts of wave height

In assessing extreme wave heights in an estuary or river ending area it is probable that some wave energy from the open sea will propagate into the estuary. Waves generated by local winds will combine with the externally generated waves to give overall wave conditions. Wave conditions are not often measured in estuaries or riverine areas and even where they are they may be representative of only one location. Other standard sources of wave data, i.e. satellites, ships and large scale meteorological models are also unlikely to be available in estuaries or riverine areas. In the absence of widespread long-term wave measurements,

global fields of one-hourly wave data were assembled by utilizing an hindcast produced with the latest stand-alone version of ECWAM wave model (Bidlot et al., 2006 / Bidlot, 2012 / ECMWF, 2015).

The ECWAM model was run on a 0.25 degrees irregular lat-lon global grid (~28 x 28 km) with fixed water depth (mean bathymetry) (i.e. no surge or tides). Note that for particular individual locations, the model may not represent the best source of wave data, but it does offer consistent coverage over the whole study area with an acceptable degree of accuracy. In simple words, even in the case that model resolution does not seem capable of simulating local topographical details, the main characteristics of the large-scale wave evolution are expected to be captured. Note that the wave hindcast was not originally designed with this study in mind, hence the relatively coarse resolution, albeit global (it was ran as part of the preparation for ERA5, the next global reanalysis from ECMWF).

For each RIEN point, hindcast wave data time series for the period of 1 January 1979 to 31 December 2014 were constructed (13,149 days) by considering the closest model grid (sea) point, with no missing records. The exact position of the 32 grid points relative to 32 (RIEN) locations is given in Table 3.3. Columns shaded in light orange correspond to lat & lon of RIEN points whereas columns shaded in light blue (wlat / wlon) refer to the grid points of WAV model being closest to RIEN locations. The resulted 315,576 records consist of significant & estimate of the individual maximum wave height, mean wave period and mean wave direction. Wind fields used (as forcing terms) for the ECWAM model were extracted from the ERA-Interim reanalysis. The ECWAM model had been configured in its CY41R1 parametrization cycle (employing 30 frequencies and 36 directions for the wave spectra). Once more, the overall conclusion has been that for a successful historical reconstruction of wave heights, it is advisable to follow a dynamical downscaling approach, as it has performed here, by utilizing ECWAV model in a resolution substantially higher than ERA-Interim's.

c. Hindcasts of river discharge

For the construction of river discharge hindcasts the LISFLOOD model was employed. The LISFLOOD model is a hydrological rainfall-runoff model that is capable of simulating the hydrological processes that occur in a catchment. LISFLOOD has been developed by the floods group of the Natural Hazards Project of the Joint Research Centre (JRC) of the European Commission. The specific development objective was to produce a tool that can be used in large and trans-national catchments for a variety of applications, including flood forecasting, capable of assessing the effects of river regulation measures, the effects of land-use change and the effects of climate change.

The LISFLOOD model (De Roo et al., 2003) is implemented in the PCRaster Environmental Modelling Language Version 3.0.0 (Wesseling et al., 1996), wrapped in a Python based interface. PCRaster is a raster GIS environment that has its own high-level computer language, which allows the construction of iterative spatio-temporal environmental models. The Python wrapper of LISFLOOD enables the user to control the model inputs and outputs and the selection of the model modules. Such an approach combines the power, relative simplicity and maintainability of code (PCRaster) and the flexibility of Python. LISFLOOD runs on any operating system for which Python and PCRaster are available.

The LISFLOOD model can run using any desired time interval, on any grid size. The model is typically run using a daily time interval to simulate the long-term catchment water balance, whereas smaller intervals (e.g. hourly) are better suited for modelling individual flood events. Both (intervals) can be combined as well. For instance, the state variables at the end of a (daily) water balance run can be used to provide the initial conditions for an (hourly) flood run. The model does not impose any limitations on the grid resolution that is used. However, its separation between runoff-generating and channel routing processes would be poorly represented at very low pixel resolutions. Since LISFLOOD has been primarily developed for the simulation of large river basins, small-scale processes are often simulated in a simplified way. Because of this, there would

be little benefit in using very high resolutions either. Most current applications of the model have employed grid resolutions of 1 or 5 km.

The LISFLOOD model is currently running within the European Flood Awareness System (EFAS) on an operational basis covering the whole of Europe on a 5 km grid. In the context of global flood modelling, the transformation from precipitation to surface and sub-surface runoff is done by HTESSEL (Balsamo et al., 2009). For routing, LISFLOOD global is set up to simulate the groundwater and routing processes. Surface runoff is routed via overland flow to the outlet of each cell. Subsurface storage and transport are modelled using two linear reservoirs. For each RIEN point, discharge hindcast series for the period of 1 January 1990 to 9 October 2013 were constructed (8,683 days) by considering the closest model grid (sea) point, with no missing records. The exact position of the 32 grid points relative to 32 (RIEN) locations is given in Table 3.3. Columns shaded in light orange (reference points) correspond to lat / lon of RIEN points whereas columns shaded in light green (dlat / dlon) contain the grid points of LISFLOOD model being closest to RIEN locations. The resulted 8,683 records comprise a time series of daily river discharge values.

3.2 Validation of hindcasts

For validation (over the selected RIEN point areas) and in harmony with hindcasts, three types of observation data were considered in this study:

- *Storm surge observations,*
- *Wave (significant & maximum) height observations and*
- *River discharge observations*

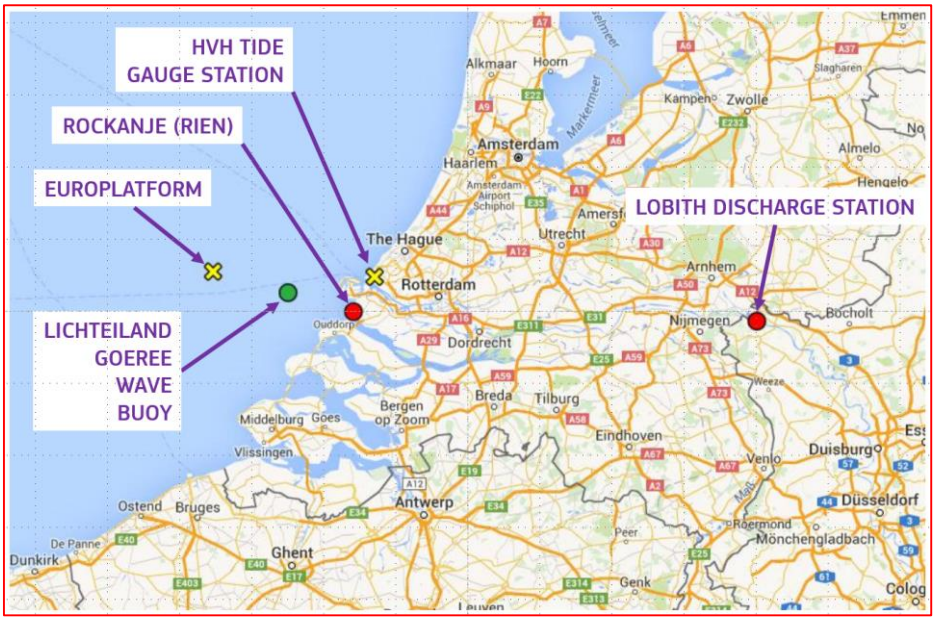

Figure 3.2. Positions of HVH tide gauge station, Rockanje RIEN, Lichteiland Goeree I wave buoy and Lobith discharge station of river Rhine (NL).

Based on these type of data, a full set of coincide observations close to the river ending (RIEN) point of river Rhine (Rockanje) was obtained from the Deltares Multifunctional Access Tool foR Operational Oceandata Services database (MATROOS) (http://noos.deltares.nl/) as shown in Table 3.5. and utilised to validate hindcasts of storm surge, significant wave height and river discharge values. For achieving this, storm surge observations were retrieved from the Hoek Van Holland (HVH) tide gauge station, whereas significant wave height observations were collected from the close by wave buoy platform of Lichteiland Goerre I (LIC).

In addition, river discharge observations were obtained from the Lobith (LOB) discharge station of Rhine river. The positions of HVH tide gauge station, Rockanje RIEN point, Lichteiland Goerre I (LIC) wave buoy and Lobith (LOB) discharge station are shown in Figure 3.2.

Table 3.5. Type and duration of HVH, LIC & LOB observations.

Variables	*Start*	*End*	*No. of days*
HVH Storm Surge	4 Apr 2010	30 Dec 2014	1,732
EUR Storm Surge	4 Apr 2010	30 Dec 2014	1,732
LIC Waves – HS	22 Sep 2010	30 Dec 2014	1,561
LIC Waves - Max	4 Apr 2010	30 Dec 2014	1,732
LOB River Discharge	4 Apr 2010	30 Dec 2014	1,732

From Table 3.5 it becomes clear that both significant and maximum wave height observations were available over Lichteiland Goerre I wave buoy platform (LIC) for time interval spanning from 1,561 to 1,732 days. For storm surge, besides HVH tide gauge station observations another set of data was available from a close by sea platform named EUROPLATFORM (EUR). A very good agreement between HVH and EUR observation values was found although a decision was made to put emphasis (selection of) on HVH platform due to its closer proximity to the RIEN point of Rockanje. It was also found that slightly higher correlation values were obtained when hindcast surge values were compared against HVH observations rather than against corresponding observations made over EUR platform.

Table 3.6. Common time intervals for hindcast and observation data sets.

Hindcasts			
Variables	*Start*	*End*	*No. of days*
Waves – HS / Storm Surge	1 Jan 1980	30 Nov 2014	12,753
Waves – HS / River Discharge	1 Jan 1990	9 Oct 2013	8,683
Storm Surge / River Discharge	1 Jan 1990	9 Oct 2013	8,683
Observations			
Variables	*Start*	*End*	*No. of days*
LIC Waves – HS / HVH Storm Surge	22 Sep 2010	30 Dec 2014	1,561
LIC Waves / LOB River Discharge	22 Sep 2010	30 Dec 2014	1,561
HVH Storm Surge / LOB River Discharge	4 Apr 2010	30 Dec 2014	1,732
Hindcasts / Observations			
Common Interval for Validation	22 Sep 2010	9 Oct 2013	1,114

The storm surge records over HVH are consisted of levels in meters (relative to Chart Datum for sea level) at hourly intervals specified to GMT with only a few missing data being flagged by error codes that were omitted during the validation assessment. It is noted that sea level is the recorded still (i.e. in the absence of waves) water level, and surge is the difference between sea level and predicted tide for that time and location. Investigating over the existence of a common (concurrent) time intervals for both hindcast and observation data sets, Table 3.6 was compiled.

A common interval of 1,114 days (from 22 September 2010 to 9 October 2013) was selected for validating all type of surge (SUR), wave (WAV) and discharge (DIS) hindcast data sets as shown in the last row of Table 3.6, highlighted by a yellow ribbon.

Both surge observations over HVH and wave observations over LIC buoy are made on an hourly basis, so, daily maximum values had to be calculated. For Lobith observation station, daily maximum river flows, generally for 00.00-24.00 GMT, were considered in harmony to surge and wave maximum daily values.

The location of Lobith station is quite far downstream without being tidally influenced while the selected common period had no missing data. Besides validating "raw" hindcasts, the main effort had been to extent such validation to both correlations but more importantly to statistical dependencies between the source variables involved in this study.

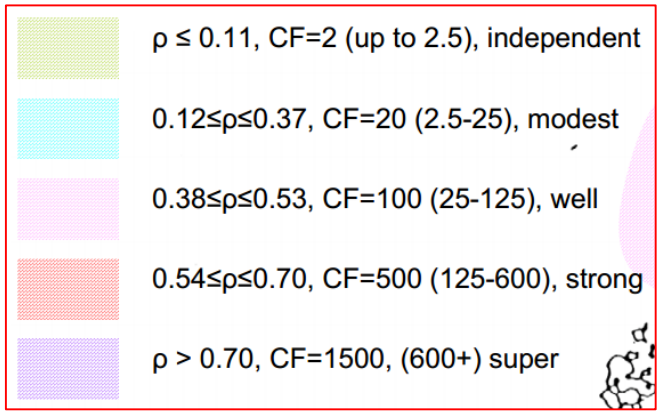

Figure 3.3. Correlation categories taken from Hawkes & Svensson (2005).

Following Hawkes and Svensson (2005) classification of correlation (as shown in Figure 3.3), Table 3.7 for correlation categories (left panel) was constructed. In the same Table (3.7) a similar classification adapted to the relatively smaller variability of dependence values (right panel) was also compiled taken into consideration similar categorisation and classification suggested by Hawkes (2005).

Table 3.7. Categories of correlation (a) & dependence (b) utilised in the current study.

	Correlation (ρ)	Category
	$\rho \le -0.06$	Negative
	$-0.05 \le \rho \le 0.05$	Zero
	$0.06 \le \rho \le 0.11$	Low
	$0.12 \le \rho \le 0.37$	Modest
	$0.38 \le \rho \le 0.53$	Well
	$0.54 \le \rho \le 0.69$	Strong
	$\rho \ge 0.70$	Very Strong

	Dependence (χ)	Category
	$\chi \le -0.06$	Negative
	$-0.05 \le \chi \le 0.05$	Zero
	$0.06 \le \chi \le 0.14$	Low
	$0.15 \le \chi \le 0.24$	Modest
	$0.25 \le \chi \le 0.34$	Well
	$0.35 \le \chi \le 0.44$	Strong
	$\chi \ge 0.45$	Very Strong

In harmony with observations, 3-hourly based storm surge and 1-hourly wave hindcasts were transformed to daily maximum hindcast values. Hindcasts of river discharges for Lobith were already referring to daily values.

a. Validation of storm surge hindcasts using Hoek Van Holland (HVH) tide gauge observations

Daily hindcast maximum levels of storm surge over Hoek Van Holland (HVH) were compared against daily maximum values of HVH tide gauge observations over the common interval of 1,114 days (see Table 3.6 for details). Storm surge levels for observations have been estimated by subtracting astronomical tide from sea level values.

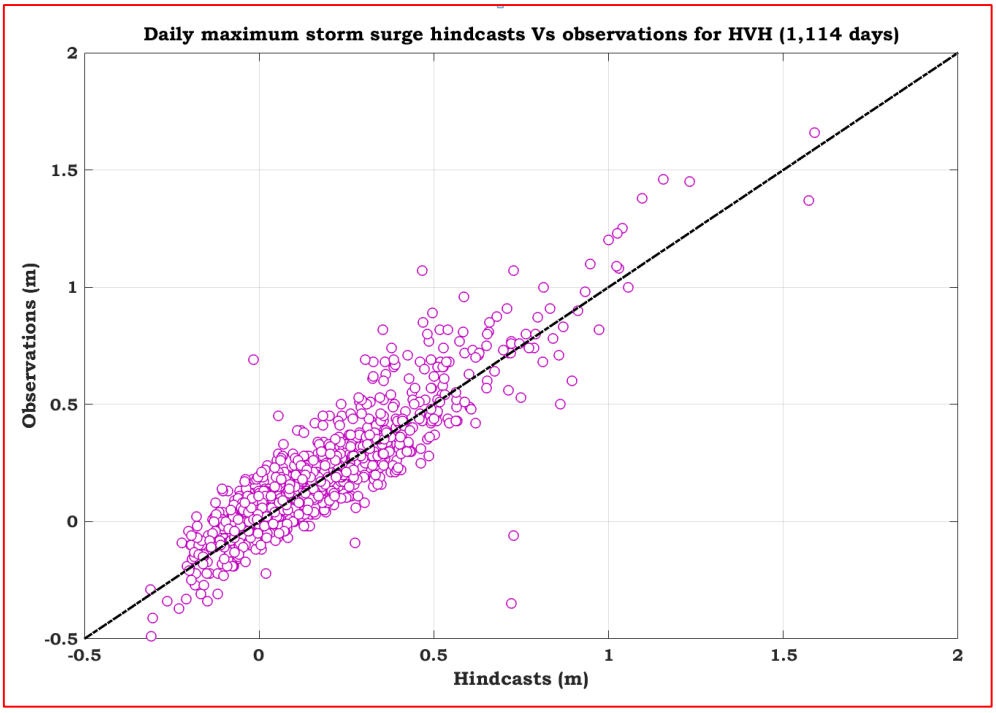

Figure 3.4. Scatterplot of storm surge hindcasts Vs observations for HVH (1,114 days).

Figure 3.4 contains the scatterplot of surge hindcasts against observations. From this scatterplot, it appears that hindcast surge values are slightly lower than their corresponding observations. This difference between observations and hindcast storm surge levels may be attributed to the (relatively low) temporal and spatial resolution of ERA-INTERIM atmospheric forcing terms.

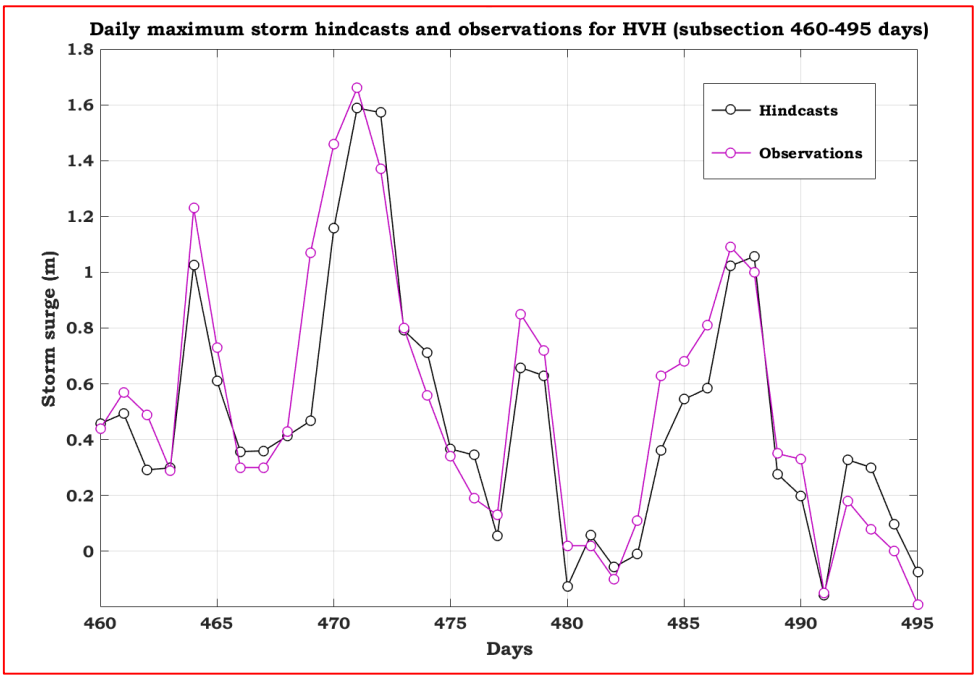

Figure 3.5. Subsection of time series for both hindcast and observation surge levels (interval of ~1 month).

Figure 3.5 contains a subsection of time series of both hindcasts and observations. From Figure 3.5 it is clear that even if the hindcast storm surge level is underestimated, the model is capable to resolve quite well the magnitude and the duration of storm events. As an example, the storm surge peak centred on day-471 (on 5 January 2012) is further investigated. This peak was found to be linked to a very intense extratropical cyclone (Ulli / Emil) affecting the greater area of North Sea. The position and details of the storm are shown on the surface weather map of 12UTC of 3 January 2012 shown in Figure 3.6 (a). The corresponding satellite picture is contained in Figure 3.6 (b).

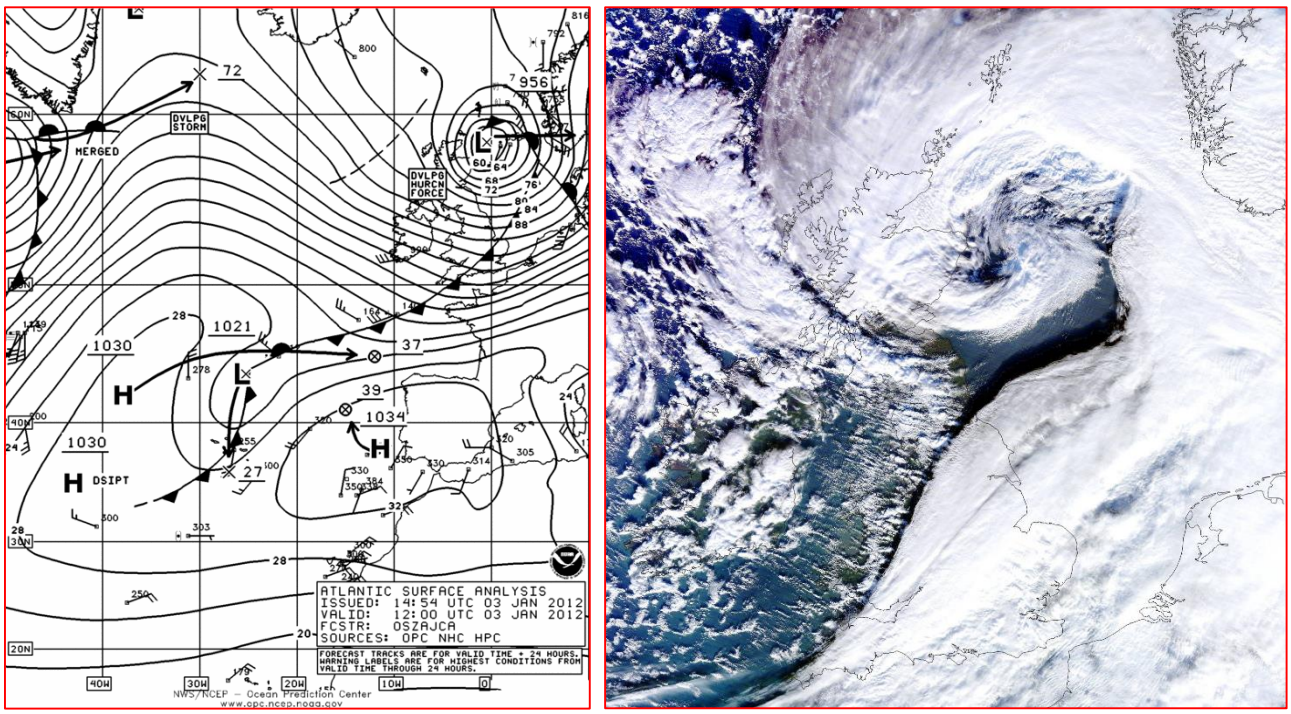

Figure 3.6. Surface weather map (a) and satellite image (b) valid for 3 January 2012 12UTC.

Studying closely both hindcast and observation values referring to Ulli storm, it seems that hindcasts could clearly resolve and identify both the phase and the magnitude of the extreme event. It is important to realise that such events are linked to intense pressure gradients as clearly seen in Figure 3.7 that prevailed during the late night hours of 5 January 2012. Besides the intensity of pressure gradients, the orientation of isobars was found to be almost vertical to the coasts of Holland (as indicated by the yellow arrow denoting the direction of isobars) that was strongly contributing to the extremity of the event.

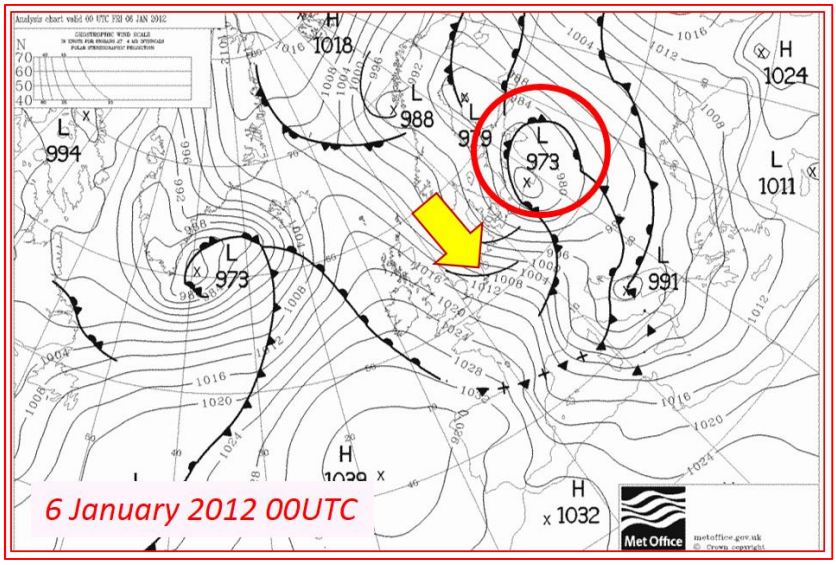

Figure 3.7. Surface weather map valid for 6 January 2012 00UTC.

Overall, storm surge hindcasts found to be somehow underestimated compared to observations as it is evident from the upper part of the diagonal line (Figure 3.4) being more populated than the lower one. This suggests a negative bias of hindcasts that has been estimated to -0.0265 meters (-2.65 cm). Nevertheless, hindcasts found to cope quite well with both the timing and magnitude of extremes. It was also found that hindcast and observation values exhibit a very strong correlation value of ~0.90.

b. Validation of significant wave height hindcasts using Lichteiland Goerre (LIC) wave buoy platform

Daily hindcast maximum values of significant wave height were compared against daily maximum values of significant wave height observations collected from the Lichteiland Goerre I (LIC) wave buoy platform (see details in the map contained in Figure 3.2).

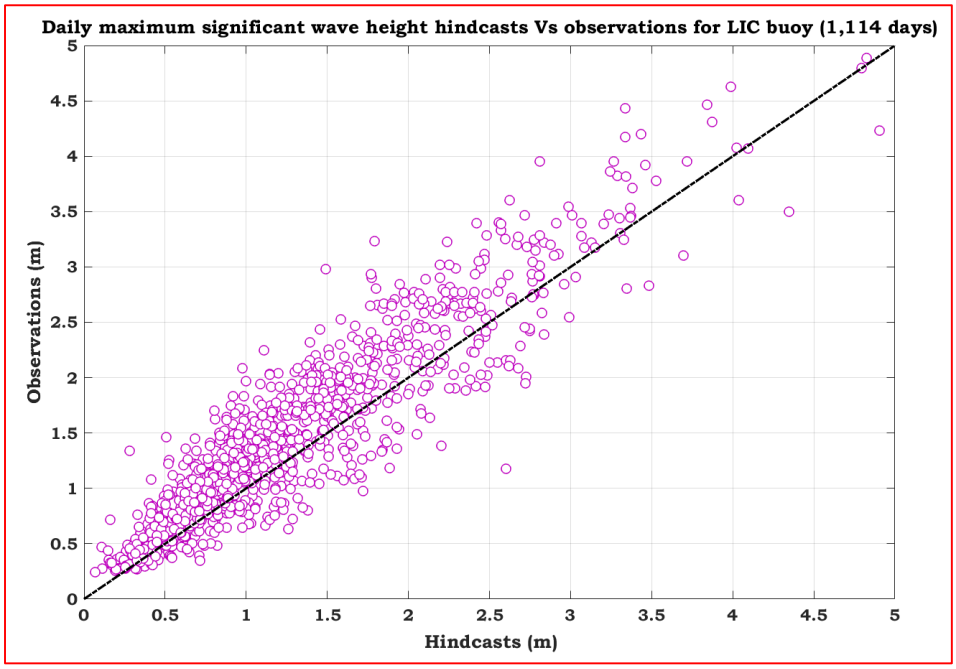

Figure 3.8. Scatterplot of significant wave height hindcasts vs observations for LIC (1,114 days).

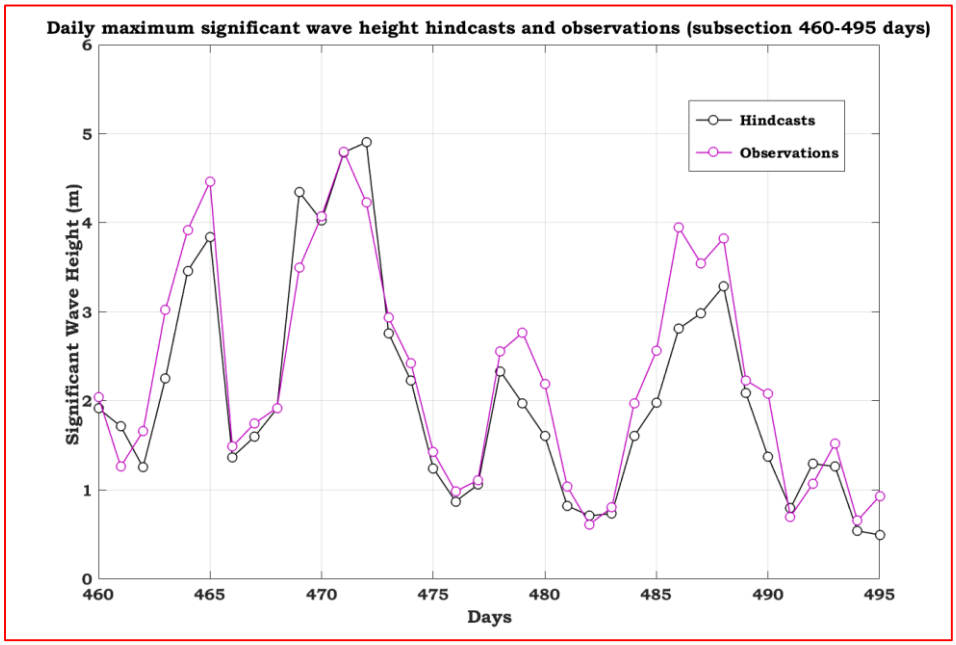

Figure 3.9. As in Figure 3.5, but for wave height hindcasts and observations.

Figure 3.8 contains the scatterplot of wave height hindcasts against observations. As in storm surge case, it appears that hindcast wave height values are slightly lower than their corresponding observations. Once more, this might be due to the smoothness of ERA-Interim reanalysis not possessing the required resolution to resolve the exact magnitude of wind and pressure fields linked to real-world wave height maxima.

The systematic bias of wave hindcasts found to be relatively small, being equal to 0.2030 meters (20.30 cm). Furthermore, wave hindcasts seem to perform quite well on how well correlate to observations since they found to exhibit a very strong correlation value of ~0.92. Such high values (of correlation) are expected to strongly contribute for achieving high values of correlation when estimating the type and magnitude of statistical dependencies between wave height and the other two variables (storm surge and river discharge).

Figure 3.9 contains a subsection of time series of both wave height hindcasts and observations. As expected (based on the scatterplot of Figure 3.8) hindcast wave values are slightly lower than their corresponding observations. An obvious explanation is the proximity of LIC buoy to the coast since WAV model puts emphasis on open seas and oceans. Another explanation could be the smoothness of ERA-Interim reanalysis fields that are used as initial and boundary terms for WAM model simulations. Such smooth fields do not possess enough resolution to resolve local (coastal) wind conditions. This fact might be the reason behind the systematic underestimation of the wave conditions by hindcasts. Utilising the example presented already in Figure 3.5, the storm surge extreme centred on day-471 found to be in absolute harmony with the wave height extreme (local maximum) observed on the same day (5 January 2012). This is also an indication that storm surge and wave extremes tend to take place in a zero-lag time mode environment.

c. Validation of river Rhine flow discharge hindcasts using Lobith discharge station

Daily hindcast mean values of river discharge were compared against daily average values of observations collected over Lobith observation station. Figure 3.10 contains the scatterplot of river discharge hindcasts against observations. Hindcasts seem to systematically underestimate observation values, as a higher number of points found to lay on the upper part than the lower one of the diagonal line. This negative bias has been estimated to 210.47 m**3 / day. Even with the presence of such negative bias, discharge hindcasts seem to perform quite well reaching to a correlation value of ~0.90.

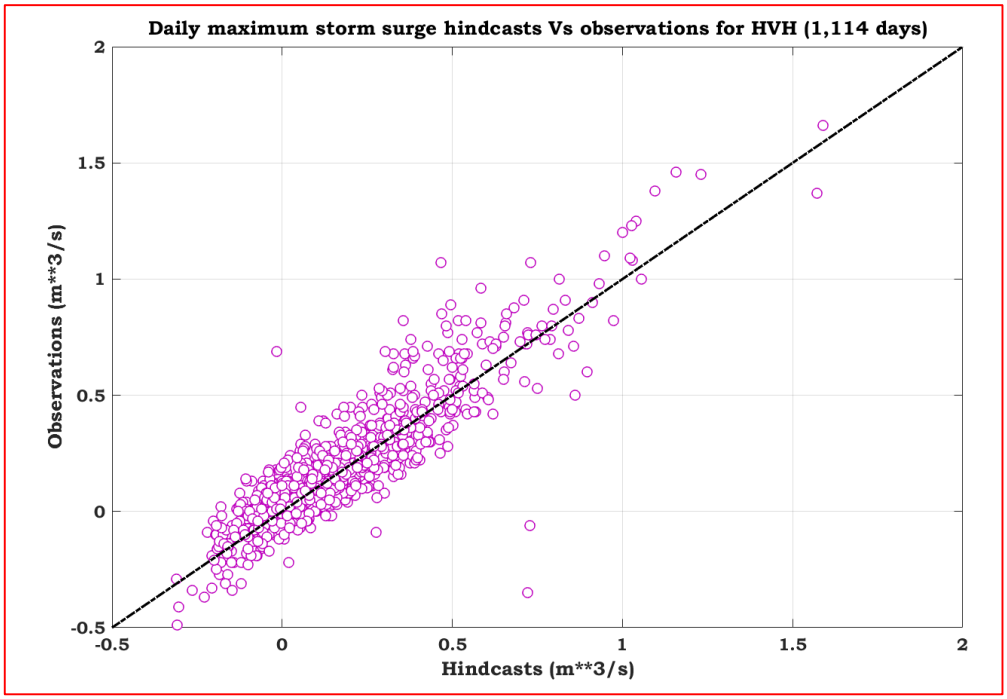

Figure 3.10. Scatterplot of river discharge hindcasts vs observations for Lobith (1,114 days).

In a similar path followed for the graph of Figure 3.5, a subsection of time series of both hindcasts and observations are contained in Figure 3.11. As expected (based on the scatterplot of Figure 3.10) hindcast discharge values are considerably lower than their corresponding observations. This might be due to the smoothness of the initial analysis fields used as forcing terms in LISFLOOD simulations. These initial fields are gridded meteorological datasets of 25 years that have been derived by interpolating weather station data.

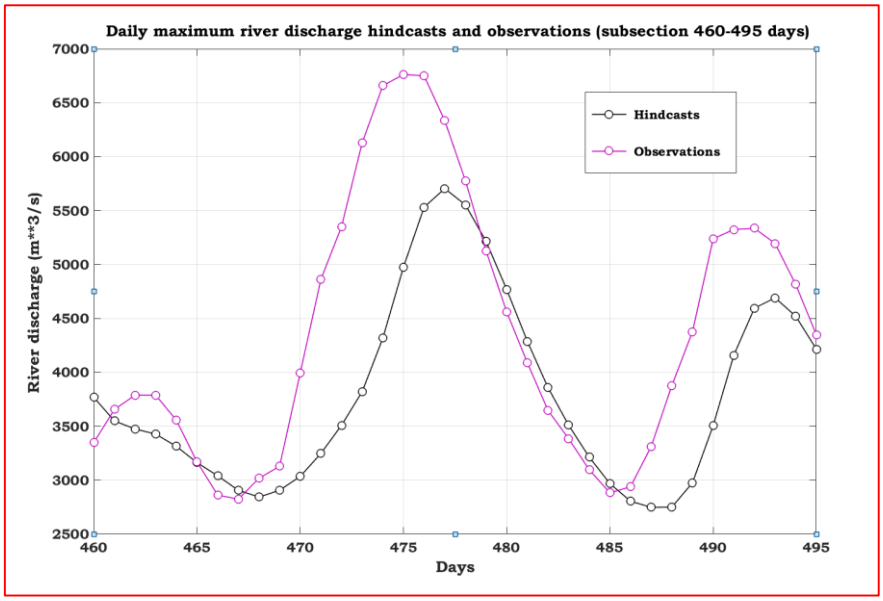

Figure 3.11. As in Figure 3.5, but for river discharge hindcasts and observations.

Furthermore, looking closely at Figure 3.10 there are cases that extreme discharge observations (outliers) are significantly underestimated by hindcasts. Focusing on Figure 3.11, the extreme of day-471 (5 January 2012) that was pronounced in surge and wave height time series (Figure 3.5 and 3.9 respectively) has been displaced into day-475 and day-476 positions.

Such displacement (lagging) is a clear sign of a lag time interval (of 4 to 5 days) between the day-471 extreme found in both surge and wave values and its corresponding extreme (day-475 / day-476) contained in river discharge values.

3.3 Capability of hindcasts resolving correctly correlations & statistical dependencies

So far, the capability of hindcasts to simulate correctly observations has been investigated. In this section the capability of hindcasts to resolve the correct type and strength of both correlation and statistical dependence among the primary variables is investigated.

At first, correlations between source variables in observations mode are calculated while the same type of correlations are calculated in hindcast mode for inter-comparison(s). Same wise, statistical dependencies in both observations and hindcast mode are assessed.

3.3.1 Correlations in observations and hindcast mode

a. Correlation between storm surge and significant wave height values

Daily maximum values of storm surge observations collected at HVH station for the common period of 1,114 days are plotted against corresponding significant wave height observations retrieved from LIC wave buoy as shown in Figure 3.12 (a). Observations of surge and wave seem to be well correlated with a

coefficient reaching to 0.69. It should be noted that this value is achieved in zero lag mode and it stands as the maximum value for any possible lag consideration of data.

Furthermore, it was found that surge values were slightly leading wave values, meaning that if there were cases with extremes taking place in different but very close dates then most probably the extreme value found in surge would be leading the extreme value found in wave height data.

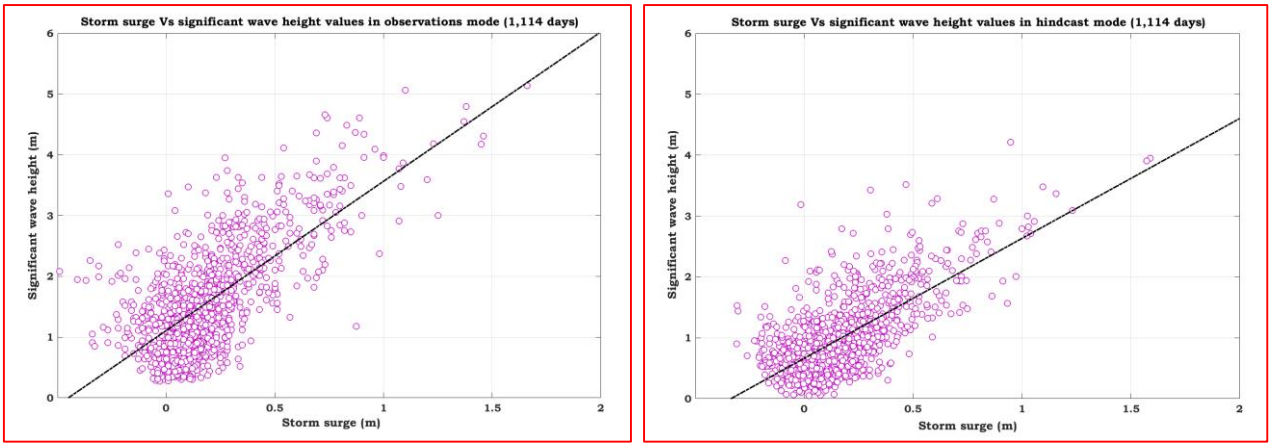

Figure 3.12. Scatterplots of storm surge Vs wave in observations (a) and hindcast (b) mode (1,114 days).

On the other hand, in hindcast mode a similar value of correlation (0.70) was found between surge and wave values during the common period of observations and hindcasts once more in a zero lag mode. Surge and wave values in hindcast mode for the common interval of observations (hind_com) are plotted in Figure 3.12 (b). A slightly higher value of correlation (0.73) was achieved when all the 12,753 of hindcasts for the total interval of surge and wave hindcasts (hind_tot) were used once more in zero-lag mode.

b. Correlation between storm surge and river discharge values

The correlation between daily maximum values of storm surge observations collected at HVH station for the common period of 1,114 days and their corresponding mean (average) river discharge observations of river Rhine at Lobith gauging station was investigated. Observations of surge and discharge found to have a low correlation for the same day (zero-lag mode) being equal to 0.15 with a clear tendency of increase to its maximum (0.30) that was reachable in a lagging mode of 5 days.

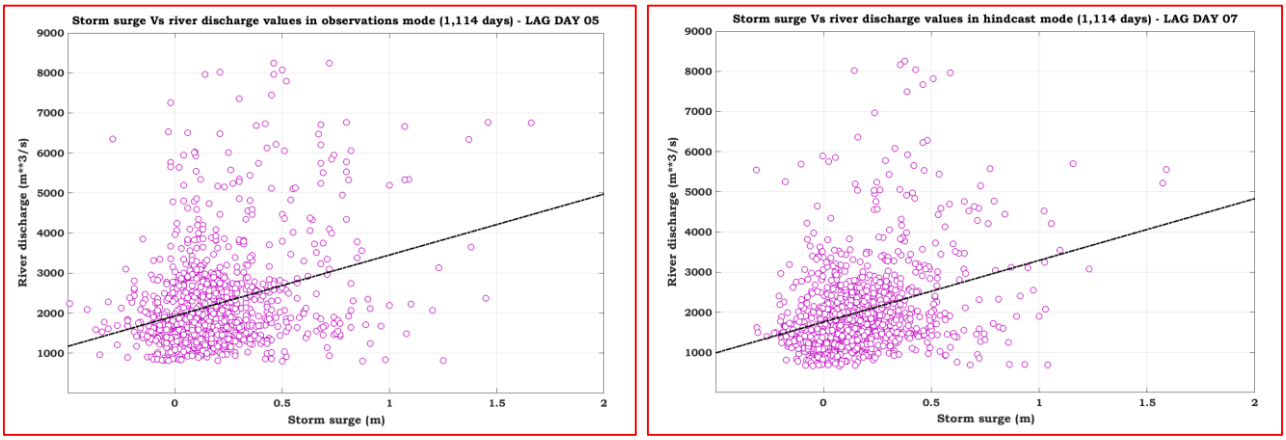

Figure 3.13. As in Figure 3.12, but for storm surge and river discharge values.

Same wise in hindcast mode (over the common interval) hindcasts of surge and discharge were found to have low correlation between them on the same day (~0.09) but as in the case of observations there was a clear tendency of increase to its maximum (0.32) in a lag mode of 7 days. The scatterplots of surge and

discharge values in both observations and hindcast mode over the common time interval are plotted in Figure 3.13 (a) and (b) respectively. It should be noted that discharge values are lagging 5 days behind surge values (observations) while this lagging becomes equal to 7 days in the case of hindcasts. It seems that a considerable lagging interval is necessary for reaching maximum values of correlation in both modes.

Similar results were found when the total number of 8,683 hindcast (hind_tot) time series were considered. A low correlation value between surges and discharges was found in zero-lag mode (~0.10) with a clear tendency of increase to its maximum (~0.33) in a lagging mode of 7 days.

c. Correlation between wave and river discharge values

The correlation between daily maximum values of wave height observations collected at LIC wave buoy station for the common period of 1,114 days and their corresponding mean (average) river discharge observations of river Rhine at Lobith gauging station was investigated. Observations of wave height and river discharge found to have a low correlation for the same day (zero-lag mode) being equal to 0.14 with a tendency of increase to its maximum (0.27) reachable in a lag mode of 6 days.

Same wise in hindcast (common) mode hindcasts of wave height and river discharge found to have low correlation between them on the same day (0.14) but as in the case of observations there was a tendency of increase to its maximum (0.37) in a lag mode of 8 days.

The scatterplots of surge and discharge values in both observations and hindcast mode over the common time interval are plotted in Figure 3.14 (a) and (b) respectively.

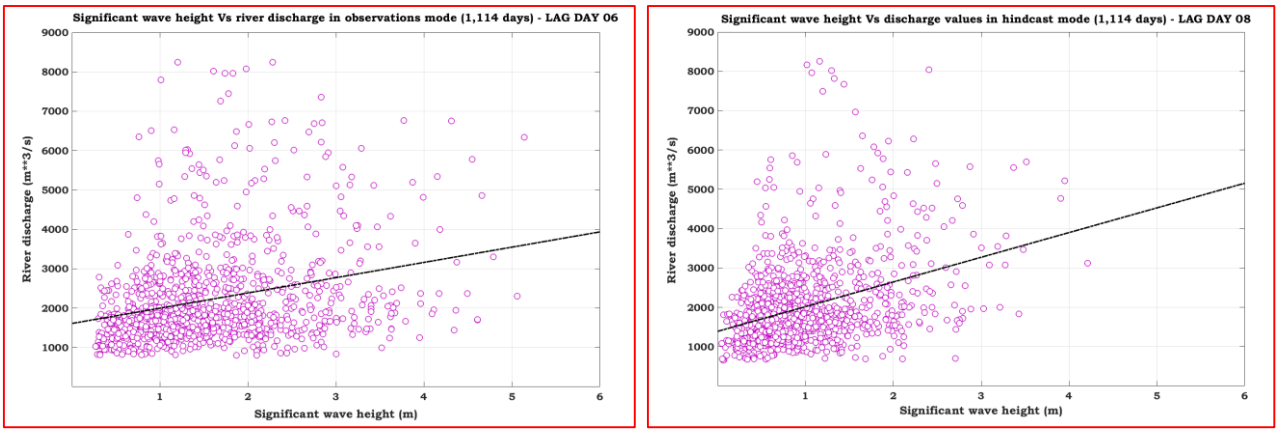

Figure 3.14. As in Figure 3.12, but for wave and river discharge values.

It should be noted that discharge values are lagging 6 days behind wave values (observations) while this lagging becomes equal to 8 days in the case of common hindcasts (hind_com). By considering such lagging intervals, maximum values of correlation are reachable in both modes. Similar results were found when the total number of 8,683 hindcasts (hind_tot) were considered. A low correlation value between waves and discharges was found in zero-lag mode (0.13) with a tendency of increase to its maximum (0.37) in a lagging mode of 7 days.

d. Assessment based on correlation value inter-comparisons

Considering the complexity of the physical drivers behind correlations investigated so far, hindcasts seem to perform quite well not only simulating quite well observation values for the common interval of interest (1,114 days) but also in resolving the type and strength of correlations between the source variables (i.e., storm surge, significant wave height and river discharge) considered in the current study. Summary of the results are contained in Table 3.8.

Table 3.8. Correlations in observations – hindcast common & hindcast total mode.

	obs_com	max (lag)	hind_com	max (lag)	hind_tot	max (lag)
SUR / WAV	0.69	0.69 (0)	0.70	0.70 (0)	0.73	0.73 (0)
SUR / DIS	0.15	0.30 (5)	0.09	0.32 (7)	0.10	0.33 (7)
WAV / DIS	0.14	0.27 (6)	0.15	0.37 (8)	0.13	0.37 (7)

Besides the obvious capability of hindcasts to resolve correctly correlations between source variables potentially acting as contributing (potential) flooding components, their capability of resolving correctly dependencies is also investigated as explained in detail in the next Subsection (3.3.2).

3.3.2 Dependencies in observations and hindcast mode

a. dependence between storm surge and significant wave height values

Statistical dependence (chi) values between daily maximum values of storm surge observations at HVH tide gauging station and their corresponding daily maximum significant wave height values collected at LIC wave buoy are plotted in Figure 3.15. A closer look for the upper percentiles acting as critical thresholds is shown in Figure 3.16.

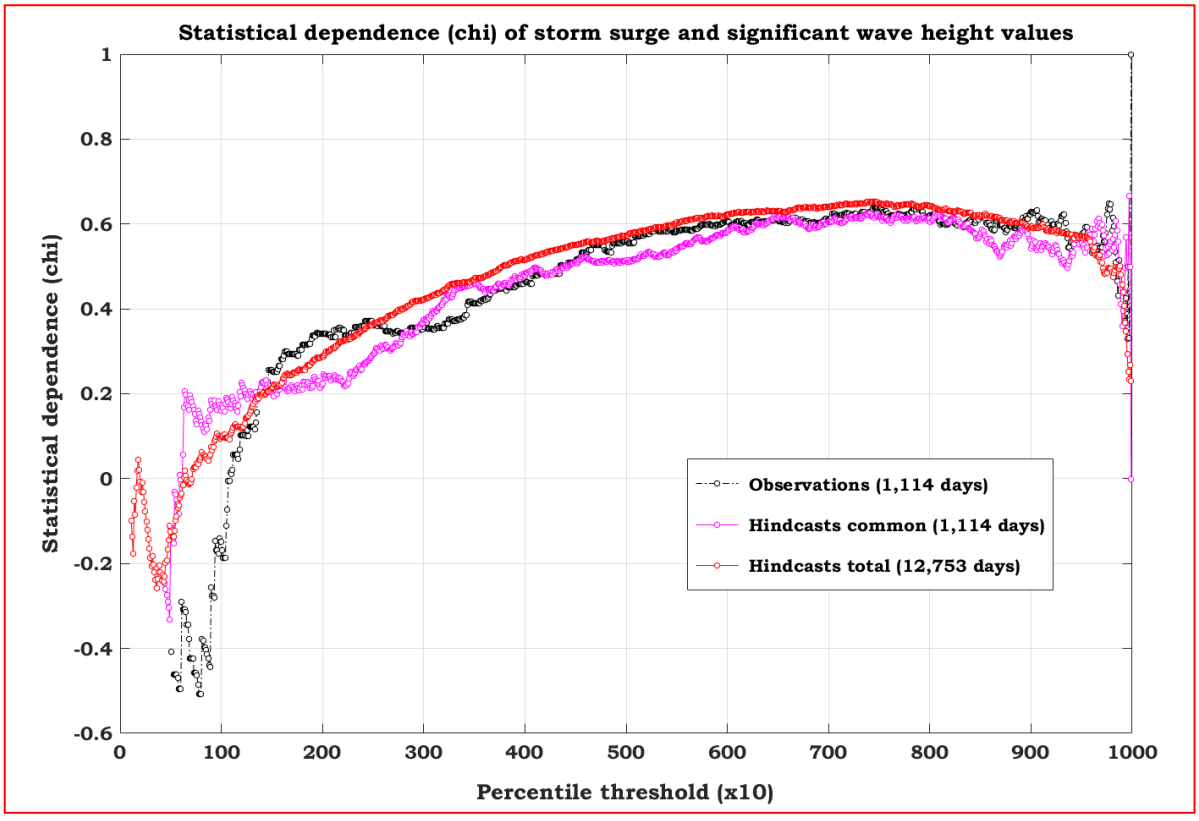

Figure 3.15. Statistical dependence (chi) of storm surge (HVH) and significant wave height (LIC) values.

The capability of hindcasts to resolve the statistical dependence between surge and wave values focusing on the upper (extreme) percentiles is investigated by inter-comparing dependencies among observations (obs_com), hindcasts (hind_com) over the common time period (1,114 days) and hindcasts (hind_tot) over the total time period of 12,753 days.

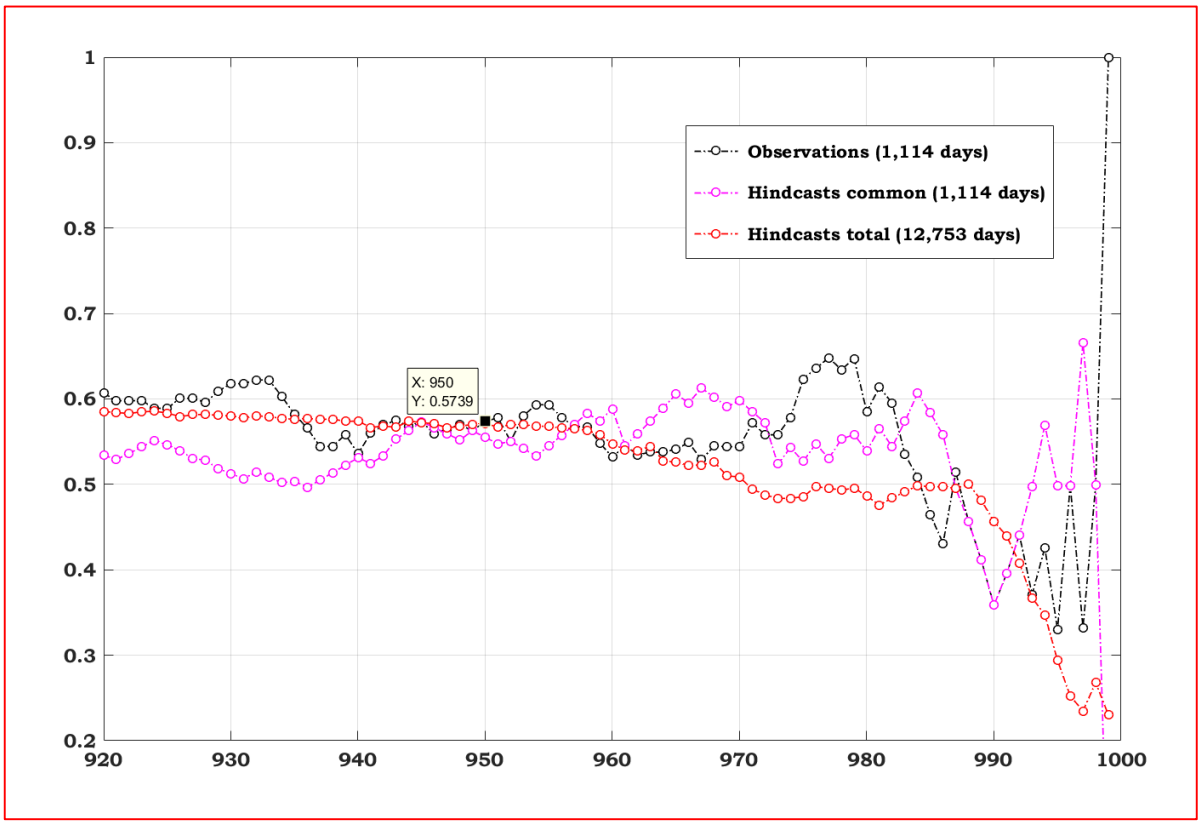

Figure 3.16. As in Figure 3.15 but for the subsection (zooming over) referring to upper thresholds ranging from 92 to 99.9% percentile values.

Very strong statistical dependence values (chi ≥ 0.45) between storm surge and significant wave height were found for all three configurations (obs_com, hind_com and hind_tot) in a zero-lag environment. In all cases surge values were found to lead the wave values when lag mode cases were investigated.

Various methodologies of estimating dependencies were utilised. Sample plots of applying matlab routines written and compiled by the JRC's Crisis Management Laboratory Team referring to techniques and methodologies documented in Coles (2001) are presented in Figures 3.15 & 3.16 (details).

Besides POT (Peaks-Over-Threshold) methodology and optimal selection of threshold for combined events (i.e., not allowing more than ~2.3 to ~2.5 events per year to exceed), emphasis was also given to the stability of graph curves representing dependencies for all obs_com, hind_com & hind_tot time series.

Table 3.9. Dependencies between storm surge & significant wave height values for observations, hindcast common and hindcast total time series.

	lead	*thres.*	*R (chiplot)*	*max*	*mat_chi*	*max (mat)*	*lag*	*R (taildep)*	*max*
obs_com	*s / w*	*95%*	*0.63*	*0.63*	*0.57*	*0.57*	*0*	*0.59*	*0.59*
hind_com	*s / w*	*95%*	*0.56*	*0.56*	*0.56*	*0.56*	*0*	*0.57*	*0.57*
hind_tot	*s / w*	*95%*	*0.57*	*0.57*	*0.57*	*0.57*	*0*	*0.59*	*0.59*

The stability issue is considered important when a relatively small amount of observation values (extreme combined events) is available resulting to a dependence graph containing intense fluctuating features. In the

case of Figure 3.16, stability on values seem to be reached for the interval between 94 to 96% percentiles. This is the primary reason of selecting the 95% percentile as a common threshold for inter-comparisons among dependence estimations.

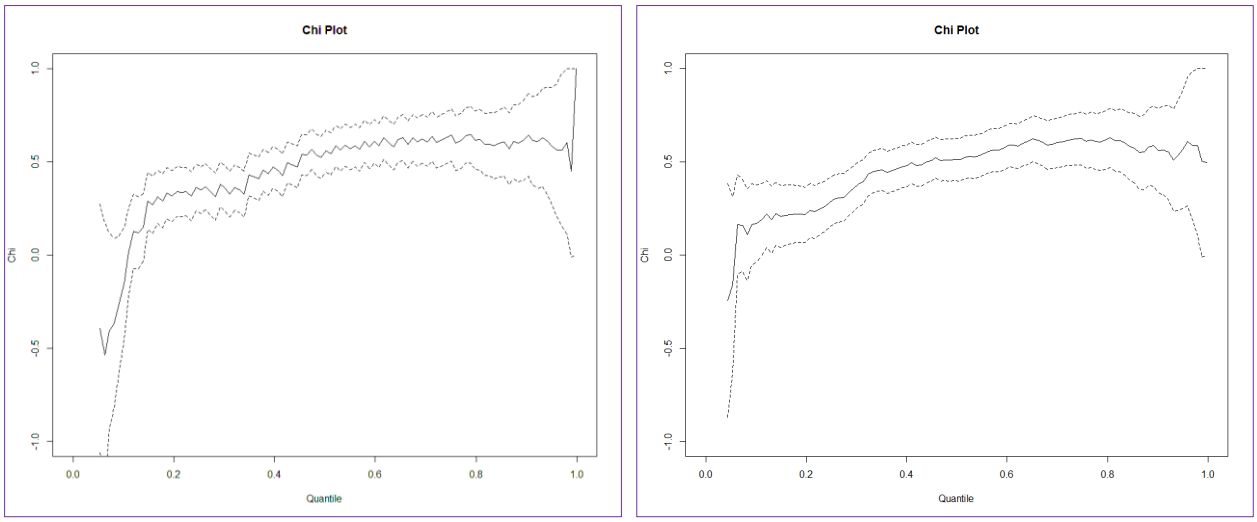

Figure 3.17. Dependence (chi) values of storm surge (HVH) and significant wave height (LIC) valid for observations mode (a) and dependence values valid for hindcast common time period (b) as estimated by the module "taildep" of the statistical package "extRemes" of application R.

Based on 95% percentile threshold as an optimal "stability" threshold, Table 3.9 is constructed containing values of dependence as they were calculated by matlab routines (mat_chi & mat_chi_lag). In the same Table (3.9) dependencies estimated by the routine "taildep" of the statistical module "extRemes" and routine "chiplot" of the statistical module "evd" of the integrated application R are presented. Studying closely Table 3.9, it becomes obvious that hindcasts were quite capable of resolving statistical dependencies between storm surge and wave height values in a zero-lag and max-lag mode. Values are contained in columns "mat_chi" and "mat (max)" being shaded by a light yellow colour. Small differences found in estimates made by R (chiplot) and R (taildep) most probably are due to the specific criteria being imposed on both mat_chi & mat_chi_lag routines concerning the selection of POT extremes.

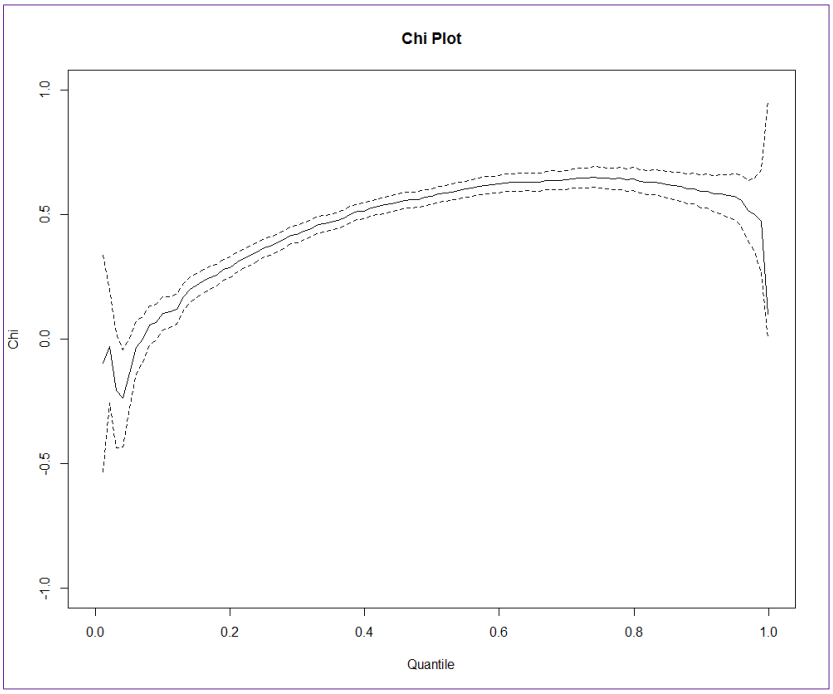

Figure 3.18. As in Figure 3.17 but valid for the total hindcast period of 12,753 days (~35 years).

Besides graphs produced by matlab routines, similar type of graphs could be created by utilising the chiplot routine of evd module (in R graphical mode). Examples of such graphs complimented also by approximate 95% confidence intervals are shown in Figures 3.17 (a) & (b) and in Figure 3.18.

b. dependence between storm surge and river discharge values

Statistical dependence (chi) values between daily maximum values of storm surge observations at HVH tide gauging station and corresponding daily average river discharge values collected at Lobith gauging station of river Rhine are plotted in Figure 3.19, referring to the maximum reachable values of chi taking place in a 6-day lag mode.

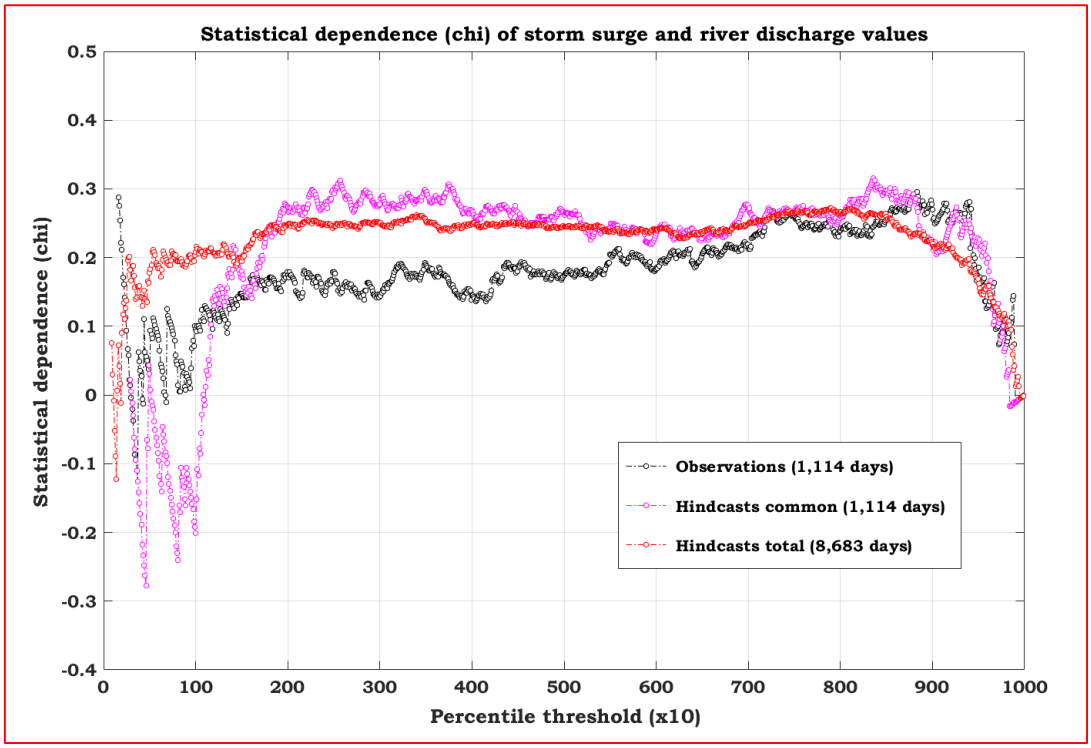

Figure 3.19. Statistical dependence (chi) of storm surge (HVH) and river discharge (LOB) values.

The capability of hindcasts to resolve the statistical dependence (focusing on the upper percentiles) between surge and river discharge values is investigated by inter-comparing dependencies coming from observations (obs_com), hindcasts (hind_com) over the common time period (1,114 days) and hindcasts (hind_tot) over the total (max common) time period of 8,683 days. As in previous surge & wave case, various methodologies of estimating dependencies were utilised. Results of applying mat_chi are presented in Table 3.10. Once more, besides POT methodology and the optimal selection of threshold not allowing more than ~2.3 to ~2.5 extreme combined events per year to exceed, emphasis was also given on the stability of curves representing dependencies for all obs_com, hind_com & hind_tot time series.

Table 3.10. Dependencies between storm surge & river discharge values for observations, hindcast common and hindcast total time series.

	lead	*thres.*	*R (chiplot)*	*max*	*mat_chi*	*max (mat)*	*lag*	*R (taildep)*	*max*
obs_com	*s / d*	*92%*	*0.18*	*0.29*	*0.14*	*0.26*	*6*	*0.20*	*0.32*
hind_com	*s / d*	*92%*	*0.11*	*0.24*	*0.10*	*0.25*	*6*	*0.16*	*0.32*
hind_tot	*s / d*	*92%*	*0.11*	*0.23*	*0.12*	*0.22*	*6*	*0.18*	*0.28*

In surge & discharge case, a relatively lower percentile (than in surge & wave case) threshold had to be selected for allowing a higher number of coincident (extreme) events to be considered in order to ensure an optimal level of stability. This was the primary reason of selecting the 92% percentile as a common threshold for inter-comparison between dependence estimations. From Table 3.10, it is clear that hindcasts were capable of resolving the maximum statistical dependence between storm surge and river discharge values in the common 6-day maximum lag mode as seen from the column labelled "max (mat)".

There seems to be a slight drawback though, since the estimation of dependence from both hindcast data sets (hind_com & hind_tot) in zero lag mode (in column mat_chi) is somehow lower than the one referring to observations (obs_com). Nevertheless, both hind_com & hind_tot seem to perform quite well in resolving both the correct value of maximum dependence and the correct duration of the lag (max) interval of 6 days. Once more, small differences found in estimates made by R and matlab routines are most probably due to the specific criteria being imposed on both mat_chi & mat_chi_lag routines concerning the optimal selection of POT extremes.

c. dependence between significant wave height and river discharge values

Statistical dependence (chi) values for daily maximum significant wave height observations collected at LIC wave buoy and their corresponding daily average river discharge values collected at Lobith gauging station of river Rhine are plotted in Figure 3.20.

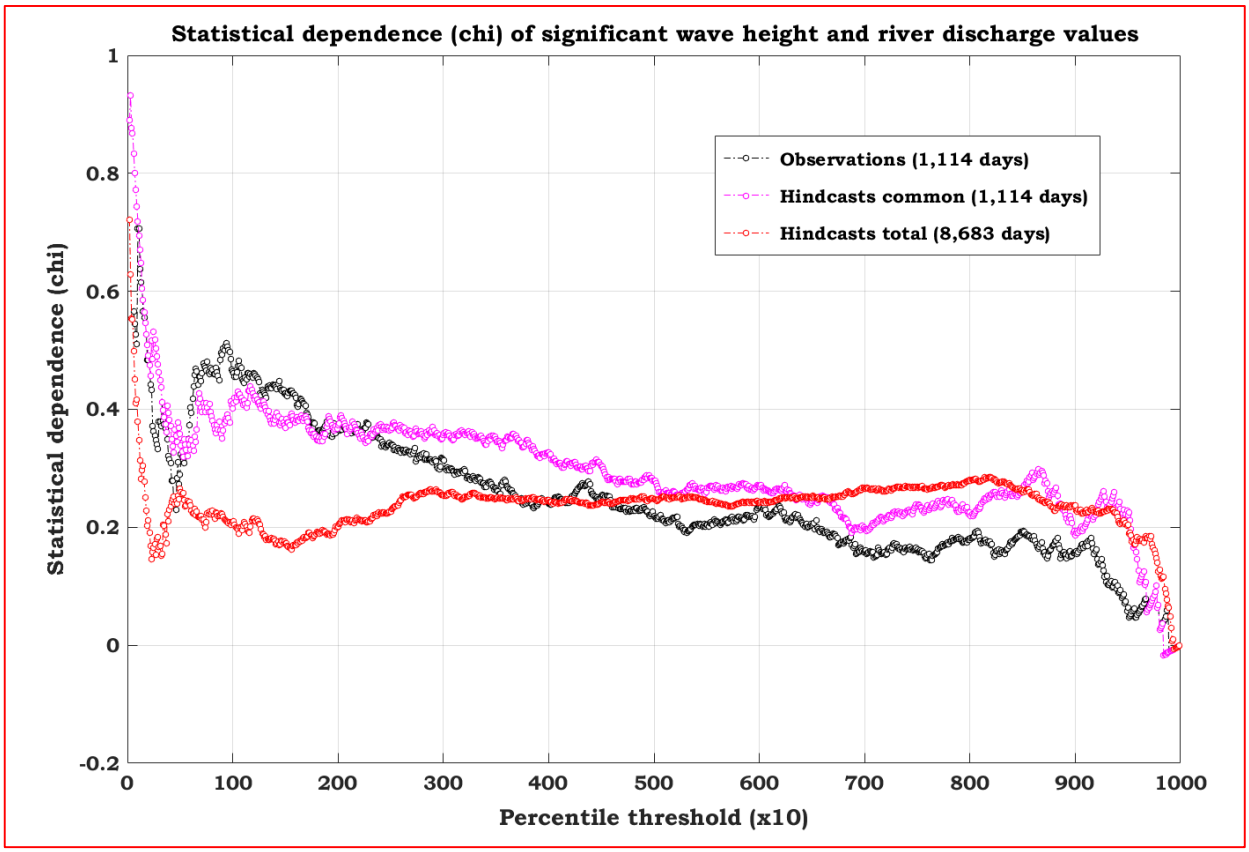

Figure 3.20. Statistical dependence (chi) of storm surge (HVH) and river discharge (LOB) values.

As in surge & river case, dependence (chi) values contained in Figure 3.20 are referring to the maximum possible values of dependence that are reachable after a considerable time lag of a few days. In observations mode (obs_com) such an interval was estimated as 6 days, whereas in hindcast mode it was found equal to 8 days (hind_com) and 7 days (hind_tot) respectively.

As in surge & river case, a relatively lower (than in surge & wave case) was selected to allow a higher number of coincident (extreme) events to be considered, ensuring an optimal stability level of graph points. This was the primary reason of selecting the 90% percentile as a common threshold for inter-comparisons of all dependence estimations. Based on such inter-comparisons, Table 3.11 was constructed.

Table 3.11. Dependencies between wave height & river discharge values for observations, hindcast common and hindcast total time series.

	lead	*thres.*	*R (chiplot)*	*max*	*matlab*	*max (mat)*	*lag*	*R (taildep)*	*max*
obs_com	*w / d*	*90%*	*0.10*	*0.21*	*0.04*	*0.16*	*6*	*0.13*	*0.25*
hind_com	*w / d*	*90%*	*0.10*	*0.30*	*0.03*	*0.23*	*8*	*0.13*	*0.33*
hind_tot	*w / d*	*90%*	*0.09*	*0.25*	*0.16*	*0.29*	*7*	*0.17*	*0.33*

From Table 3.11, it becomes clear that hindcasts were capable of resolving relatively well the statistical dependence between wave height and river discharge values. There seems to be a slight disagreement concerning dependence values based on observations from those based on hind_tot time series (in zero-lag mode) but this may be expected since obs_com & hind_tot durations differ substantially. Furthermore, in max lag mode (6 days for obs_com and 8 days for hind_com), hindcasts found to be slightly overshooting during the common time interval in harmony with hindcasts (hind_tot) made over the total time interval.

Overall, considering the complexity of physical drivers behind such dependencies, hindcasts seem to perform quite well not only simulating observations over the common interval of interest but also in resolving the type and strength of both correlations and statistical dependencies between the source variables (i.e., storm surge, significant wave height & river discharge) considered in the current study.

Furthermore, the routines mat_chi & mat_chi_lag (see Table 2.2) being coded as matlab functions were the primary routines used for the estimation of dependencies between source variables. Both routines are capable of providing the user with dependence values based on a wide range of upper percentile (critical) thresholds. These routines not only make use of the POT (Peaks-Over-Threshold) methodology but they also allow the user to select the maximum number of combined (compound) events on a yearly basis by defining and applying an appropriate upper percentile threshold. For the current study, this maximum number of yearly compound events has been set to ~2.3 to ~2.5 based mainly on suggestions by Svensson and Jones (2005) and it was modulated only in cases that stability of dependence graph curve had to be ensured.

Besides matlab functions additional routines from the integrated statistical package R were used for the estimation and inter-comparison of dependence values. The main module "extRemes" of R has been able to provide estimations of dependence referring to specific single percentile thresholds by utilising the powerful "taildep" routine. Another "powerful" tool of R used for estimations of dependence has been the "evd" module that stands for “Extreme Value Distributions” that contains the routine "chiplot". Utilising "chiplot" a detailed plot of dependence (chi) values is possible based on a wide range of percentile values. The routine "chiplot" besides chi values is also able to provide selected confidence intervals for chi. Another significant ability of "chiplot" is the plotting of the "sister" graph of chi, namely the parameter "chibar" with selected confidence intervals (of chibar). It is important to point out that chi refers to asymptotic behaviour of statistical dependent variables (and this the area on which this Report is focusing on), whereas chibar refer to the statistical dependence of asymptotically independent values (not investigated yet).

4. Results

Results based on total (max time period) hindcasts are given below. Estimations of correlation and statistical dependence between flooding components are given by means of Tables & Maps.

4.1 Correlation assessment of combined event components over RIEN points

The type and strength of correlation for all combined events considered in this study are presented in this section. The existence and magnitude of lag periods are also presented together with the leading parameter.

4.1.1 Storm surge & wave height for MAX12 (maxima over 12 hours)

Strong correlations (0.54 ≤ ρ ≤ 0.69) between storm surge and significant wave height values were found mainly over the coastal areas of English Channel, Irish Sea and North Sea as shown in Table 4.1.

Table 4.1. Correlations between surge & wave values for MAX12.

RIEN	River	Ocean / Sea	Lead	Correl.	Max	Lag (d)	Type
01	Po (IT)	Adriatic Sea	SUR / WAV	0.30	0.33	0.5	mod
02	Metauro (IT)	Adriatic Sea	SUR / WAV	0.26	0.29	0.5	mod
03	Vibrata (IT)	Adriatic Sea	SUR / WAV	0.29	0.35	0.5	mod
04	Foix (ES)	Balearic Sea	SUR / WAV	0.12	0.14	0.5	mod
05	Ebro (ES)	Balearic Sea	SUR / WAV	0.17	0.21	0.5	mod
06	Velez (ES)	Alboran Sea	SUR / WAV	0.06	0.07	0.5	low
07	Sella (ES)	Bay of Biscay	SUR / WAV	-0.08	-0.05	0.5	zero
08	Rhone (FR)	Gulf of Lion	SUR / WAV	0.13	0.23	1.0	mod
09	Bethune (FR)	English Channel	SUR / WAV	0.64	*	0.0	strong
10	Moros (FR)	Bay of Biscay	SUR / WAV	0.26	*	0.0	mod
11	Aven (FR)	Bay of Biscay	SUR / WAV	0.29	*	0.0	mod
12	Blavet (FR)	Bay of Biscay	SUR / WAV	0.28	*	0.0	mod
13	Owenavorragh (IE)	Irish Sea	SUR / WAV	0.55	*	0.0	strong
14	Goeta Aelv (SE)	North Sea	WAV / SUR	0.58	0.62	0.5	strong
15	Orkla (NO)	Norwegian Sea	SUR / WAV	0.49	*	0.0	well
16	Vantaa (FI)	Baltic Sea	WAV / SUR	0.44	0.44	0.5	well
17	Rhine (NL)	North Sea	SUR / WAV	0.64	*	0.0	strong
18	Weser (DE)	North Sea	SUR / WAV	0.65	*	0.0	strong
19	Schelde (BE)	North Sea	WAV / SUR	0.48	0.52	0.5	well
20	Severn (UK)	Bristol Channel	SUR / WAV	0.29	*	0.0	mod
21	Mersey (UK)	Irish Sea	SUR / WAV	0.51	0.51	0.5	well
22	Tyne (UK)	North Sea	WAV / SUR	0.19	0.22	0.5	mod
23	Tamar (UK)	English Channel	SUR / WAV	0.40	*	0.0	well
24	Avon (UK)	English Channel	SUR / WAV	0.49	*	0.0	well
25	Thames (UK)	North Sea	WAV / SUR	-0.01	0.18	1.0	mod
26	Exe (UK)	English channel	WAV / SUR	0.43	*	0.0	well
27	Humber (UK)	North Sea	SUR / WAV	0.28	*	0.0	mod
28	Danube (RO)	Black Sea	SUR / WAV	0.09	0.15	0.5	mod
29	Tagus (PT)	Atlantic Ocean	SUR / WAV	-0.11	-0.11	0.5	neg
30	Sado (PT)	Atlantic Ocean	SUR / WAV	-0.10	-0.09	0.5	neg
31	Douro (PT)	Atlantic Ocean	SUR / WAV	0.09	0.10	0.5	low
32	Guadianna (ES)	Atlantic Ocean	SUR / WAV	0.15	*	0.0	mod

In Mediterranean Sea, correlations were found to be of moderate importance (0.12 ≤ ρ ≤ 0.37) with the case of river Velez RIEN (Alboran Sea) belonging in the lowest category (0.06 ≤ ρ ≤ 0.11). The lag period in most cases in Mediterranean was half a day (12 hours). Such 12-hour lagging was found to be the case for some other coastal areas meaning that in most cases the events of interest were taken place during the same day. The maximum lag period of one day (24 hours) found over Thames RIEN linked to a moderate value of correlation (~0.19). Correlation spatial details are shown in the map contained in Figure 4.1.

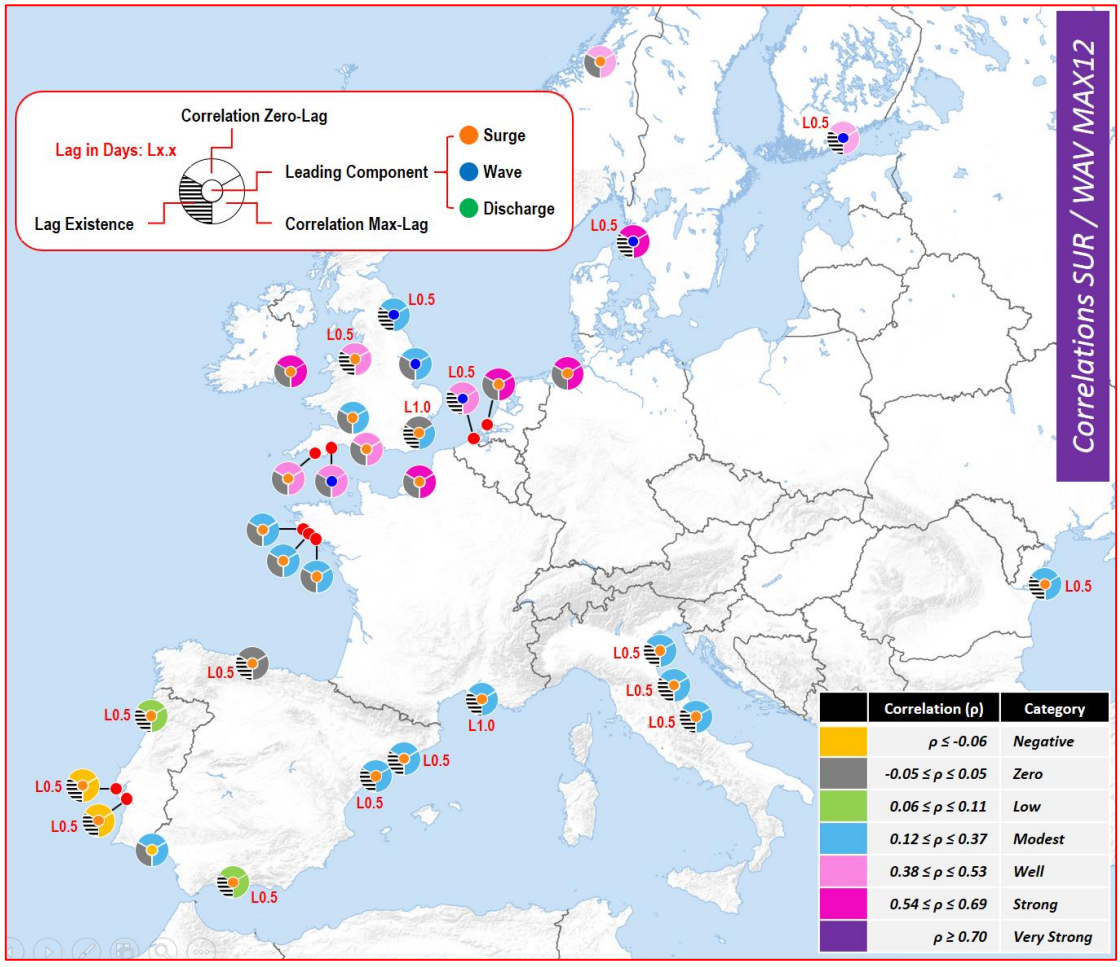

Figure 4.1. Map with local values of correlations between surge & wave for MAX12.

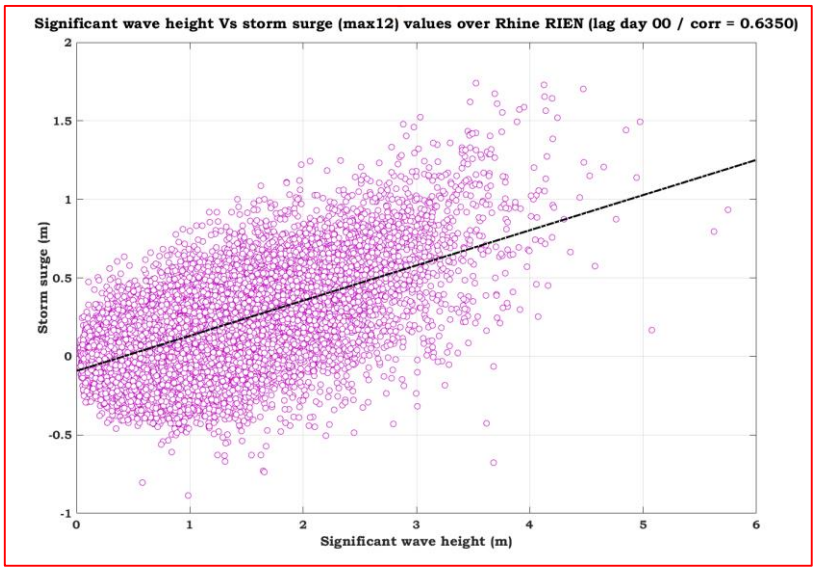

Figure 4.2. Scatterplot of surge & wave height (max12) values valid for RIEN of river Rhine (NL).

By studying closely lag correlations, storm surge was found to lead wave values in most RIEN points of this report. This was not true for the ending points of Goeta Aelv (SE), Vantaa (FI), Schelde (BE), Tyne, Thames & Exe (UK), not showing strong correlation values also (except Goeta Aelv). Overall, strong correlations appear to take place mostly on the same 12-hour interval reflecting to a zero-lag mode. An example of such strong correlation with zero lag time interval is shown in Figure 4.2 valid for the ending point (RIEN) of river Rhine (NL) in hindcast (total) mode.

4.1.2 Storm Surge & wave height for MAX24 (maxima over 24 hours)

Very strong ($\rho \geq 0.70$) and strong correlations ($0.54 \leq \rho \leq 0.69$) between storm surge and significant wave height values were found mainly over coastal areas of English Channel, Irish Sea, North Sea and Norwegian Sea (as shown in Table 4.2, whereas correlation spatial details are shown in Figure 4.3).

Table 4.2. Correlations between surge & wave values for MAX24.

RIEN	River	Ocean / Sea	Lead	Correl.	Max	Lag (d)	Type
01	Po (IT)	Adriatic Sea	SUR / WAV	0.39	*	0	well
02	Metauro (IT)	Adriatic Sea	SUR / WAV	0.33	*	0	mod
03	Vibrata (IT)	Adriatic Sea	SUR / WAV	0.36	0.38	1	well
04	Foix (ES)	Balearic Sea	SUR / WAV	0.12	0.13	1	mod
05	Ebro (ES)	Balearic Sea	SUR / WAV	0.19	0.22	1	mod
06	Velez (ES)	Alboran Sea	SUR / WAV	0.10	0.10	1	low
07	Sella (ES)	Bay of Biscay	SUR / WAV	-0.03	-0.02	1	zero
08	Rhone (FR)	Gulf of Lion	SUR / WAV	0.17	0.25	1	mod
09	Bethune (FR)	English Channel	SUR / WAV	0.72	*	0	v. strong
10	Moros (FR)	Bay of Biscay	SUR / WAV	0.31	*	0	mod
11	Aven (FR)	Bay of Biscay	SUR / WAV	0.34	*	0	mod
12	Blavet (FR)	Bay of Biscay	SUR / WAV	0.334	*	0	mod
13	Owenavorragh (IE)	Irish Sea	SUR / WAV	0.62	*	0	strong
14	Goeta Aelv (SE)	North Sea	WAV / SUR	0.64	0.65	1	strong
15	Orkla (NO)	Norwegian Sea	SUR / WAV	0.54	*	0	strong
16	Vantaa (FI)	Baltic Sea	WAV / SUR	0.51	*	0	well
17	Rhine (NL)	North Sea	SUR / WAV	0.61		0	strong
18	Weser (DE)	North Sea	SUR / WAV	0.70	*	0	~v. strong
19	Schelde (BE)	North Sea	WAV / SUR	0.61	*	0	strong
20	Severn (UK)	Bristol Channel	SUR / WAV	0.37	*	0	mod
21	Mersey (UK)	Irish Sea	SUR / WAV	0.60	*	0	strong
22	Tyne (UK)	North Sea	WAV / SUR	0.30	*	0	mod
23	Tamar (UK)	English Channel	SUR / WAV	0.46	*	0	well
24	Avon (UK)	English Channel	SUR / WAV	0.57	*	0	strong
25	Thames (UK)	North Sea	WAV / SUR	0.15	0.26	1	mod
26	Exe (UK)	English channel	WAV / SUR	0.50	*	0	well
27	Humber (UK)	North Sea	SUR / WAV	0.43	*	0	well
28	Danube (RO)	Black Sea	SUR / WAV	0.14	0.18	1	mod
29	Tagus (PT)	Atlantic Ocean	SUR / WAV	-0.08	*	0	neg
30	Sado (PT)	Atlantic Ocean	SUR / WAV	-0.06	*	0	neg
31	Douro (PT)	Atlantic Ocean	SUR / WAV	0.15	*	0	mod
32	Guadianna (ES)	Atlantic Ocean	SUR / WAV	0.19	*	0	mod

Such significant correlations appear to take place on the same 24-hour interval in zero-lag mode (except for Goeta Aelv RIEN in Sweden). Such lag issues (of one-day maximum) seem to be important mainly for the coastal areas of Mediterranean Sea (RIEN) points. Once more by studying closely lag correlations, storm surge found to lead wave values in most of coastal areas in a similar way as in the previous Subsection (Max12). In Mediterranean Sea correlations were found to belong mostly in moderate ($0.12 \leq \rho \leq 0.37$) to well ($0.38 \leq \rho \leq 0.53$) categories except in case of Velez river RIEN area at Alboran Sea that was found belonging in the lowest correlation category ($\rho \leq 0.11$).

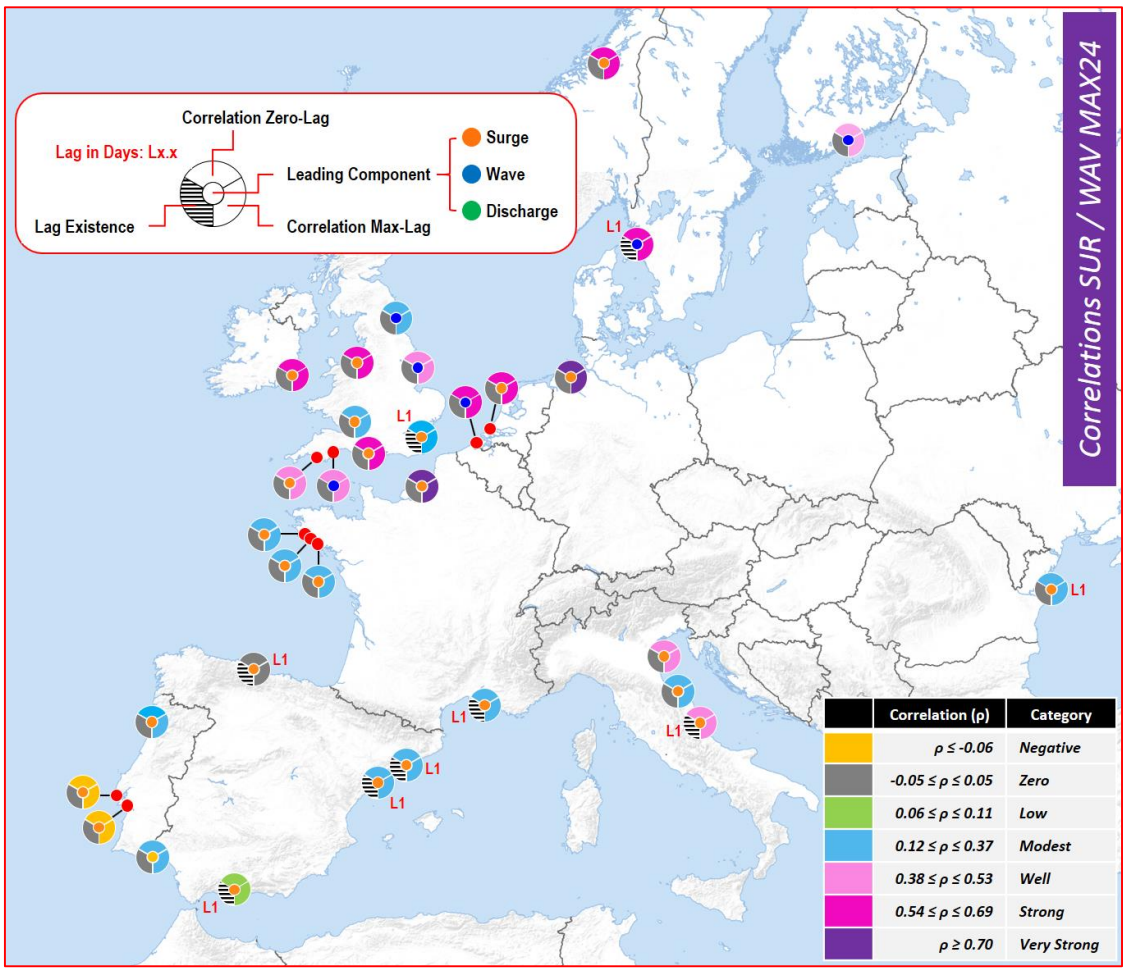

Figure 4.3. Map with local values of correlations between surge & wave for MAX24.

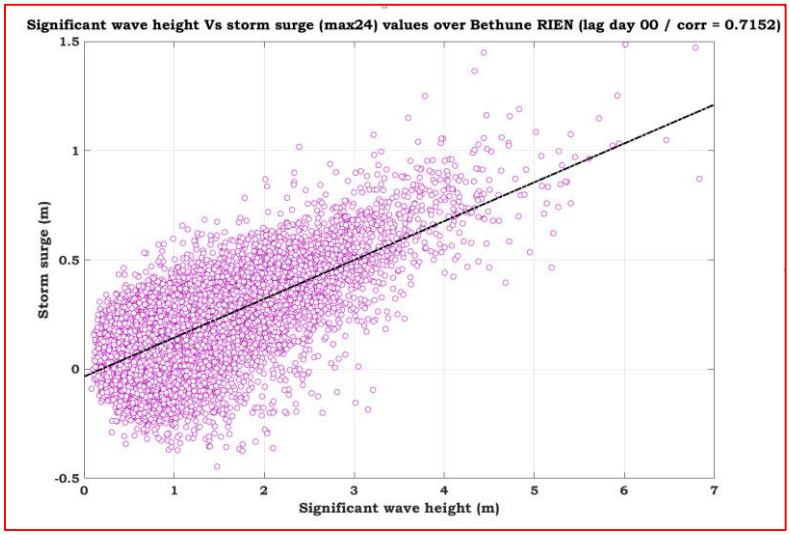

Figure 4.4. Scatterplot of surge & wave height (max24) values valid for RIEN of river Bethune (FR).

Overall, both very strong and strong correlations appear to take place mostly on the same 24-hour interval in zero-lag mode. An example of very strong correlation with zero-lag time interval is shown in Figure 4.4 valid for the ending point (RIEN) of river Bethune (FR) in hindcast (total) mode.

4.1.3 Storm surge & river discharge for MAX24 (maxima over 24 hours)

Moderate correlations ($0.12 \leq \rho \leq 0.37$) between storm surge and river discharge values were found in most cases. Only two cases belonging to the higher "well" category ($0.38 \leq \rho \leq 0.53$) were found for Rhine (NL) and Mersey (UK) RIEN points, while zero correlations were found for Ebro (ES), Orkla (NO), Thames (UK), Guadianna (ES), Tagus & Sado (PT). Most of moderate correlations were not valid for the same day (i.e., in zero-lag mode) but they refer to a considerable lag interval (of a few days) while there were even some cases that time lag interval was found to extend well above seven days as clearly shown in Table 4.3.

Table 4.3. Correlations between surge & river discharge values for MAX24.

RIEN	River	Ocean / Sea	Lead	Correl.	Max	Lag (d)	Type
01	Po (IT)	Adriatic Sea	SUR / DIS	0.10	0.29	4	mod
02	Metauro (IT)	Adriatic Sea	SUR / DIS	0.36	*	0	mod
03	Vibrata (IT)	Adriatic Sea	SUR / DIS	0.26	0.31	3	mod
04	Foix (ES)	Balearic Sea	SUR / DIS	0.11	*	0	mod
05	Ebro (ES)	Balearic Sea	SUR / DIS	-0.05	-0.02	3	zero
06	Velez (ES)	Alboran Sea	SUR / DIS	0.17	*	0	mod
07	Sella (ES)	Bay of Biscay	SUR / DIS	0.08	0.12	1	mod
08	Rhone (FR)	Gulf of Lion	SUR / DIS	0.19	0.36	4	mod
09	Bethune (FR)	English Channel	SUR / DIS	0.22	0.33	5	mod
10	Moros (FR)	Bay of Biscay	SUR / DIS	0.16	*	0	mod
11	Aven (FR)	Bay of Biscay	SUR / DIS	0.07	0.12	5	mod
12	Blavet (FR)	Bay of Biscay	SUR / DIS	0.17	*	0	mod
13	Owenavorragh (IE)	Irish Sea	SUR / DIS	0.22	0.31	7	mod
14	Goeta Aelv (SE)	North Sea	SUR / DIS	0.06	0.11	>7	mod
15	Orkla (NO)	Norwegian Sea	SUR / DIS	-0.07	-0.05	2	zero
16	Vantaa (FI)	Baltic Sea	SUR / DIS	0.22	0.23	2	mod
17	Rhine (NL)	North Sea	SUR / DIS	0.22	0.37	5	well
18	Weser (DE)	North Sea	SUR / DIS	0.19	0.35	7	mod
19	Schelde (BE)	North Sea	SUR / DIS	0.28	0.33	2	mod
20	Severn (UK)	Bristol Channel	SUR / DIS	0.20	0.33	3	mod
21	Mersey (UK)	Irish Sea	SUR / DIS	0.37	0.41	1	well
22	Tyne (UK)	North Sea	SUR / DIS	0.30	*	0	mod
23	Tamar (UK)	English Channel	SUR / DIS	0.26	0.27	1	mod
24	Avon (UK)	English Channel	SUR / DIS	0.23	0.31	5	mod
25	Thames (UK)	North Sea	DIS / SUR	0.02	0.04	1	zero
26	Exe (UK)	English channel	SUR / DIS	0.31	0.34	1	mod
27	Humber (UK)	North Sea	SUR / DIS	0.15	0.15	1	mod
28	Danube (RO)	Black Sea	SUR / DIS	0.02	0.20	>7	mod
29	Tagus (PT)	Atlantic Ocean	SUR / DIS	-0.09	-0.01	>7	zero
30	Sado (PT)	Atlantic Ocean	SUR / DIS	0.02	0.05	4	zero
31	Douro (PT)	Atlantic Ocean	SUR / DIS	0.24	0.27	1	mod
32	Guadianna (ES)	Atlantic Ocean	SUR / DIS	-0.03	0.01	>7	zero

Investigating over the existence of lag correlations, surge values were found to be leading discharge ones in almost every (RIEN) point. The only exception was for river Thames that discharge values were found to lead storm surge values by one day. No case of correlation belonging to a higher than moderate category was found in zero-lag mode. In the case of Mersey (with max correlation of "well" category) it appears that a lag interval of 1-day is required for such value (0.41) to be reached, whereas in Rhine case the max correlation value of 0.38 can be reached in a 5-day lag mode. Spatial correlation details are shown in Figure 4.5.

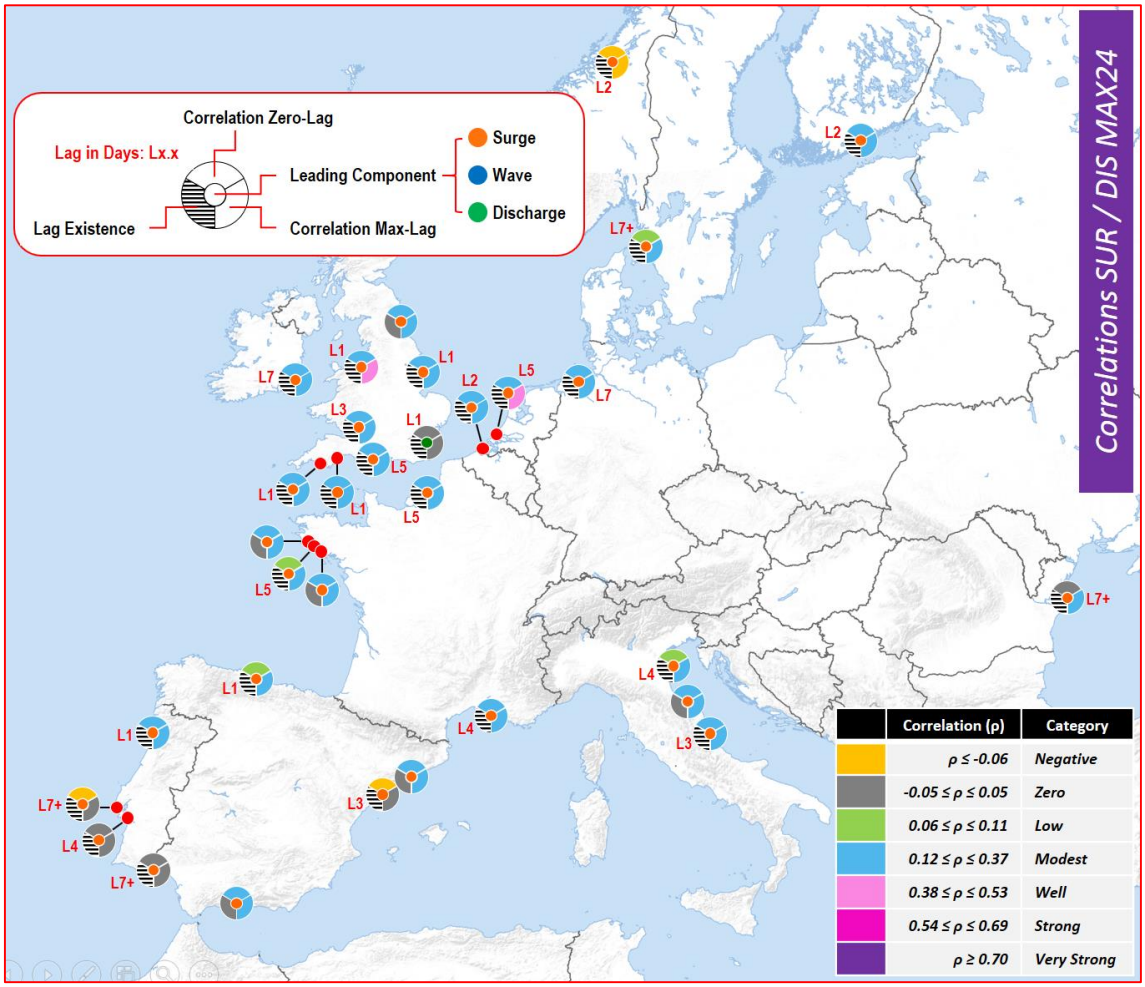

Figure 4.5. Map with spatial correlations between surge & river discharge values for MAX24.

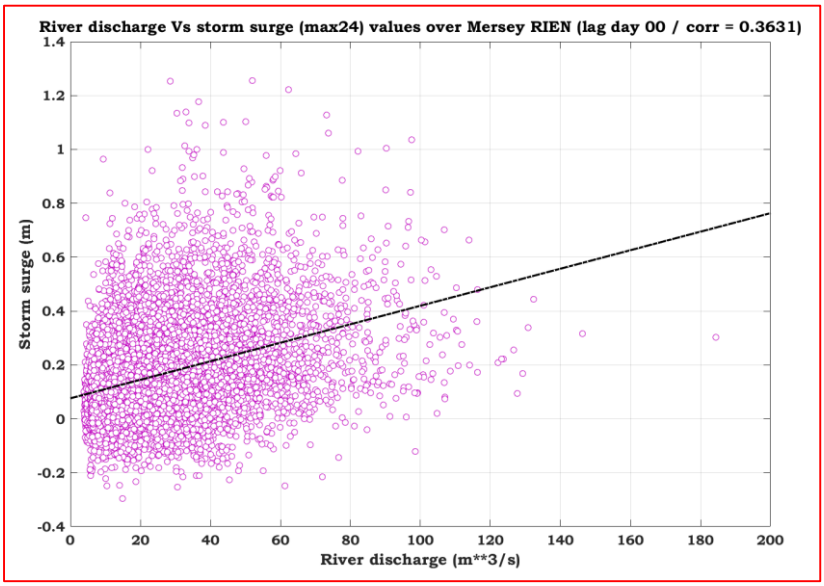

Figure 4.6. Scatterplot of storm surge & river discharge (max24) values valid for RIEN of river Mersey (UK).

Overall, even for moderate correlations between storm surge and river discharge values, a considerable number of days (time lag interval) seems to be an absolute necessity. An example of the highest correlation of ~0.37 (in zero-lag mode) is shown in Figure 4.6 valid for the river Mersey RIEN at Irish Sea.

4.1.4 Wave height & river discharge for MAX24 (maxima over 24 hours)

Strong correlations ($0.54 \leq \rho \leq 0.69$) between significant wave height and river discharge values were found in a considerable number of RIEN in Bay of Biscay, English Channel and Atlantic Sea, whereas zero correlations were found for Orkla (NO) and Danube (RO). Correlations falling into moderate and well categories were found for the rest of RIEN points. It should be noted (as in surge & discharge cases) most of max correlation values (see Table 4.4) are not valid for the same day (i.e., in zero-lag mode) but they refer to a considerable lag interval (of few days). Correlation spatial details are shown in Figure 4.7.

Table 4.4. Correlations between significant wave height & river discharge values for MAX24.

RIEN	River	Ocean / Sea	Lead	Correl.	Max	Lag (d)	Type
01	Po (IT)	Adriatic Sea	WAV / DIS	0.03	0.14	3	mod
02	Metauro (IT)	Adriatic Sea	DIS / WAV	0.30	*	0	mod
03	Vibrata (IT)	Adriatic Sea	WAV / DIS	0.32	0.33	1	mod
04	Foix (ES)	Balearic Sea	WAV / DIS	0.23	*	0	mod
05	Ebro (ES)	Balearic Sea	WAV / DIS	0.19	0.30	>7	mod
06	Velez (ES)	Alboran Sea	DIS / WAV	0.24	*	0	mod
07	Sella (ES)	Bay of Biscay	WAV / DIS	0.38	0.38	1	well
08	Rhone (FR)	Gulf of Lion	WAV / DIS	0.18	0.26	3	mod
09	Bethune (FR)	English Channel	WAV / DIS	0.32	0.40	4	well
10	Moros (FR)	Bay of Biscay	WAV / DIS	0.52	*	0	well
11	Aven (FR)	Bay of Biscay	WAV / DIS	0.51	0.55	3	strong
12	Blavet (FR)	Bay of Biscay	WAV / DIS	0.57	*	0	strong
13	Owenavorragh (IE)	Irish Sea	WAV / DIS	0.42	0.46	3	well
14	Goeta Aelv (SE)	North Sea	WAV / DIS	0.08	0.15	>7	mod
15	Orkla (NO)	Norwegian Sea	WAV / DIS	-0.04	-0.03	1	zero
16	Vantaa (FI)	Baltic Sea	WAV / DIS	0.13	0.14	2	mod
17	Rhine (NL)	North Sea	WAV / DIS	0.29	0.44	5	well
18	Weser (DE)	North Sea	WAV / DIS	0.21	0.31	6	mod
19	Schelde (BE)	North Sea	WAV / DIS	0.36	0.41	2	well
20	Severn (UK)	Bristol Channel	WAV / DIS	0.38	0.49	3	well
21	Mersey (UK)	Irish Sea	WAV / DIS	0.39	0.40	1	well
22	Tyne (UK)	North Sea	WAV / DIS	0.34	*	0	mod
23	Tamar (UK)	English Channel	WAV / DIS	0.58	0.58	1	strong
24	Avon (UK)	English Channel	WAV / DIS	0.44	0.50	4	well
25	Thames (UK)	North Sea	WAV / DIS	0.32	0.34	2	mod
26	Exe (UK)	English channel	WAV / DIS	0.50	0.54	1	strong
27	Humber (UK)	North Sea	WAV / DIS	0.28	0.30	1	mod
28	Danube (RO)	Black Sea	WAV / DIS	-0.04	*	0	zero
29	Tagus (PT)	Atlantic Ocean	WAV / DIS	0.43	0.47	4	well
30	Sado (PT)	Atlantic Ocean	WAV / DIS	0.45	0.47	1	well
31	Douro (PT)	Atlantic Ocean	WAV / DIS	0.54	0.56	1	strong
32	Guadianna (ES)	Atlantic Ocean	WAV / DIS	0.39	0.45	>7	well

The necessity of a lag interval is true especially for Ebro (ES), Goeta Aelv (SE) and Guadianna (ES) with lag intervals extending well above seven days. Looking into the lag correlations, wave values were found to be leading river discharge ones in almost every (RIEN) point. The only two exceptions were for river Metauro (IT) and river Velez (ES) that discharges were leading waves. It was also found that in both of these cases there was no lagging time interval. Only one case of correlation belonging to the strong category was found in a zero-lag mode. This was the case of Blavet (FR) RIEN with a correlation reaching 0.57 (zero-lag mode). It became also obvious for this case that significant wave height was leading over river discharge values.

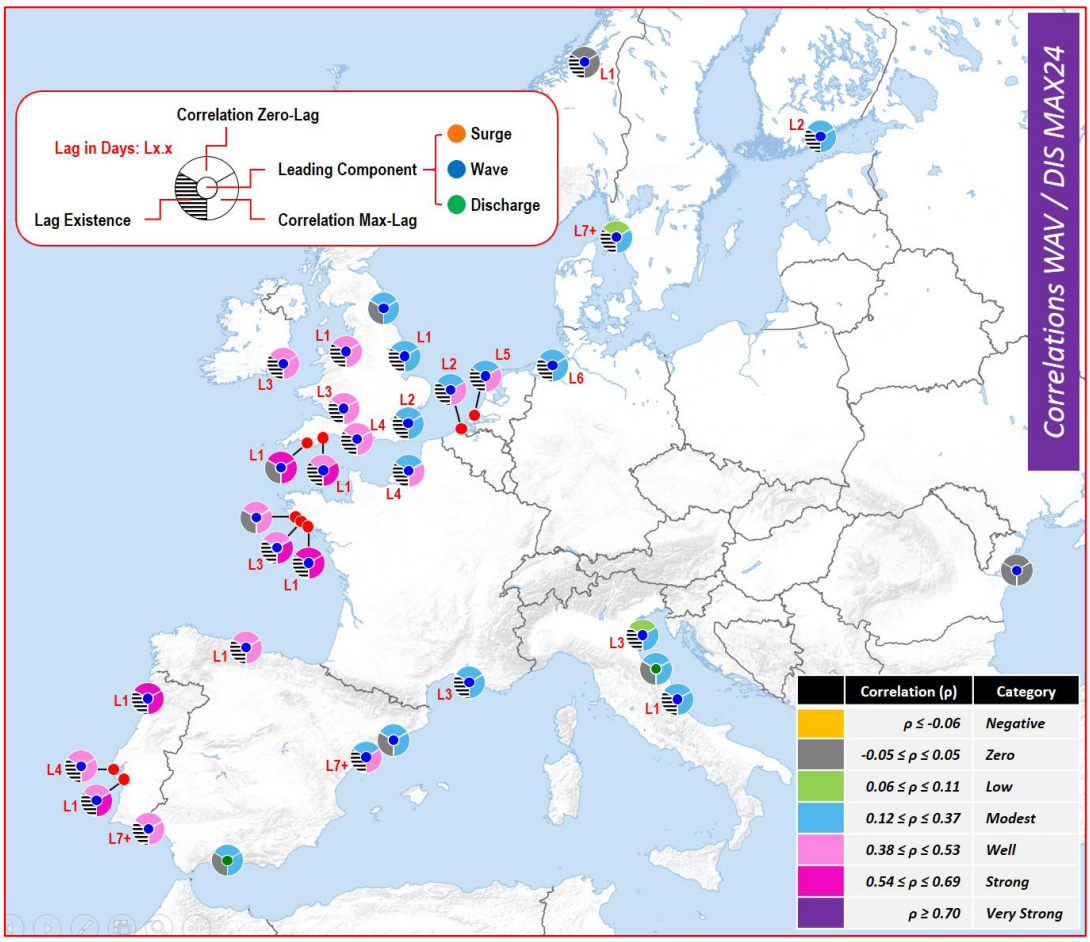

Figure 4.7. Map with spatial correlations between wave & river discharge values for MAX24.

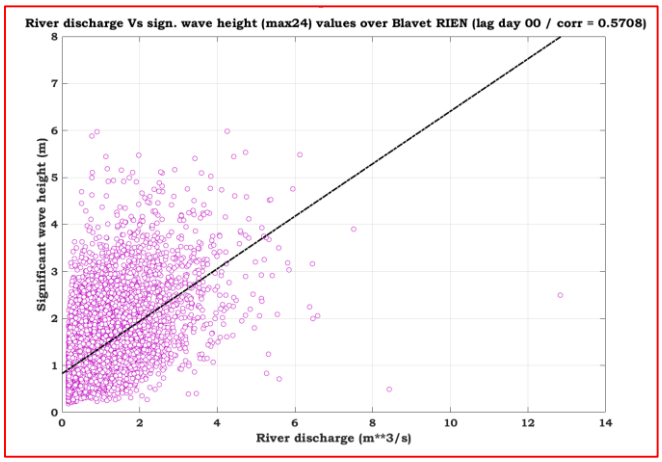

Figure 4.8. Scatterplot of wave & river discharge (max24) values valid for RIEN of river Blavet (FR).

Overall, correlations for wave & discharge cases seem to be quite higher than surge & discharge cases, although being considerable lower than surge & wave ones. The issue of lag time interval that seems as absolute necessity for a high value of correlation to be reached was quite pronounced once more as in the

previous surge & discharge case. Nevertheless, there were cases with high correlation values in zero-lag mode as well. An example of such high correlation (0.57) is shown in Figure 4.8 for RIEN of river Blavet (FR).

4.2 Statistical dependence assessment of combined event components over RIEN points

The type of statistical dependence for all combined events over the RIEN points considered in this study are presented in this section. The existence and magnitude of lag periods are also presented. Details concerning the leading source variables have already been presented in the corresponding subsections of correlation.

4.2.1 Storm surge & wave height for MAX12 (maxima over 12 hours)

Very strong statistical dependence values (chi ≥ 0.45) between storm surge and wave height values were found mainly over the coastal areas of English Channel and North Sea as shown in Table 4.5.

Table 4.5. Dependencies between surge & wave values for MAX12.

RIEN	River	CHI	Max	Type	Lag (d)	CHI (R)	Max (R)	Type (R)
01	Po (IT)	0.20	*	mod	0.0	0.24	*	mod
02	Metauro (IT)	0.15	*	mod	0.0	0.21	*	mod
03	Vibrata (IT)	0.21	*	mod	0.0	0.21	*	mod
04	Foix (ES)	0.07	*	low	0.0	0.15	*	mod
05	Ebro (ES)	0.19	*	mod	0.0	0.23	*	mod
06	Velez (ES)	0.08	*	low	0.0	0.13	*	low
07	Sella (ES)	0.12	0.12	low	0.5	0.18	0.19	mod
08	Rhone (FR)	0.10	0.12	low	0.5	0.16	0.18	mod
09	Bethune (FR)	0.56	*	v. strong	0.0	0.57	*	v. strong
10	Moros (FR)	0.20	*	mod	0.0	0.23	*	mod
11	Aven (FR)	0.22	*	mod	0.0	0.25	*	well
12	Blavet (FR)	0.22	*	mod	0.0	0.26	*	well
13	Owenavorragh (IE)	0.36	*	strong	0.0	0.38	*	strong
14	Goeta Aelv (SE)	0.38	0.42	strong	0.5	0.40	0.44	v. strong
15	Orkla (NO)	0.30	*	well	0.0	0.33	*	well
16	Vantaa (FI)	0.32	*	well	0.0	0.34	*	strong
17	Rhine (NL)	0.51	*	v. strong	0.0	0.52	*	v. strong
18	Weser (DE)	0.54	*	v. strong	0.0	0.55	*	v. strong
19	Schelde (BE)	0.41	*	strong	0.0	0.42	*	strong
20	Severn (UK)	0.18	*	mod	0.0	0.22	*	mod
21	Mersey (UK)	0.31	*	well	0.0	0.32	*	well
22	Tyne (UK)	0.13	0.13	low	0.5	0.18	0.18	mod
23	Tamar (UK)	0.27	*	well	0.0	0.29	*	well
24	Avon (UK)	0.39	*	strong	0.0	0.41	*	strong
25	Thames (UK)	0.08	0.18	mod	1.0	0.15	0.25	well
26	Exe (UK)	0.32	*	well	0.0	0.34	*	~strong
27	Humber (UK)	0.27	*	well	0.0	0.29	*	well
28	Danube (RO)	0.21	0.36	strong	0.5	0.24	0.39	strong
29	Tagus (PT)	0.14	0.15	mod	0.5	0.20	0.21	mod
30	Sado (PT)	0.16	*	mod	0.0	0.20	*	mod
31	Douro (PT)	0.21	*	mod	0.0	0.25	*	well
32	Guadianna (ES)	0.2484	*	well	0.0	0.29	*	well

In the Mediterranean Sea, most dependencies were found to belong in the moderate category (0.15 ≤ chi ≤ 0.24) with river Velez RIEN (Alboran Sea) belonging in the lowest category (0.06 ≤ chi ≤ 0.14). The lag period in most cases in the Mediterranean was found to be zero. For the rest of the coastal areas, a certain lagging of 12-hour was found in six cases only, meaning that combined events of interest might have taken place during the same day. The maximum lag period of one day (24 hours) was found over Thames RIEN linked to a dependence of 0.25 belonging to "well" category. Spatial details of dependence are shown in Figure 4.9.

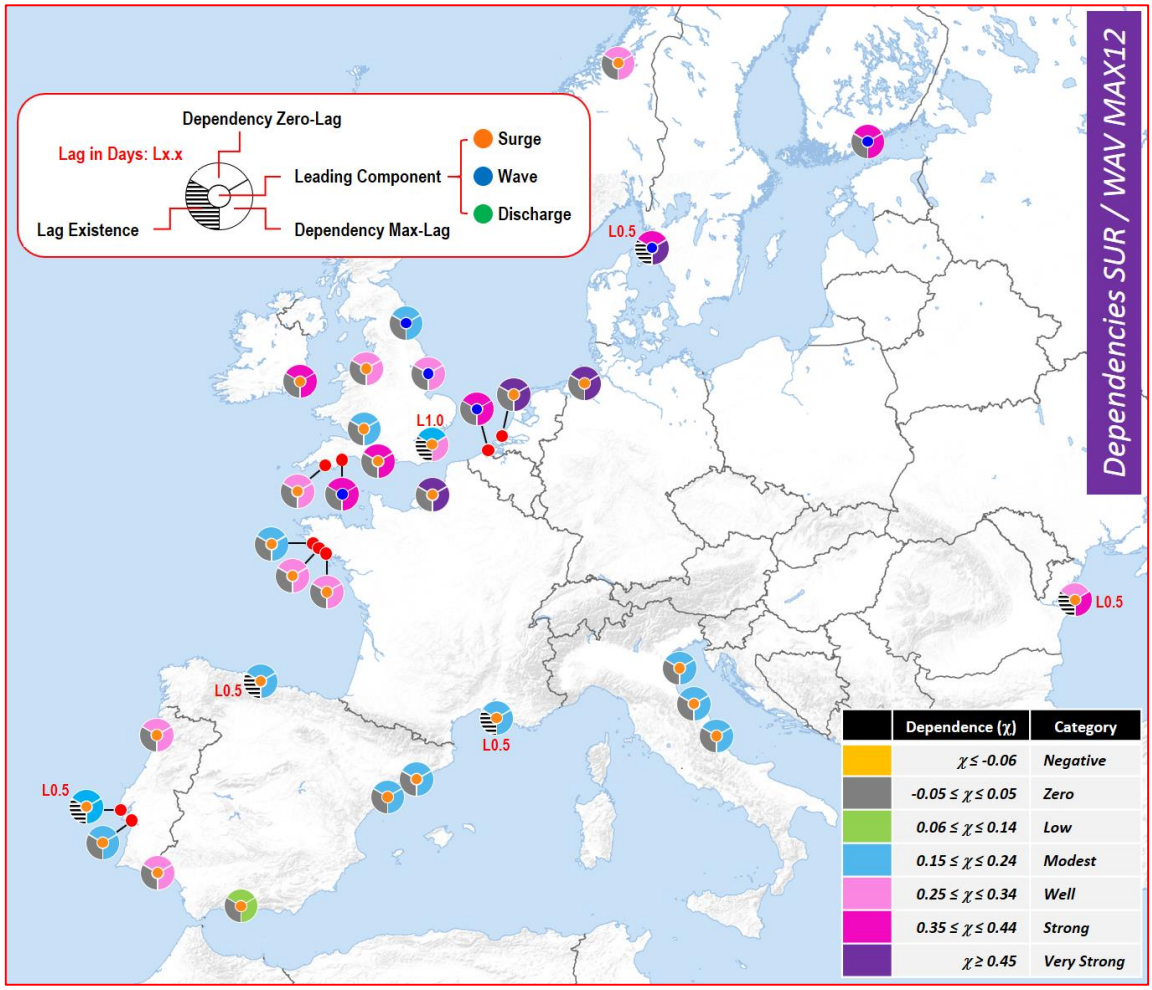

Figure 4.9. Map with local values of dependence between surge & wave for MAX12.

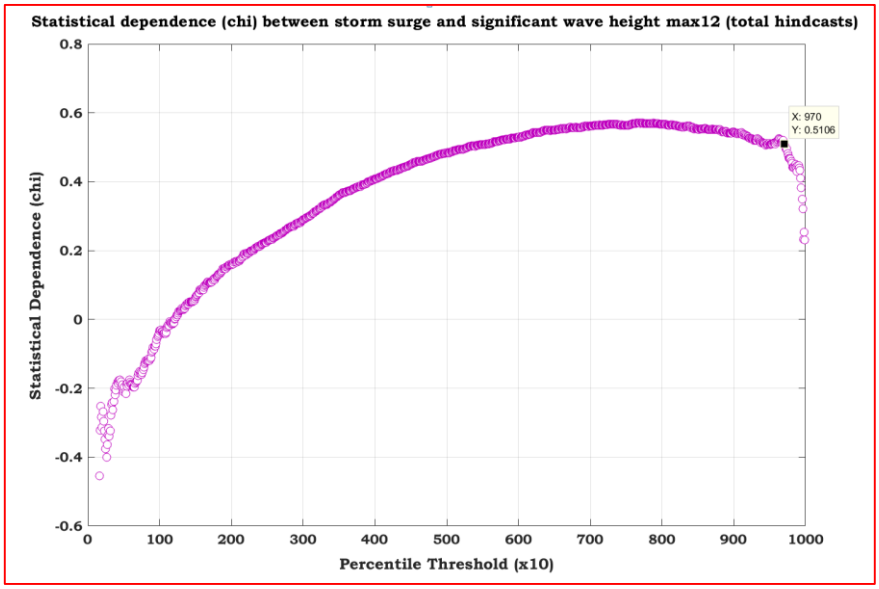

Figure 4.10. Dependence of storm surge & wave height (max12) values valid for RIEN of river Rhine (NL).

Overall, very strong and strong values of dependence were found mostly on the same 12-hour interval (zero-lag mode) as shown in Table 4.5. An example of such (very) strong dependence with zero-lagging is shown in Figure 4.10. It is valid for the RIEN point of river Rhine (NL) in hindcast (total) mode being produced by utilising mat_chi (matlab) function routines. Studying closely Figure 4.10 it obvious that dependence values after 97% percentile threshold seem to break down and become quite erratic due to the fact that there are not enough joint extremes for calculating certain terms of the dependence equation.

It is important to point out that in case of matlab (mat_chi & mat_chi_lag) routines applied for the estimation of dependence values (shown in Figure 4.10), besides POT (Peaks-Over-Threshold) methodology, an additional criterion concerning the selection of the critical threshold has been applied. This criterion ensures that not more than ~2.3 to ~2.5 events per year are to be exceed as in Svensson and Jones (2005).

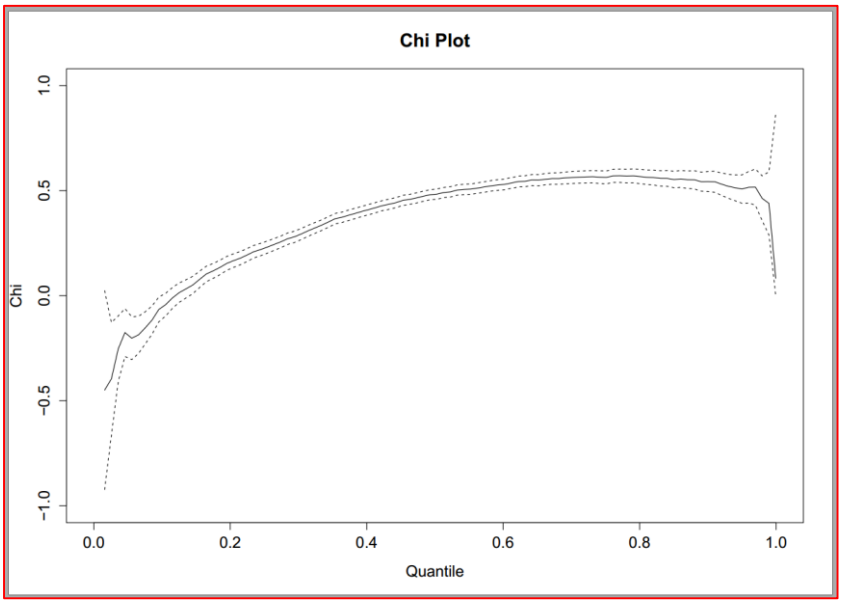

Figure 4.11. Dependence of storm surge & wave height (max12) values valid for RIEN of river Rhine (NL).

Besides mat_chi & mat_chi_lag dependence matlab routines, results from routines contained in the statistical package evd (chiplot) of R with the approximate 95% confidence intervals are shown in Figure 4.11. Values of chi estimated by R routines were found to be slightly higher than matlab routines most probably due to the different set of criteria concerning the selection of critical (percentile) thresholds.

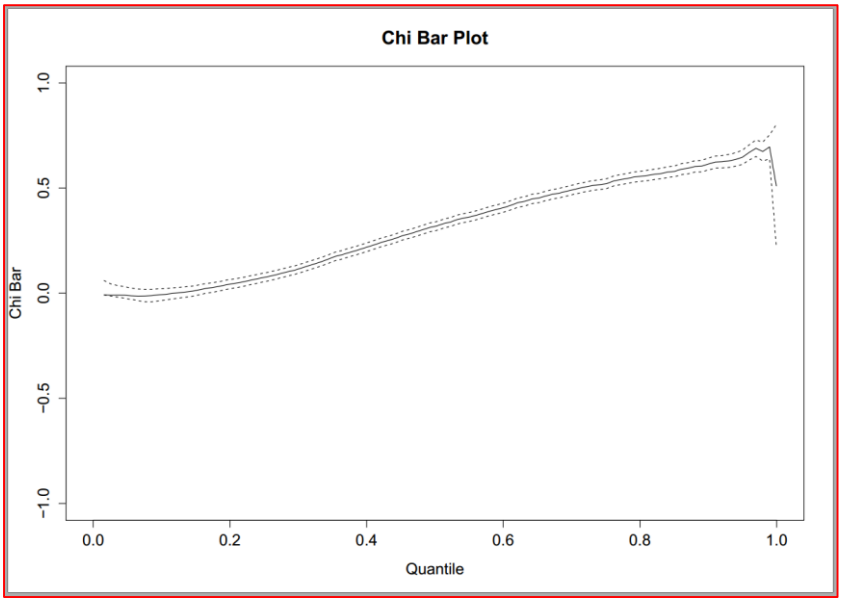

Figure 4.12. Dependence (BAR) of surge & wave height (max12) values valid for RIEN of river Rhine (NL).

Furthermore, the "sister" plot of dependence chi, the plot of parameter "chibar" with its 95% significance intervals is shown in Figure 4.12. It should be pointed out that "chibar" provides the strength of dependence within the class of asymptotically independent variables whereas chi (dependence) values provide a measure summarizing the strength of dependence within the class of asymptotically dependent variables.

4.2.2 Storm surge & wave height for MAX24 (maxima over 24 hours)

Very strong statistical dependence values (chi ≥ 0.45) between storm surge and wave height values were found in three cases over the coastal areas of English Channel and North Sea in zero-lag mode. This zero-lag found to be the case for additional six cases of strong dependencies (0.35 ≤ chi ≤ 0.44) over the same coastal areas including the Irish Sea (see Table 4.6). Spatial details of dependence are shown in Figure 4.13.

Table 4.6. Dependencies between surge & wave values for MAX24.

RIEN	River	CHI	Max	Type	Lag (d)	CHI (R)	Max (R)	Type (R)
01	Po (IT)	0.21	*	mod	0	0.24	*	mod
02	Metauro (IT)	0.15	*	mod	0	0.19	*	mod
03	Vibrata (IT)	0.24	*	low	0	0.23	*	mod
04	Foix (ES)	0.08	*	low	0	0.13	*	low
05	Ebro (ES)	0.19	*	mod	0	0.23	*	mod
06	Velez (ES)	0.08	*	low	0	0.13	*	low
07	Sella (ES)	0.12	*	low	0	0.17	*	mod
08	Rhone (FR)	0.12	*	low	0	0.16	*	mod
09	Bethune (FR)	0.63	*	v. strong	0	0.64	*	v. strong
10	Moros (FR)	0.23	*	mod	0	0.26	*	well
11	Aven (FR)	0.26	*	well	0	0.28	*	well
12	Blavet (FR)	0.25	*	well	0	0.28	*	well
13	Owenavorragh (IE)	0.37	*	strong	0	0.38	*	strong
14	Goeta Aelv (SE)	0.38	0.39	strong	1	0.40	0.42	strong
15	Orkla (NO)	0.30	*	well	0	0.31	*	well
16	Vantaa (FI)	0.32	*	well	0	0.34	*	strong
17	Rhine (NL)	0.55	*	v. strong	0	0.57	*	v. strong
18	Weser (DE)	0.54	*	v. strong	0	0.55	*	v. strong
19	Schelde (BE)	0.41	*	strong	0	0.42	*	strong
20	Severn (UK)	0.21	*	mod	0	0.24	*	mod
21	Mersey (UK)	0.32	*	well	0	0.34	*	well
22	Tyne (UK)	0.12	*	low	0	0.16	*	mod
23	Tamar (UK)	0.29	*	well	0	0.31	*	well
24	Avon (UK)	0.43	*	strong	0	0.44	*	strong
25	Thames (UK)	0.11	0.17	mod	1	0.16	0.22	mod
26	Exe (UK)	0.33	*	well	0	0.35	*	strong
27	Humber (UK)	0.28	*	well	0	0.30	*	well
28	Danube (RO)	0.23	*	mod	0	0.26	*	well
29	Tagus (PT)	0.17	*	mod	0	0.22	*	mod
30	Sado (PT)	0.18	*	mod	0	0.22	*	mod
31	Douro (PT)	0.23	*	mod	0	0.26	*	well
32	Guadianna (ES)	0.27	*	well	0	0.30	*	well

In the Mediterranean Sea, most of dependencies were found to fall in the moderate category (0.15 ≤ chi ≤ 0.24) whereas river Velez RIEN (Alboran Sea) and Foix RIEN were found to belong in the lowest category (0.06 ≤ chi ≤ 0.14). The lag period in all cases in the Mediterranean was zero. Such zero lagging was found to be the case for almost all the cases in this max24 section. The maximum lag period of one day was found over Thames RIEN (UK) linked to a dependence value of 0.22 belonging to "well" category and over Goeta Aelv RIEN (SE) linked to a strong value of 0.42. It should be noted that dependencies for max24 found to be slightly higher than max12. Also, in most cases the lag period for max24 was equal to zero.

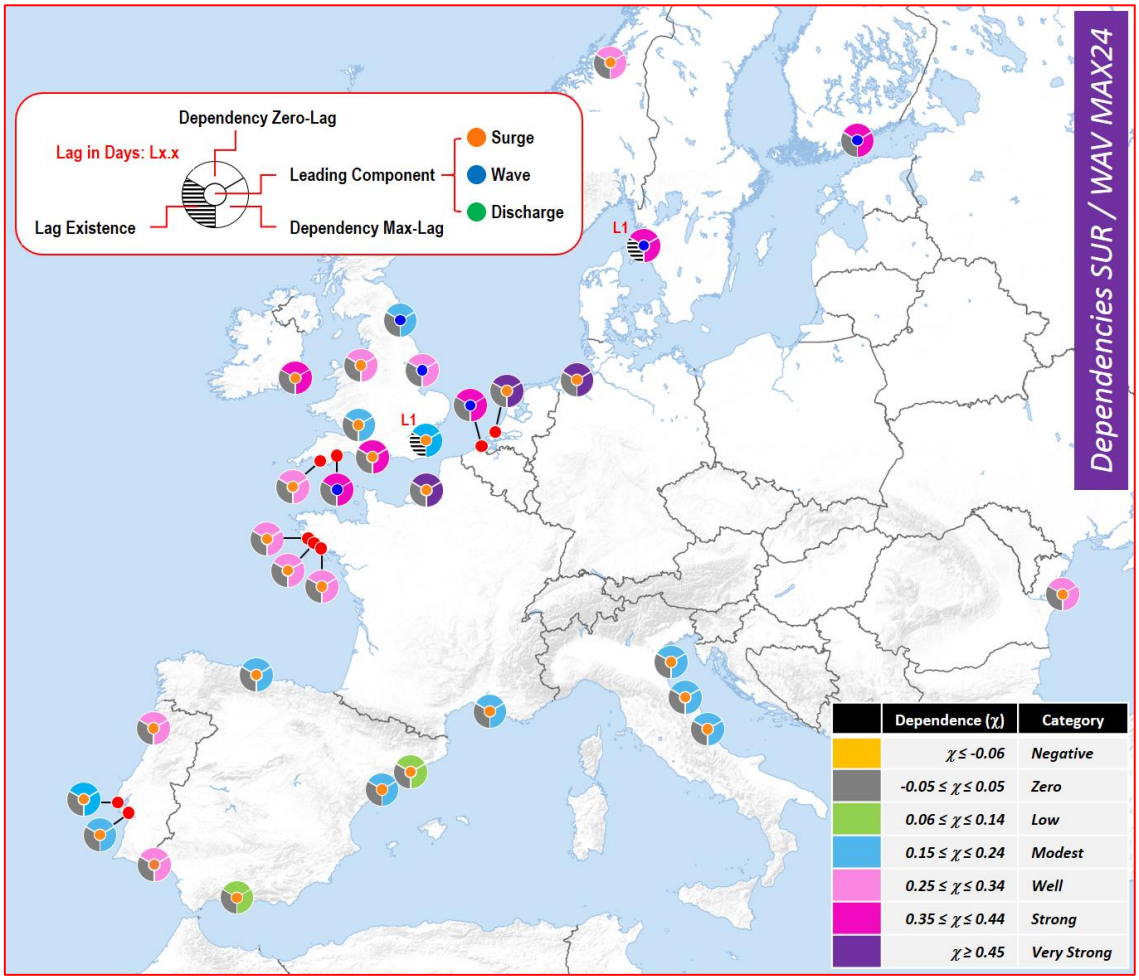

Figure 4.13. Map with local values of dependence between surge & wave values for MAX24.

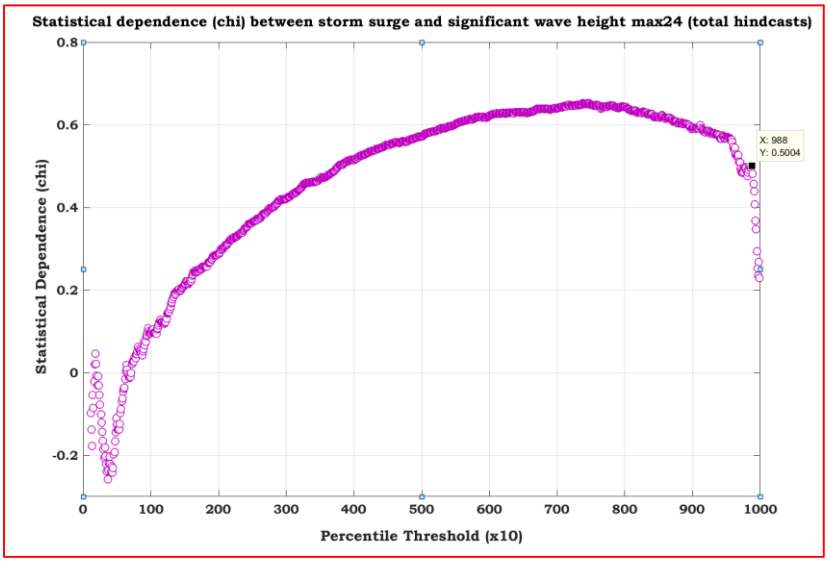

Figure 4.14. Dependence of storm surge & wave (max24) values valid for RIEN of river Rhine (NL).

Overall, very strong and strong dependencies appear mostly on the same 24-hour interval in zero-lag mode. In accordance with max12 section, an example of such (very) strong dependence (in zero-lag) is shown in Figure 4.14 valid for the RIEN of river Rhine (NL) in hindcast (total) mode by utilizing mat_chi (matlab) function routines. Details of how dependence varies within upper percentiles are shown in Figure 4.15. Stability seems to suggest the 96% threshold resulting to a very high value of dependence (0.55).

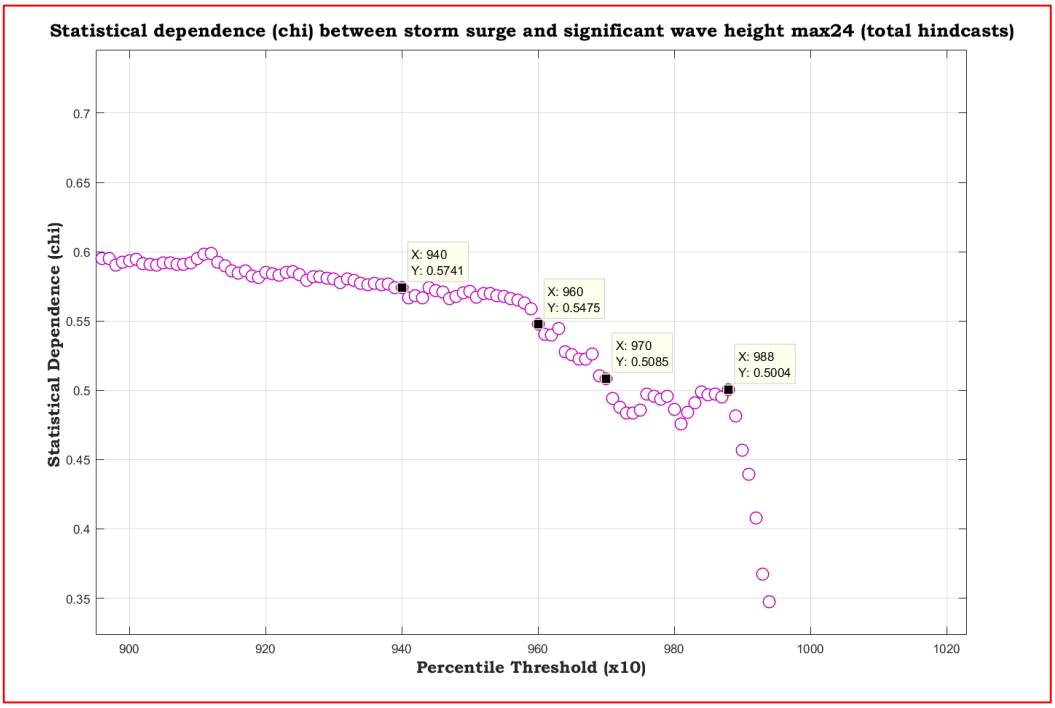

Figure 4.15. Details of dependence of surge & wave (max24) values valid for RIEN of river Rhine (NL).

Additional plot of chi (for inter-comparison with Figure 4.14 & Figure 4.15) containing the 95% confidence intervals by utilizing the routine "chiplot" of module "evd" (Extreme Value Distributions) of the integrated statistical package R is shown below in Figure 4.16.

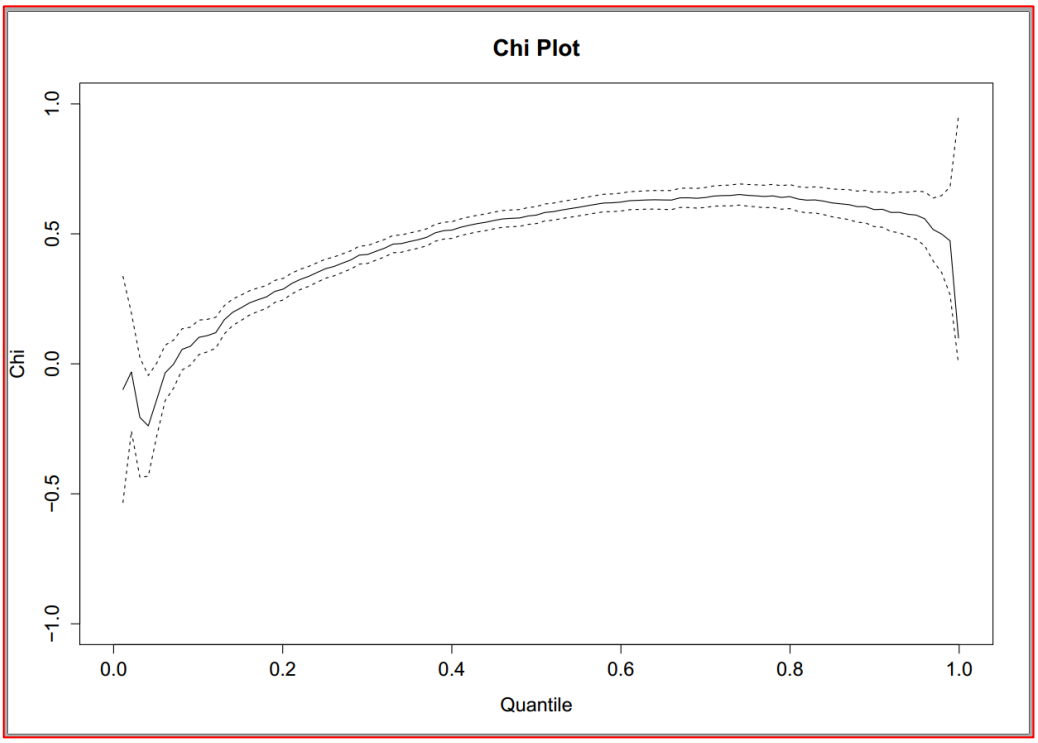

Figure 4.16. Dependence of storm surge & wave (max24) values valid for RIEN of river Rhine (NL).

4.2.3 Storm surge & river discharge for MAX24 (maxima over 24 hours)

Moderate (0.15 ≤ chi ≤ 0.24) to well (0.25 ≤ chi ≤ 0.34) values of statistical dependence between storm surge and river discharge were found in most cases. Only two cases belonging in the low category (0.06 ≤ ρ ≤ 0.14) were found for Orkla (NO) and Avon (UK) RIEN points. Spatial details of dependence are contained in Table 4.7.

Table 4.7. Dependencies between surge & river discharge values for MAX24.

RIEN	River	CHI	Max	Type	Lag (d)	CHI (R)	Max (R)	Type (R)
01	Po (IT)	0.05	0,14	mod	4	0.13	0.23	mod
02	Metauro (IT)	0.21	*	mod	0	0.25	*	well
03	Vibrata (IT)	0.15	0.19	mod	2	0.20	0.24	well
04	Foix (ES)	0.09	0.10	low	1	0.16	0.17	mod
05	Ebro (ES)	0.05	0.08	low	3	0.15	0.17	mod
06	Velez (ES)	0.18	*	mod	0	0.23	*	mod
07	Sella (ES)	0.13	0.16	mod	1	0.18	0.22	mod
08	Rhone (FR)	0.11	0.23	mod	4	0.18	0.30	well
09	Bethune (FR)	0.14	0.20	mod	4	0.20	0.26	well
10	Moros (FR)	0.15	*	mod	0	0.20	*	mod
11	Aven (FR)	0.13	*	low	0	0.18	*	mod
12	Blavet (FR)	0.17	*	mod	0	0.22	*	mod
13	Owenavorragh (IE)	0.16	0.19	mod	2	0.21	0.24	mod
14	Goeta Aelv (SE)	0.07	0.07	low	1	0.18	0.18	mod
15	Orkla (NO)	-0.07	-0.05	zero	2	0.09	0,11	low
16	Vantaa (FI)	0.10	*	low	0	0.19	*	mod
17	Rhine (NL)	0.12	0.22	mod	4	0.19	0.28	well
18	Weser (DE)	0.15	0.25	well	6	0.21	0.30	well
19	Schelde (BE)	0.15	0.16	mod	1	0.20	0.22	mod
20	Severn (UK)	0.13	0.20	mod	3	0.19	0.25	well
21	Mersey (UK)	0.16	0.18	mod	2	0.21	0.24	mod
22	Tyne (UK)	0.14	*	mod	0	0.20	*	mod
23	Tamar (UK)	0.20	*	mod	0	0.24	*	well
24	Avon (UK)	0.20	0.23	mod	2	0.24	0.27	well
25	Thames (UK)	0.01	*	zero	0	0.12	*	low
26	Exe (UK)	0.22	*	mod	0	0.26	*	well
27	Humber (UK)	0.07	*	low	0	0.15	*	mod
28	Danube (RO)	-0.01	0.07	low	>7	0.11	0.20	mod
29	Tagus (PT)	0.08	0.15	mod	>7	0.18	0.25	well
30	Sado (PT)	0.15	0.17	mod	3	0.23	0.25	well
31	Douro (PT)	0.24	0.26	well	1	0.29	0.31	well
32	Guadianna (ES)	0.12	0.14	mod	3	0.22	0.24	well

It should be noted that most of the cases belonging to moderate and well categories were not assessed on the same day (i.e., in zero-lag mode) but they were referring to a considerable lag interval (of a few days). There were even two cases with time lags extending well above seven days, e.g., for Danube (RO) and Tagus (PT) RIEN points. The issue of lagging appears to be quite important in estimating dependencies between surge and river discharge values since a certain lag interval seems to be necessary in order for some considerable / significant value of statistical dependence to be reached.

Based on this, it comes as no surprise that in order for relatively high values of dependence to be reached (the well category for example) a considerable lagging is required in most of the cases analysed here. Same wise, substantial lower values of dependence should be expected in most cases when a zero-lag mode environment is considered.

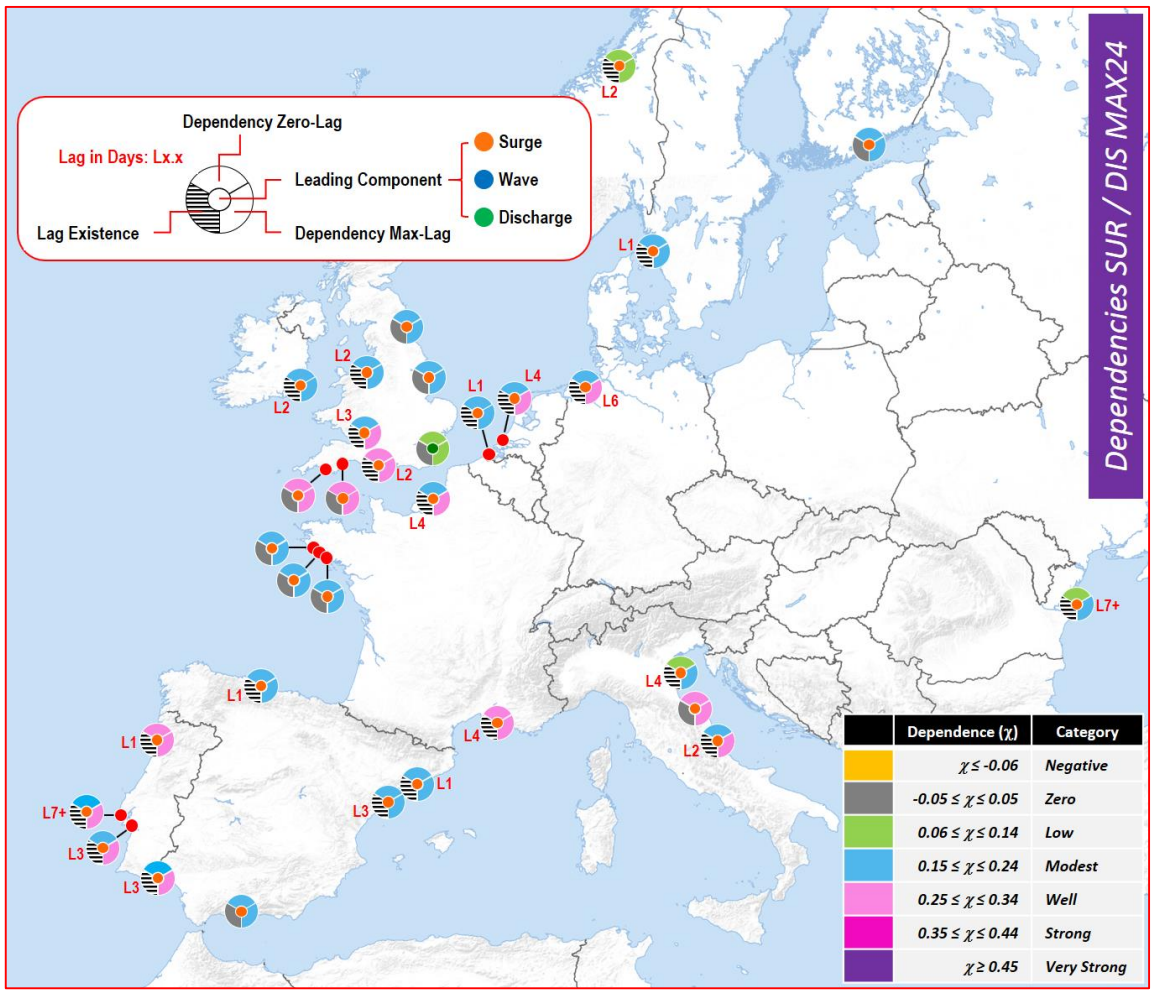

Figure 4.17. Map with local values of dependence between surge & river discharge values for MAX24.

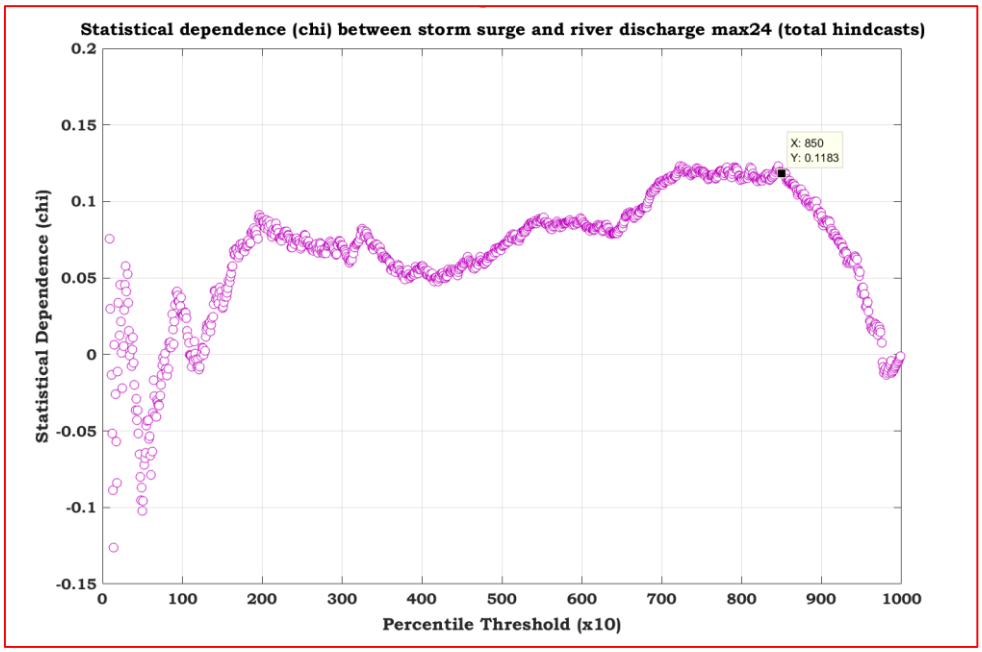

Figure 4.18. Dependence of surge & river discharge (max24) values valid for RIEN of river Rhine (NL).

In contrary to surge & wave max12 and max 24 cases examined in previous subsections, an example of a low dependence (as zero-lag is considered) is shown in Figure 4.18 valid for the RIEN point of river Rhine (NL) in hindcast (total) mode by utilizing mat_chi (matlab) function routines. It should be noted that in a lag mode environment of 4 days, substantial higher values of dependence should be expected, as the ones shown in Table 4.7, contained in columns Max & Max (R).

4.2.4 Wave height & river discharge for MAX24 (maxima over 24 hours)

Strong statistical dependence values (0.35 ≤ chi ≤ 0.44) between wave height and river discharge values were found for six cases over the coastal areas of Bay of Biscay and eastern Atlantic Ocean (Table 4.8). In Mediterranean Sea, most of dependencies were found to belong in the moderate category (0.15 ≤ chi ≤ 0.24) with river Ebro RIEN (Balearic Sea) belonging in the well category (0.25 ≤ chi ≤ 0.34) with a lagging of a few days, while for river Ebro (RIEN) this lagging was found to be extended even beyond 7 days.

Table 4.8. Dependencies between wave & river discharge values for MAX24.

RIEN	River	CHI	MAX	Type	Lag (d)	CHI (R)	Max (R)	Type (R)
01	Po (IT)	0.02	0.07	low	3	0.12	0.17	mod
02	Metauro (IT)	0.15	*	mod	0	0.20	*	mod
03	Vibrata (IT)	0.16	0.17	mod	1	0.21	0.21	mod
04	Foix (ES)	0.14	*	mod	0	0.21	*	mod
05	Ebro (ES)	0.09	0.16	mod	>7	0.17	0.24	well
06	Velez (ES)	0.19	*	mod	0	0.23	*	mod
07	Sella (ES)	0.18	0.18	mod	1	0.23	0.24	mod
08	Rhone (FR)	0.07	0.11	low	2	0.15	0.18	mod
09	Bethune (FR)	0.16	0.22	mod	3	0.22	0.28	well
10	Moros (FR)	0.32	*	well	0	0.35	*	strong
11	Aven (FR)	0.29	0.33	well	3	0.33	0.37	strong
12	Blavet (FR)	0.30	0.32	well	1	0.33	0.35	strong
13	Owenavorragh (IE)	0.17	0.19	mod	3	0.21	0.23	mod
14	Goeta Aelv (SE)	0.04	0.06	low	2	0.14	0.15	mod
15	Orkla (NO)	-0.02	*	zero	0	0.11	*	low
16	Vantaa (FI)	0.04	0.06	low	2	0.12	0.15	mod
17	Rhine (NL)	0.12	0.29	well	5	0.21	0.34	well
18	Weser (DE)	0.13	0.20	mod	6	0.19	0.27	well
19	Schelde (BE)	0.19	0.24	mod	2	0.24	0.29	well
20	Severn (UK)	0.20	0.29	well	3	0.24	0.33	well
21	Mersey (UK)	0.16	0.16	mod	1	0.21	0.22	mod
22	Tyne (UK)	0.10	*	low	0	0.16	*	mod
23	Tamar (UK)	0.30	*	well	0	0.33	*	well
24	Avon (UK)	0.25	0.28	well	3	0.29	0.32	well
25	Thames (UK)	0.14	0.16	mod	1	0.20	0.22	mod
26	Exe (UK)	0.27	0.29	well	1	0.30	0.32	well
27	Humber (UK)	0.09	0.10	low	1	0.16	0.17	mod
28	Danube (RO)	-0.04	*	zero	0	0.10	*	low
29	Tagus (PT)	0.23	0.28	well	4	0.29	0.33	well
30	Sado (PT)	0.28	0.31	well	4	0.32	0.35	strong
31	Douro (PT)	0.31	0.33	well	1	0.35	0.37	strong
32	Guadianna (ES)	0.27	0.29	well	3	0.32	0.34	~strong

As in surge & discharge case, a well pronounced characteristic of wave & discharge dependencies seems to be the lag time interval that seems to be necessary in order for high values of statistical dependence to be reached. Only a limited (8) cases found to exhibit zero-lag time characteristics and only one of them (RIEN of river Moros) reached a strong value of dependence (0.35). Investigating further over lag dependencies, wave values were found to lead discharge ones as already highlighted in the corresponding section of correlations (Table 4.4). This applies for all cases except Metauro river (Adriatic Sea) and Velez river (Alboran Sea) RIEN points. Spatial details of dependence can be seen in Figure 4.19.

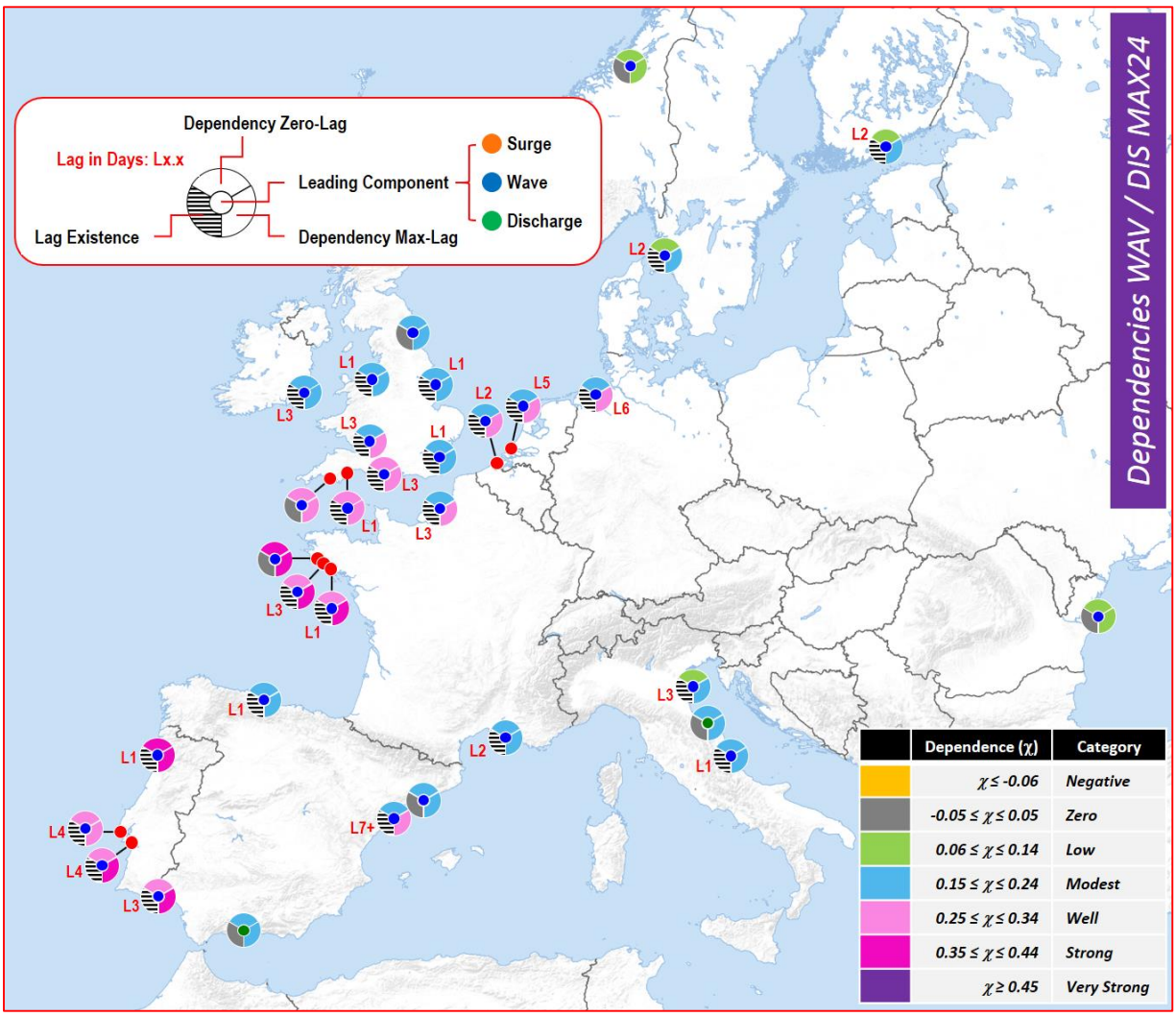

Figure 4.19. Map with local values of dependence between wave & river discharge values for MAX24.

In accordance with previous dependence examples presented already in previous subsections, an example of dependence belonging to well category in zero-lag mode is contained in Figure 4.20 valid for the ending point (RIEN) of river Rhine (NL) in hindcast (total) mode by utilizing mat_chi (matlab) function routines. It should be noted that in a lagging mode environment of 5 days, considerably higher values of dependence were estimated (as shown in Table 4.8).

Details (zooming over) referring to upper percentiles of Figure 4.20 are shown in Figure 4.21. The plot referring to zero lag mode highlights the difficulties and limitations concerning the selection of an optimal threshold for the estimation of dependence. For instance, if all "conservative" rules are applied by mat_chi routines, then the 94% percentile is to be selected (corresponding to ~2.5 combined events on a yearly basis). This gives a quite low value of dependence (0.12). On the other hand, if someone is after a more stable computational environment, then the 84% percentile appears to be more appropriate resulting to a substantial higher value of dependence (0.24). Nevertheless, the more "conservative" dependence value (0.12) was kept in this case (Table 4.8) for harmonising results over the coastal areas considered in this study.

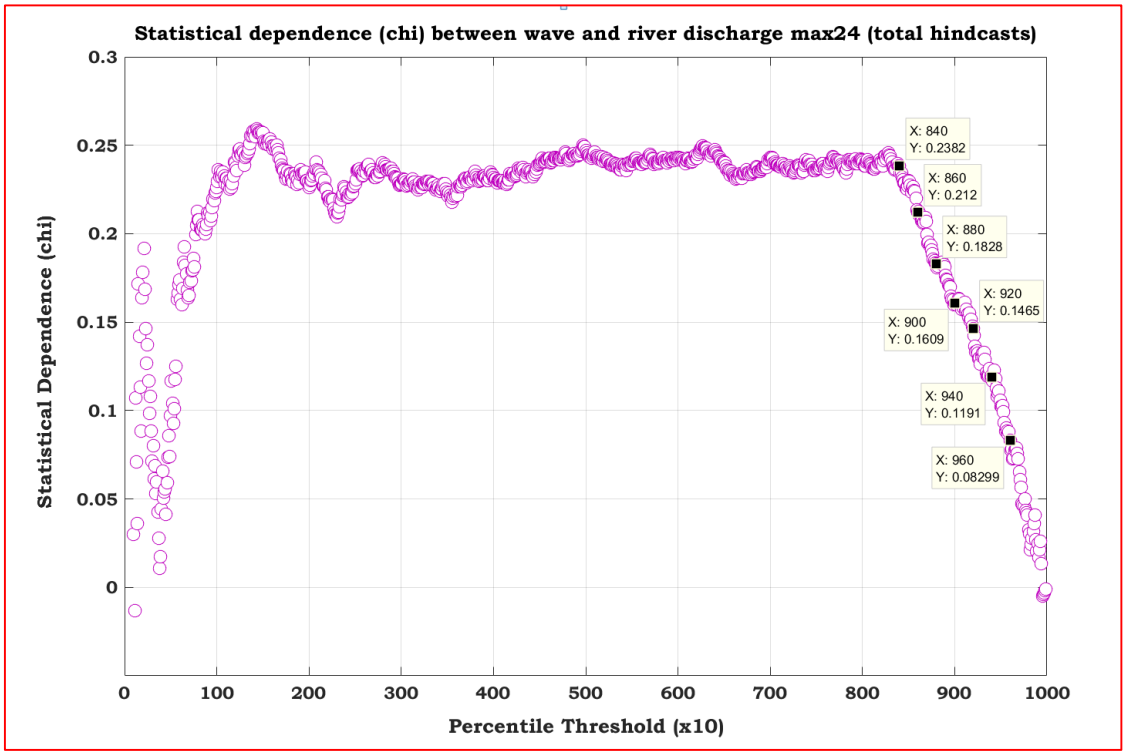

Figure 4.20. Dependence of wave & river discharge (max24) values valid for RIEN of river Rhine (NL).

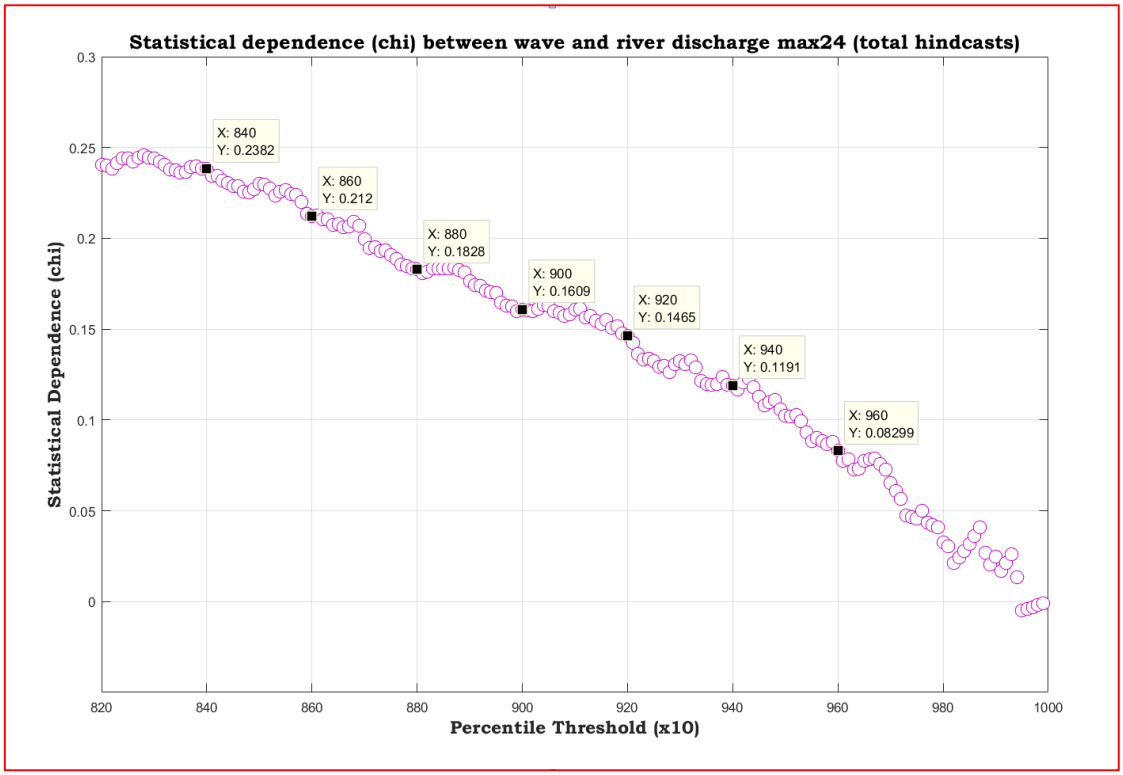

Figure 4.21. Dependence of wave & discharge (max24) values valid for RIEN of river Rhine (NL) details.

Two Tables (4.9 & 4.10) summarizing the results on dependence are shown below for zero-lag and max-lag cases correspondingly. A categorisation of the coastal / sea areas is also performed. Changes with previous detailed Tables are highlighted by a yellow colour. The different sea areas of the Mediterranean Sea (North Adriatic Sea, Gulf of Lion, Balearic Sea & Alboran Sea), the Bay of Biscay, the English Channel, the Irish Sea & Bristol Channel, the Norwegian Sea & the Baltic Sea, the North Sea, the Black Sea and the North-eastern Atlantic Ocean are depicted also in different colour shades.

Table 4.9. Correlations & dependencies between surge, wave & discharge values for zero-lag mode.

RIEN	River	Ocean / Sea	S / W12	S / W24	S / R24	W / R24
01	Po (IT)	Adriatic Sea	mod	mod	low	low
02	Metauro (IT)	Adriatic Sea	mod	mod	well	mod
03	Vibrata (IT)	Adriatic Sea	mod	mod	mod	mod
08	Rhone (FR)	Gulf of Lion	mod	mod	mod	mod
04	Foix (ES)	Balearic Sea	mod	low	mod	mod
05	Ebro (ES)	Balearic Sea	mod	mod	mod	mod
06	Velez (ES)	Alboran Sea	low	low	mod	mod
07	Sella (ES)	Bay of Biscay	mod	mod	mod	mod
10	Moros (FR)	Bay of Biscay	mod	well	mod	strong
11	Aven (FR)	Bay of Biscay	well	well	mod	well
12	Blavet (FR)	Bay of Biscay	well	well	mod	well
13	Owenavorragh (IE)	Irish Sea	strong	strong	mod	mod
21	Mersey (UK)	Irish Sea	well	well	mod	mod
20	Severn (UK)	Bristol Channel	mod	mod	mod	well
15	Orkla (NO)	Norwegian Sea	well	well	low	low
16	Vantaa (FI)	Baltic Sea	strong	strong	mod	low
22	Tyne (UK)	North Sea	mod	mod	mod	mod
27	Humber (UK)	North Sea	well	well	mod	mod
14	Goeta Aelv (SE)	North Sea	v. strong	strong	mod	low
17	Rhine (NL)	North Sea	v. strong	v. strong	mod	mod
18	Weser (DE)	North Sea	v. strong	v. strong	mod	mod
19	Schelde (BE)	North Sea	strong	strong	mod	~well
25	Thames (UK)	North Sea	mod	mod	low	mod
09	Bethune (FR)	English Channel	v. strong	v. strong	mod	mod
24	Avon (UK)	English Channel	strong	strong	well	well
26	Exe (UK)	English channel	~strong	strong	well	well
23	Tamar (UK)	English Channel	well	well	well	well
28	Danube (RO)	Black Sea	strong	well	low	low
31	Douro (PT)	Atlantic Ocean	well	well	well	strong
29	Tagus (PT)	Atlantic Ocean	mod	mod	mod	well
30	Sado (PT)	Atlantic Ocean	mod	mod	mod	well
32	Guadianna (ES)	Atlantic Ocean	well	well	mod	well

Table 4.10. Correlations & dependencies between surge, wave & discharge values in max-lag mode.

RIEN	River	Ocean / Sea	L	S / W12	L	S / W24	L	S / R24	L	W / R24
01	Po (IT)	Adriatic Sea	0	mod	0	mod	4	mod	3	mod
02	Metauro (IT)	Adriatic Sea	0	mod	0	mod	0	well	0	mod
03	Vibrata (IT)	Adriatic Sea	0	mod	0	mod	2	well	1	mod
08	Rhone (FR)	Gulf of Lion	0.5	mod	0	mod	4	well	2	mod
04	Foix (ES)	Balearic Sea	0	mod	0	low	1	mod	0	mod
05	Ebro (ES)	Balearic Sea	0	mod	0	mod	3	mod	>7	well
06	Velez (ES)	Alboran Sea	0	low	0	low	0	mod	0	mod
07	Sella (ES)	Bay of Biscay	0.5	mod	0	mod	1	mod	1	mod
10	Moros (FR)	Bay of Biscay	0	mod	0	well	0	mod	0	strong
11	Aven (FR)	Bay of Biscay	0	well	0	well	0	mod	3	strong
12	Blavet (FR)	Bay of Biscay	0	well	0	well	0	mod	1	strong
13	Owenavorragh (IE)	Irish Sea	0	strong	0	strong	2	mod	3	mod
21	Mersey (UK)	Irish Sea	0	well	0	well	2	mod	1	mod
20	Severn (UK)	Bristol Channel	0	mod	0	mod	3	well	3	well
15	Orkla (NO)	Norwegian Sea	0	well	0	well	2	low	0	low
16	Vantaa (FI)	Baltic Sea	0	strong	0	strong	0	mod	2	mod
22	Tyne (UK)	North Sea	0.5	mod	0	mod	0	mod	0	mod
27	Humber (UK)	North Sea	0	well	0	well	0	mod	1	mod
14	Goeta Aelv (SE)	North Sea	0.5	v. strong	1	strong	1	mod	2	mod
17	Rhine (NL)	North Sea	0	v. strong	0	v. strong	4	well	5	well
18	Weser (DE)	North Sea	0	v. strong	0	v. strong	6	well	6	well
19	Schelde (BE)	North Sea	0	strong	0	strong	1	mod	2	well
25	Thames (UK)	North Sea	1	well	1	mod	0	low	1	mod
09	Bethune (FR)	English Channel	0	v. strong	0	v. strong	4	well	3	well
24	Avon (UK)	English Channel	0	strong	0	strong	2	well	3	well
26	Exe (UK)	English channel	0	~strong	0	strong	0	well	1	well
23	Tamar (UK)	English Channel	0	well	0	well	0	well	0	well
28	Danube (RO)	Black Sea	0.5	strong	0	well	>7	mod	0	low
31	Douro (PT)	Atlantic Ocean	0	well	0	well	1	well	1	strong
29	Tagus (PT)	Atlantic Ocean	0.5	mod	0	mod	>7	well	4	well
30	Sado (PT)	Atlantic Ocean	0	mod	0	mod	3	well	4	strong
32	Guadianna (ES)	Atlantic Ocean	0	well	0	well	3	well	3	~strong

Overall, the highest values of (strong / very strong) correlations and dependencies were found between surge and wave values mainly over the North Sea and the English Channel taking place (as a combined event) on the same day (zero-lag mode) in most of the cases.

Considering the compound events of surge and river discharge, moderate to well category values were found in most cases but not in a zero-lag mode as in the previous surge & wave combined events. It also became clear that in order to achieve such (moderate to well) values, a considerable lag time interval (in most cases of few days) was required with surge clearly leading discharge values.

For the case of wave and river discharge, well to strong category values were found but once more mostly in a non-zero mode indicating the necessity of a considerable lag time interval for such (well to strong) values to be reached.

Inter-comparisons with previous research results was not easy since there have not been so many journal papers covering the wide range of the areas and combination of source variables being investigated in the current Report. Nevertheless, based on existing work so far an inter-comparison of this Report's results to some published results taken from "Use of Joint Probability Methods in Flood Management: A Guide to Best Practice" Technical Report by Hawkes (2005) are presented in Figure 4.22.

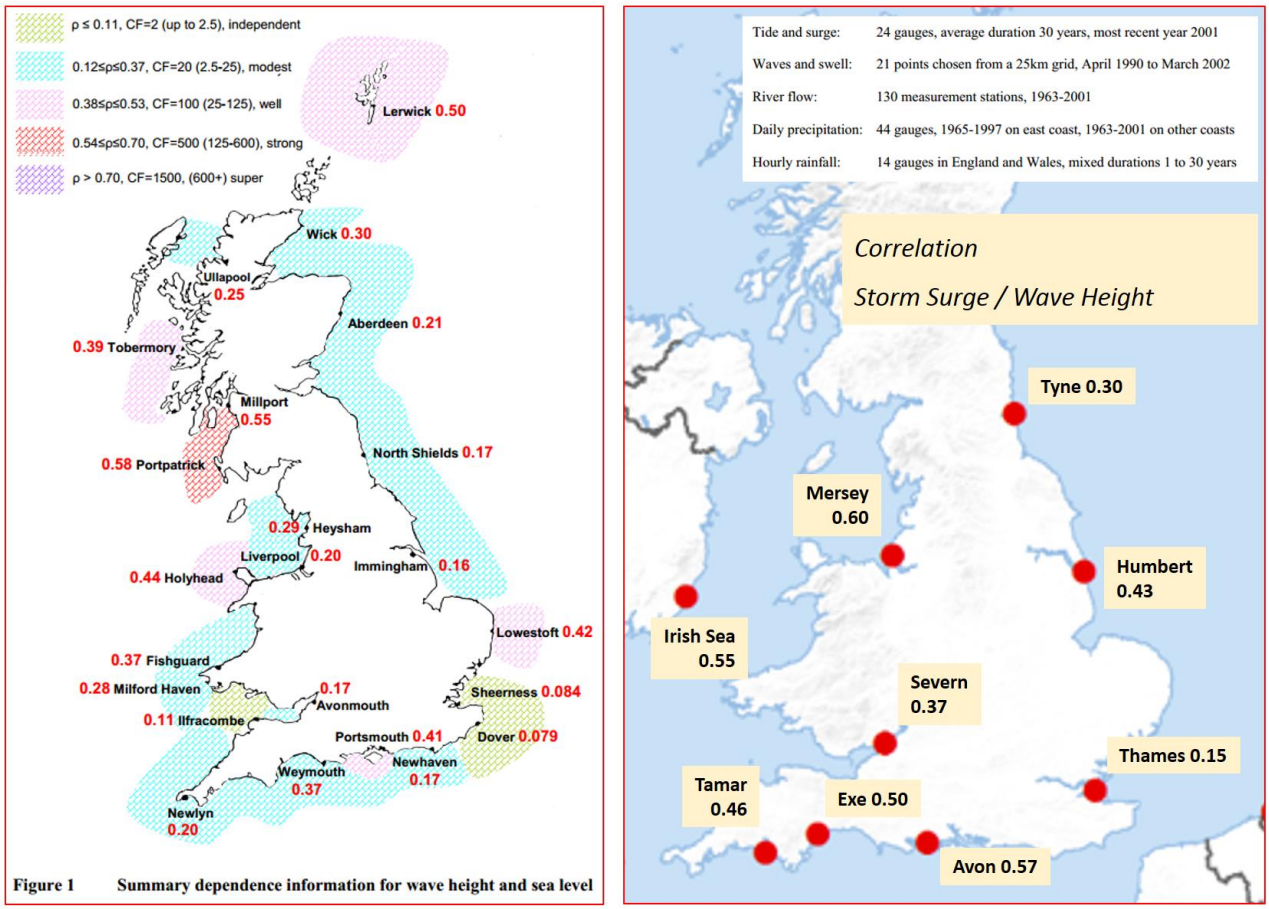

Figure 4.22. Inter-comparison of storm surge & wave height correlation values.

It should be noted that the left panel of Figure 4.22 is referring to results found by Hawkes (2005) concerning correlations between sea level & wave height while the right panel is referring to storm surge & wave height correlations found in this Report. Although the variable of sea level differs from the variable of storm surge there seems to be a satisfactory general agreement of the results. Local differences most probably are not attributed only to the fact of considering storm surge in the place of sea level but also due to the positions of the model grid points (both for storm surge and for wave height) that are somehow placed more inside the sea. This is because in practice the closest model sea point to the RIEN point is used for both correlation and statistical dependence estimations.

5. Discussion & conclusion

In this Report, the possibility of utilising joint probability methods in coastal flood hazard component calculations is investigated since flood risk is rarely a function of just one source variable but mostly of two or three variables such as river discharge, storm surge, waves etc. Joint probability values (expressed as joint return periods also) provide the likelihood of source variables taking high values simultaneously resulting to a situation where flooding may occur.

This report focuses on data preparation, parameter selection, methodology application and presentation of the results. The source variable-pairs considered in this report, including enough information for calculations, are shown below:

(i) storm surge & wave height, relevant to most coastal flood defence studies,

(ii) storm surge & river discharge, relevant to most riverine / estuary flood defence studies and

(iii) wave height & river discharge, relevant to most coastal flood defence studies.

The analysis is focused over 32 river ending (RIEN) points being selected to cover a variety of coastal environments along European riverine and estuary areas. These RIEN points refer to the:

(i) Mediterranean Sea (Central & North Adriatic Sea, Gulf of Lion, Balearic Sea & Alboran Sea),

(ii) Bay of Biscay,

(iii) English Channel,

(iv) Irish Sea & Bristol Channel,

(v) Norwegian Sea & Baltic Sea,

(vi) North Sea

(vii) Black Sea and

(viii) North-eastern Atlantic Ocean

In the absence of widespread coincident long-term measurements of storm surge, wave height and river discharge, the methodology of simulating data observations by modelling (hindcasts) was followed resulting to a set of model simulations (hindcasts) for the three primary variables (surge, wave height & discharge) considered in the study. Storm surge hindcasts were performed by utilising the hydrodynamic model Delft3D-Flow of Deltares (on a horizontal grid of 0.20x0.20 degrees) being forced by wind and pressure terms from ECMWF ERA-Interim reanalysis fields of 0.75x0.75 resolution. In a similar way, wave hindcasts were generated by utilizing the ECMWF ECWAM wave (stand-alone) model with a spatial resolution of ~28 km, forced by neutral wind terms from ERA-Interim. For the construction of river discharge hindcasts the LISFLOOD model - developed by the floods group of the Natural Hazards Project of the Joint Research Centre (JRC) - was employed. The LISFLOOD model is a hydrological rainfall-runoff model that is capable of simulating the hydrological processes that occur in a catchment with a horizontal resolution of 5x5 km forced by a gridded meteorological dataset of 25 years collected from a wide range of weather and climatological stations.

Validation of hindcasts was made over the selected RIEN point of river Rhine (NL). Considering the physical driver complexity behind interactions among surge, wave height and discharge variables, hindcasts found to perform quite well, not only simulating observations over the common interval of interest (1,114 days), but also in resolving the right type and strength of both correlations and statistical dependencies existing between source variables.

Since the concept of the statistical dependence (as defined by Reed, 1999) is uniquely linked to the tendency for critical values of source variables to occur at the same time resulting to an increase in frequency of an

extreme, results of the current study are presented by means of analytical tables and detailed maps referring to both correlation and dependence (χ) values being estimated over RIEN points. In particular, dependence (χ) values form such analytical tables can be used in an easy way to calculate the joint return period for any combined event by inserting the value of χ in a simple formula containing the individual return periods of source variables. It is then straightforward to estimate the joint probability as the inverse of the joint return period.

Based on the above, special oriented routines as mat_chi & mat_chi_lag (see Table 2.2) being coded as matlab functions were the primary routines used for the estimation of dependencies between source variables. Both routines are capable to provide the user with dependence values based on a wide range of upper percentile (critical) thresholds. Both routines not only make use of the POT (Peaks-Over-Threshold) methodology but they also allow the user to select the maximum number of combined (compound) events on a yearly basis by applying an appropriate upper percentile threshold. For the current study, this maximum number of yearly compound events has been set to ~2.3 to ~2.5 (depending also on the stability of the graph curve of dependence points) based mainly on suggestions by Svensson and Jones (2005).

Besides matlab functions, additional routines from the integrated statistical package R were used for the estimation and inter-comparison of dependence values. The main module "extRemes" of R has been capable to provide estimations of dependence referring to specific single percentile thresholds by utilising the powerful "taildep" routine. Another "powerful" tool of R used for estimations of dependence has been the "evd" module that stands for “Extreme Value Distribution” that contains the routine "chiplot". Utilising "chiplot" a detailed plot of dependence (chi) values is possible based on a wide range of percentile values. The routine "chiplot" besides chi (χ) values is also capable of providing confidence intervals of chi (in most cases the 95% value was utilized). Another significant capability of "chiplot" is the plotting of the "sister" graph of chi (χ), namely the parameter "chibar" with its corresponding (95% in most cases) confidence intervals (of chibar).

It is important to point out that chi (χ) refers to the asymptotic behavior of statistical dependent variables (and this is the area on which this Report is focusing on), whereas chibar refers to the statistical dependence of asymptotically independent values (not investigated in details yet). The main idea of constructing analytical tables and detailed maps by using the combination of mat_chi, mat_chi_lag, taildep and chiplot routines is very straightforward. if someone is after details concerning the maximum number of combined events on a yearly basis he should use the mat_chi routine for better handling and selecting the appropriate percentile threshold although he should also take under serious consideration possible stability issues. On the same wavelength, if someone is interested in dependence values in lag time mode, the appropriate selection should be the mat_chi_lag that is also capable of providing the leading of the two source variables besides the maximum lag interval.

On the other hand, taildep routine of the module extRemes of R should be used if someone is after chi & chibar dependence values for a single (already selected) critical upper percentile threshold. Furthermore, if someone is after defining confidence intervals (95% for example), the usage of chiplot of the module evd of R appears to be the most appropriate one. Both chi and chibar parameters can be plotted together with their (selected) confidence interval range.

Small differences, in general, were found in estimations of statistical dependence between matlab and R routines most probably attributed to the methodology of selecting critical percentile thresholds and how to identify and define POT extremes in every case. It should be noted that in most cases both matlab and R routine estimations of dependence were found to fall in the same category, but nevertheless, in few cases in which matlab and R routine estimations were found to belong in a different category, the maximum possible category was considered in both Tables & Maps.

By inter-comparison of results, very strong ($\rho \geq 0.70$) and strong ($0.54 \leq \rho \leq 0.69$) correlations and dependencies ($\chi \geq 0.45$ & $0.35 \leq \chi \leq 0.44$) between storm surge and wave height values were found mainly over the coastal areas of English Channel, Irish Sea, North Sea and Norwegian Sea with surge to slightly lead wave values (in MAX12 mode). Such significant correlations and dependencies appear to take place mostly on the same 24-hour (daily) time interval (i.e., in zero-lag mode). Furthermore, moderate ($0.15 \leq \chi \leq 0.24$) to well ($0.25 \leq \chi \leq 0.34$) category dependencies were found for most of the remaining sea areas, also on a zero-lag mode, whereas, in the Mediterranean Sea, dependencies were found to belong mostly in moderate category with some cases of even lower values ($0.06 \leq \chi \leq 0.14$) as the ones prevailing over the Balearic and Alboran Sea.

Concerning storm surge & river discharge in zero-lag mode, most of dependencies found to belong to moderate category with some cases (mainly over English Channel) reaching the higher (well) category. An important element in this case had been the necessity of a considerable time lag interval – extending over a few (mostly 2 to 4) days – for achieving even higher values of both correlations and dependencies. In such (max lag-mode) case, surge values clearly were leading discharge ones in most of the cases, meaning that storm surge maxima were taking place before river discharge maxima.

The existence of a time lag interval necessary for achieving relatively high values of correlations and dependencies was also pronounced between wave and discharge values. Nevertheless, in zero-lag mode, most of dependencies found to belong to moderate and well categories with some cases (mainly over the Bay of Biscay and North-eastern Atlantic Ocean) reaching the higher (strong) category. In max lag-mode, more cases of strong dependence were found over the Bay of Biscay and North-eastern Atlantic Ocean with wave to lead discharge values in almost all cases.

Overall, the highest values of (strong / very strong) correlations and dependencies were found between surges and waves mainly over the North Sea and the English Channel with (such combined) events to take place on the same day (zero-lag mode). Moderate to well category dependencies were found for most of sea areas, also on a zero-lag mode. In the case of surge & river discharge, moderate to well category values were found in most cases but not in a zero-lag mode as in surge & wave case. It became clear that in order to achieve such (relatively high) values, a considerable lag time interval of a few days was required with surge clearly leading discharge values. For the case of wave & river discharge, well to strong category values were found but once more mostly in non-zero lag mode indicating the necessity of a considerable lag time interval for dependence to reach such (well / strong) values with wave distinctly leading discharge values.

Closing, the suggested methodology of estimating joint probabilities appears to be simple and straightforward. This can be achieved by utilising appropriate analytical tables and detailed maps contained in the report referring to dependence values for combined events of interest over RIEN areas, the same way that was applied by DEFRA (UK) and documented by Hawkes (2005). For the joint probability assessment, the estimated value of dependence (χ) – taken from the analytical tables and maps – could be utilised to calculate the joint return period of the combined event of interest by inserting this (χ) value in a simple formula (described by Equation 2.4.10) containing the individual return periods of the source variables involved. It is then a one-step procedure to estimate the joint probability value as the inverse of the joint return period.

It is obvious that this is only the first step to the direction of studying and investigating over (joint) probabilities of such compound events that could be considered by the Coastal-Alert-Risk Project. An obvious second step should be the estimation of the individual return periods over RIEN points by fitting EVA (Extreme Value Analysis) distributions on the available set (time-series) of hindcasts. It is also obvious that more primary and proxy variables should be studied. For instance, besides the significant wave height values, the maximum wave height or/and the period or/and the direction of waves should be considered. Another important point here is the effect of seasonal circulation and water-mass distribution (currents & tides) besides the prevailing weather system and atmospheric circulation contained in relevant weather maps.

References

Acreman, M.C., 1994. Assessing the joint probability of fluvial and tidal floods in the River Roding. J. IWEM, 8, 490–496.

AR & R Project 18, 2009. AR & R Project No. 18 – Coastal Processes and Severe Weather Events: Discussion Paper, Water Technology report to Australia Rainfall & Runoff (2009) referring to the report of Department of Science, Information Technology, Innovation and the Arts (2012) "Coincident Flooding in Queensland: Joint probability and dependence methodologies", Science Delivery, October 2012.

Balsamo, G., Viterbo, P., Beljaars, A., van den Hurk, B., Hirschi, M., Betts, A.K. and K. Scipal, 2009. A revised hydrology for the ECMWF model: Verification from field site to terrestrial water storage and impact in the Integrated Forecast System, J. Hydrometeorol., 10, 623–643.

Bidlot, J.-R., Janssen, P. and S. Abdalla, 2006. Impact of the revised formulation for ocean wave dissipation on ecmwf operational wave model. ECMWF Techn. Memo. No. 509, ECMWF, Reading, U.K., 27 pp.

Bidlot J.-R., 2012: Present status of wave forecasting at ECMWF. Proceeding from the ECMWF Workshop on Ocean Waves, 25-27 June 2012.

ECMWF, 2015. IFS DOCUMENTATION – Cy41R1, Operational implementation 12 May 2015, PART VII: Wave Model, ECMWF IFS documentation.

Blank, L., 1982. Statistical Procedures for Engineering, Management, and Science, McGraw Hill.

Coles, S.G., 2001: An Introduction to Statistical Modelling of Extreme Values. Springer Series in Statistics. Springer Verlag London. 208p

Coles, S.G. and J.A. Tawn, 1991. Modelling extreme multivariate events. J. R. Statist. Soc., B53, 377–392.

Coles, S.G. and J.A. Tawn, 1994. Statistical methods for multivariate extremes: an application to structural design. Appl. Statist., 43, 1–48.

Coles, S.G., Heffernan, J. and J.A. Tawn, 2000. Dependence measures for extreme value analyses. Extremes, 2, 339–365.

Dee, D.P., Uppala, S.M., Simmons, A.J., Berrisford, P., Poli, P., Kobayashi, S., Andrae, U., Balmaseda, M.A., Balsamo, G., Bauer, P., Bechtold, P., Beljaars, A., van de Berg, L., Bidlot, J., Bormann, N., Delsol, C., Dragani, R., Fuentes, M., Geer, A.J., Haimberger, L., Healy, S.B., Hersbach, H., Hólm, E.V., Isaksen, L., Kallberg, P., Köhler, M., Matricardi, M., McNally, A.P., Monge-Sanz, B.M., Morcrette, J.-J., Park, B.K., Peubey, C., de Rosnay, P., Tavolato, C., Thépaut, J.-N., and F. Vitart, 2011. The ERA-Interim reanalysis: configuration and performance of the data assimilation system, Q. J. Roy. Meteorol. Soc., 137, 553– 597, doi:10.1002/qj.828, 2011.

Deltares Delft3D-FLOW, 2014. Simulation of multi-dimensional hydrodynamic flows and transport phenomena, including sediments. User Manual. Deltares, Delft, The Netherlands.

De Roo, A.P.J., Bartholmes, J., Bates, P.D., Beven, K., Bongioannini-Cerlini, B., Gouweleeuw, B., Heise, E., Hils, M., Hollingsworth, M., Holst, B., Horritt, M., Hunter, N., Kwadijk, J., Pappenburger, F., Reggiani, P., Rivin, G., Sattler, K., Sprokkereef, E., Thielen, J., Todini, E. and M. Van Dijk, 2003. Development of a European Flood Forecasting System. International Journal of River Basin Management, 1, 49-59.

Dixon, M.J. and J.A. Tawn, 1994. Extreme sea-levels at the UK A-class sites: site-by-site analyses. Internal Document No. 65, Proudman Oceanographic Laboratory, UK.

Dwyer, I.J., 1995. Confluence flood joint probability. Report to MAFF, project number FD0417. Institute of Hydrology, UK.

Gould, M., Colleter, G. and M. Erpf, 2008. Sunshine Coast Regional Council Storm Tide Management, IPWEA National Conference on Climate Change, Coffs Harbour, NSW, Australia, 2008.

Hawkes, P.J., 2003. Extreme water levels in estuaries and rivers: the combined influence of tides, river flows and waves. R&D Technical Report FD0206/TR1 to Defra. HR Wallingford, UK.

Hawkes, P.J., 2004. Use of joint probability methods for flood & coastal defence: a guide to best practice. R&D Interim Technical Report FD2308/TR2 to Defra. HR Wallingford, UK.

Hawkes, P.J., 2005. Use of joint probability methods in flood management: a guide to best practice. R&D Technical Report FD2308/TR2 to Defra. HR Wallingford, UK.

Hawkes, P.J. and C. Svensson, 2003. Joint probability: dependence mapping & best practice. R&D Interim Technical Report FD2308/TR1 to Defra. HR Wallingford and CEH Wallingford, UK.

Hawkes, P.J. and C. Svensson, 2005. Joint probability: dependence mapping & best practice. R&D Final Technical Report FD2308/TR1 to Defra. HR Wallingford and CEH Wallingford, UK.

Hawkes, P.J., Svensson C. and S. Surendran (2005). The joint probability of pairs of variables relevant to flood risk: Dependence mapping and best practice. Defra Flood and Coastal Management Conference, University of York.

Hawkes, P.J. and J.A. Tawn, 2000. Joint probability of waves and water levels: JOIN-SEA: A rigorous but practical new approach. Internal Document No. SR 537, HR Wallingford with Lancaster University, UK. (Originally dated Nov. 1998, re–issued with minor adjustments in final form May 2000).

IPCC, 2012. Managing the Risks of Extreme Events and Disasters to Advance Climate Change Adaptation. A Special Report of Working Groups I and II of the Intergovernmental Panel on Climate Change [Field, C.B., V. Barros, T.F. Stocker, D. Qin, D.J. Dokken, K.L. Ebi, M.D. Mastrandrea, K.J. Mach, G.-K. Plattner, S.K. Allen, M. Tignor, and P.M. Midgley (eds.)]. Cambridge University Press, Cambridge, UK, and New York, NY, USA, 582 pp.

Ibidapo-Obe, O. and M. Beran, 1988. Hydrological aspects of combined effects of storm surges and heavy rainfall on river flow. Report No. 30 in the Operational Hydrology Series, WMO Report No. 704. World Meteorological Organisation, Geneva.

Jones, D.A., 1998. Joint probability fluvial-tidal analyses: structure functions and historical emulation. Report to MAFF, project number FD0417. Institute of Hydrology, UK.

Meadowcroft, I., Hawkes, P.J. and S. Surendran, 2004. Joint probability best practice guide: practical approaches for assessing combined sources of risk for flood and coastal risk managers. In Proceedings from the DEFRA 39th Flood & Coastal Management Conference, York, UK, July 2004, 6A.2.1– 6A.2.12.

Need, S.F., Lambert, M.F. A.V. Metcalfe, 2008. A total probability approach to flood analysis in tidal rivers reaches, World Environmental and Water Resources Congress, ASCE, Honolulu, Hawaii, 2008.

Prandle, D. and J. Wolf, 1978. The interaction of surge and tide in the North Sea and River Thames. Geophysical J. Royal Astronomical Soc., 55, 203–216.

Reed, D.W., 1999. Flood Estimation Handbook, Vol. 1: Overview. Institute of Hydrology, Wallingford, UK.

Sembiring, L., van Ormondt, M., van Dongeren, A. and D. Roelvink, 2015. A validation of an operational wave and surge prediction system for the Dutch coast. Nat. Hazards Earth Syst. Sci. 15:1231-1242.

Svensson, C. and D.A. Jones, 2000. Dependence between extreme sea surge, river flow and precipitation: a study in eastern Britain. Report to MAFF, project number FD0206. CEH Wallingford, UK.

Svensson, C. and D.A. Jones, 2002. Dependence between extreme sea surge, river flow and precipitation in eastern Britain. Int. J. Climatol., 22 (10), 1149–1168.

Svensson, C. and D.A. Jones, 2003. Dependence between extreme sea surge, river flow & precipitation: a study in south & west Britain. R&D Interim Technical Report FD2308/TR3 to Defra. CEH Wallingford, UK.

Svensson, C. and D.A. Jones, 2004a. Dependence between sea surge, river flow & precipitation in south & west Britain. Hydrol. Earth Sys. Sci., 8, 973–992

Svensson, C. and D.A. Jones, 2004b. Sensitivity to storm track of the dependence between extreme sea surges and river flows around Britain. In Hydrology: Science and Practice for the 21st Century, Vol. 1. Proc. from the British Hydrological Society's international conference, London, UK, July 2004, 239a–245a (addendum).

Svensson, C. and D.A. Jones, 2005. Climate change impacts on the dependence between sea surge, precipitation and river flow around Britain. In Proceedings from the DEFRA 40th Flood & Coastal Management Conference, York, UK, July 2005, 6A.3.1–6A.3.9.

Tawn, J.A., 1992. Estimating probabilities of extreme sea-levels. Journal of the Royal Statistical Society: Series C, 41. 77–93. ISSN 1467-9876.

Teakle, I., Gildas, C., Khondker, R., Breen, M. and D. McGarry, 2005. Boundary conditions for estuarine flood modelling using joint probability analysis, Proc. of Coasts and Ports: Coastal Living – Living Coast, Australasian Conference, 613–619.

Vongvisessomjai, S. and S. Rojanakamthorn, 1989. Interaction of tide and river flow. J. Waterway Port Coastal Ocean Eng. (ASCE), 115, 86–104.

Vousdoukas, M.I., Voukouvalas, E., Annunziato, A., Giardino, A. and L. Feyen, 2016. Projections of extreme storm surge levels along Europe. Clim. Dyn. in press. DOI: 10.1007/s00382-016-3019-5.

Walden, A.T., Prescott, P. and N.B. Webber, 1982. The examination of surge–tide interaction at two ports on the central south coast of England. Coastal Engineering, 6, 59–70.

Wesseling, C., van Deursen, W. and P. Burrough, 1996. A spatial modelling language that unifies dynamic environmental models and GIS. In Proceedings, Third International Conference/Workshop on Integrating GIS and Environmental Modelling, Santa Fe, NM, January 21-26.

Weston, A.E., 1979. The measurement of interactive freshwater and tidal flows in the River Dee, North Wales. J. Inst. Water Eng. Sci., 33, 69–79.

White, C.J., 2007. The use of joint probability analysis to predict flood frequency in estuaries and tidal rivers, PhD Thesis, School of Civil Engineering and the Environment, University of Southampton, p343.

List of abbreviations and definitions

AA	"Applied Approach" methodology for estimating joint probabilities (Hawkes and Tawn, 2000).
CAR	CoastAlRisk (Coastal-Alert-Risk) Exploratory Project for 2015-2016.
CEH	Center for Ecology & Hydrology, Wallingford (UK).
GDACS	Global Disaster Alerts & Coordination System (http://gdacs.org/).
chiplot	Specialised routine of evd module for the estimation and production of "chi" and "chibar" statistical dependence measures between two source variables.
DEFRA	Department of Environmental & Food Rural Affairs (UK).
ERCC	Emergency Response Coordination Centre (ERCC) of the EC (European commission).
evd	Set of routines focusing on EVD (Extreme Value Distribution) module of the integrated statistical platform R.
extRemes	Set of routines focusing on EVA (Extreme Value Analysis) module of the integrated statistical platform R.
GFDS	Global Flood Detection System (http://www.gdacs.org/flooddetection/).
GloFAS	Global Flood Awareness System of JRC (http://www.globalfloods.eu/).
GPCP	Global Precipitation Climatology Project (http://precip.gsfc.nasa.gov/).
HVH	Hoek Van Holland Tide Gauge Station (NL).
HR	(Wallingford). Civil Engineering & Environmental Hydraulics (http://www.hrwallingford.com/).
HTESSEL	Land Surface Scheme (http://www.globalfloods.eu/user-information/data-and-methods).
IPSC	Institute for the Protection and Security of the Citizen of the JRC.
IES	Institute for the Environment and Sustainability of the JRC.
IPTS	Institute for Prospective Technological Studies of the JRC.
LIC	Wave buoy platform of Lichteiland Goerre I (NL).
mat_chi	Matlab routines for the estimation of statistical dependence following Coles (2001).
mat_chi_lag	Matlab routines for the estimation of statistical dependence in lag-mode of various time intervals and identification of the leading source variable.
POL	http://noc.ac.uk/about-us/history/proudman-oceanographic-laboratory.
RIEN	RIver ENding (points).
SSCS	Storm Surge Calculation System of GDACS.
SA	"Simplified Approach" methodology for estimating joint probabilities (Hawkes, 2000).
taildep	Specialised routine of the extRemes module (R) for the estimation of statistical dependence between two source variables.

List of figures

Figure 1.1. Main components of the Coast-Alert-Risk (CoastAlRisk / CAR) exploratory research project.

Figure 1.2. Main elements of the Joint Return Period module of CAR Project.

Figure 1.3. Storm surge Vs significant wave height observations at HVH / LIC.

Figure 2.1. Storm surge and significant wave height time series of observations at HVH / LIC.

Figure 3.1. Positions of the 32 RIEN points used in the study.

Figure 3.2. Positions of HVH tide gauge station, Rockanje RIEN, Lichteiland Goeree wave buoy and Lobith discharge station of river Rhine (NL).

Figure 3.3. Correlation categories taken from Hawkes & Svensson (2005).

Figure 3.4. Scatterplot of storm surge hindcasts Vs observations for HVH (1,114 days).

Figure 3.5. Subsection of time series for both hindcast and observation values (interval of ~1 month).

Figure 3.6. Surface weather map (a) and satellite image (b) valid for 3 January 2012 12UTC.

Figure 3.7. Surface weather map valid for 6 January 2012 00UTC.

Figure 3.8. Scatterplot of significant wave height hindcasts vs observations for LIC (1,114 days).

Figure 3.9. As in Figure 3.5, but for wave hindcasts and observations.

Figure 3.10. Scatterplot of significant wave height hindcasts vs observations for HVH (1,114 days).

Figure 3.11. As in Figure 3.5, but for river discharge hindcasts and observations.

Figure 3.12. Scatterplots of storm surge Vs wave in observations (a) and hindcast (b) mode (1,114 days).

Figure 3.13. As in Figure 3.12, but for storm surge and river discharge values.

Figure 3.14. As in Figure 3.12, but for storm surge and river discharge values.

Figure 3.15. Statistical dependence (chi) of storm surge (HVH) and significant wave height (LIC) values.

Figure 3.16. As in Figure 3.15 but for the subsection (zooming over) referring to upper thresholds ranging from 92 to 99.9% percentile values.

Figure 3.17. Dependence (chi) values of storm surge (HVH) and significant wave height (LIC) valid for observations mode (a) and dependence values valid for hindcast common time period (b) as estimated by the module “taildep” of the statistical package “extRemes” of application R.

Figure 3.18. As in Figure 3.17 but valid for the total hindcast period of 12,753 days (~35 years).

Figure 3.19. Statistical dependence (chi) of storm surge (HVH) and river discharge (LOB) values.

Figure 3.20. Statistical dependence (chi) of storm surge (HVH) and river discharge (LOB) values.

Figure 4.1. Map with local values of correlations between surge & wave for MAX12.

Figure 4.2. Scatterplot of surge & wave height (max12) values valid for RIEN of river Rhine (NL).

Figure 4.3. Map with local values of correlations between surge & wave for MAX24.

Figure 4.4. Scatterplot of surge & wave height (max24) values valid for RIEN of river Bethune (FR).

Figure 4.5. Map with spatial correlations between surge & river discharge values for MAX24.

Figure 4.6. Scatterplot of storm surge & river discharge (max24) values for RIEN of river Mersey (UK).
Figure 4.7. Map with spatial correlations between wave & river discharge values for MAX24.
Figure 4.8. Scatterplot of wave & river discharge (max24) values valid for RIEN of river Blavet (FR).
Figure 4.9. Map with local values of dependence between surge & wave for MAX12.
Figure 4.10. Dependence of storm surge & wave height (max12) values valid for RIEN of river Rhine (NL).
Figure 4.11. Dependence of storm surge & wave height (max12) values valid for RIEN of river Rhine (NL).
Figure 4.12. Dependence (BAR) of surge & wave height (max12) values valid for RIEN of river Rhine (NL).
Figure 4.13. Map with local values of dependence between surge & wave values for MAX24.
Figure 4.14. Dependence of storm surge & wave (max24) values valid for RIEN of river Rhine (NL).
Figure 4.15. Details of dependence of surge & wave (max24) values valid for RIEN of river Rhine (NL).
Figure 4.16. Dependence of storm surge & wave (max24) values valid for RIEN of river Rhine (NL).
Figure 4.17. Map with local values of dependence between surge & river discharge values for MAX24.
Figure 4.18. Dependence of surge & river discharge (max24) values valid for RIEN of river Rhine (NL).
Figure 4.19. Map with local values of dependence between wave & river discharge values for MAX24.
Figure 4.21. Dependence of wave & discharge (max24) values valid for RIEN of river Rhine (NL) details.
Figure 4.22. Inter-comparison of storm surge & wave height results.

List of tables

Table 2.1. Different methodologies for estimating joint probabilities.

Table 2.2. Statistical modules & routines used for the estimation of dependence.

Table 2.3. Example of utilising dependence to estimate joint return periods.

Table 3.1. List of the River Ending (RIEN) points.

Table 3.2. Duration of simulations (Hindcasts).

Table 3.3. Positions of RIEN points Vs model grid points used for hindcasts.

Table 3.4. Details of Delft3D model setup.

Table 3.5. Type and duration of HVH, LIC & LOB observations.

Table 3.6. Common time intervals for hindcast and observation data sets.

Table 3.7. Categories of correlation (a) & dependence (b) utilised in the current study.

Table 3.8. Correlations in observations – hindcast common & hindcast total mode.

Table 3.9. Dependencies between storm surge & significant wave height values for observations, hindcast common and hindcast total time series.

Table 3.10. Dependencies between storm surge & river discharge values for observations, hindcast common and hindcast total time series.

Table 3.11. Dependencies between wave height & river discharge values for observations, hindcast common and hindcast total time series.

Table 4.1. Correlations between surge & wave values for MAX12.

Table 4.2. Correlations between surge & wave values for MAX24.

Table 4.3. Correlations between surge & river discharge values for MAX24.

Table 4.4. Correlations between significant wave height & river discharge values for MAX24.

Table 4.5. Dependencies between surge & wave values for MAX12.

Table 4.6. Dependencies between surge & wave values for MAX24.

Table 4.7. Dependencies between surge & river discharge values for MAX24.

Table 4.8. Dependencies between wave & river discharge values for MAX24.

Table 4.9. Correlations & dependencies between surge, wave & discharge values for zero-lag mode.

Table 4.10. Correlations & dependencies between surge, wave & discharge values in max-lag mode.

LB-NA-27824-EN-N

JRC Mission

As the Commission's in-house science service, the Joint Research Centre's mission is to provide EU policies with independent, evidence-based scientific and technical support throughout the whole policy cycle.

Working in close cooperation with policy Directorates-General, the JRC addresses key societal challenges while stimulating innovation through developing new methods, tools and standards, and sharing its know-how with the Member States, the scientific community and international partners.

Serving society
Stimulating innovation
Supporting legislation

Publications Office

doi:10.2788/677778

ISBN 978-92-79-57665-2